FORMULATIONS, ISSUES, AND COMPARISON OF CAR-FOLLOWING MODELS

Venkata Siva Praveen Pasumarthy

Thesis Submitted to the Faculty of Virginia Polytechnic Institute and State University
in partial fulfillment of the requirements for the degree of

Master of Science
in
Civil Engineering

Dr. Hesham Rakha, Chair
Dr. Antonio Trani
Dr. Slimane Adjerid

February 3, 2004
Blacksburg, Virginia

Keywords: Car-Following Models, Traffic Stream Models, Speed and Acceleration Formulations, Discharge Headways and Capacity Drop

FORMULATIONS, ISSUES, AND COMPARISON OF CAR-FOLLOWING MODELS

Venkata Siva Praveen Pasumarthy

ABSTRACT

Microscopic simulation software use car-following models to capture the interaction of a vehicle and the preceding vehicle traveling in the same lane. In the literature, much research has been carried out in the field of car-following and traffic stream modeling. Microscopic car-following models have been characterized by using the relationship between a vehicle's desired speed and the distance headway (h) between the lead and follower vehicles. On the other hand, macroscopic traffic stream models describe the motion of a traffic stream by approximating for the flow of a continuous compressible fluid. This research work develops and compares three different formulations of car-following models – speed formulation, molecular acceleration, and fluid acceleration formulation. First, four state-of-the-art car-following models namely, Van Aerde, Greenshields, Greenberg and Pipes models, are selected for developing the three aforementioned formulations. Then a comprehensive car-following behavior encompassing steady-state conditions and two constraints – acceleration and collision avoidance – is presented. Specifically, the variable power vehicle dynamics model proposed by Rakha and Lucic (2002) is utilized for the acceleration constraint.

Subsequently, the thesis describes the issues associated with car-following formulations. Recognizing that many different traffic flow conditions exist, three distinct scenarios are selected for comparison purposes. The results demonstrate that the speed formulation ensures that vehicles typically revert to steady-state conditions when vehicles experience a perturbation from steady-state conditions. On the other hand, both acceleration formulations are unable to converge to steady-state conditions when the system experiences a perturbation from a steady-state.

The thesis also attempts to address the question of capacity drop associated with vehicles accelerating from congested conditions. Specifically, the capacity drop proposition is analyzed for the case of a backward recovery (typical of a signalized intersection) and stationary shockwave (typical of a capacity drop on a freeway). In the case of the backward recovery shockwave, the acceleration constraint results in a temporally and spatially confined capacity drop as vehicles accelerate to their desired steady-state speed. This temporally and spatially confined capacity drop results in what is typically termed the start loss of a signalized phase. Subsequently, vehicles attain steady-state conditions, in the case of the speed and molecular acceleration formulations, at the traffic signal stop bar after the initial five vehicle departures. The analysis also demonstrates that after

attaining steady-state conditions the capacity may drop for the initial vehicle departures as a result of traffic stream dispersion. This traffic dispersion capacity drop increases as vehicles travel further downstream. Alternatively, in the case of a stationary bottleneck the aggressiveness of vehicle accelerations plays a major role in defining the capacity drop downstream of a bottleneck. The study demonstrates that any temporal headways that may be lost while vehicles accelerate to steady-state conditions may not be recuperated and thus result in capacity drops downstream of a bottleneck. A typical example of this scenario is the traffic stream flow rate downstream of a stop sign, which is significantly less than the roadway capacity. The reduction in capacity is caused by losses in temporal headways between successive vehicles which are not recuperated. The study also demonstrates that the ability to model such a capacity drop does not require the use of a dual-regime traffic stream model as is proposed in the Highway Capacity Manual (HCM). Instead, the use of a single-regime model captures the observed capacity with the introduction of an acceleration constraint to the car-following system of equations.

ACKNOWLEDGEMENTS

This work would not have been possible without the support and encouragement of many people. I would like to take this opportunity to thank them.

First and foremost, I thank my advisor, Dr. Hesham Rakha for providing the necessary financial assistance to pursue a Master's degree and help me out of a difficult phase in my life. I am also very grateful to him for his guidance through my research work and for his valuable suggestions regarding my career.

I also express my appreciation to the members of my committee, Dr. Antonio Trani and Dr. Slimane Adjerid for their precious comments and support. Also, I am thankful to my friends and colleagues whom I worked with at VTTI and Civil Engineering Department, who made my study all the more enjoyable.

I cannot end without thanking my family. I am grateful to my parents for the many sacrifices they made to shape my career and to my sister for the wonderful times we spent together.

TABLE OF CONTENTS

LIST OF TABLES

LIST OF FIGURES

NOMENCLATURE

h_i	=	Distance headway between vehicle "i" and vehicle "i-1" (km);
s_i	=	Time headway between vehicle "i" and vehicle "i-1" (h);
$\bar{h}, \bar{s}$	=	Average distance and time headway between successive vehicles, respectively (km, h);
h_b	=	Boundary distance headway above which a lower sensitivity factor is introduced (km);
$h_n(t)$	=	Distance headway of vehicle "n" at instant "t" (km);
$\tilde{h}_{n+1}(t)$	=	Projected headway of vehicle "n+1" as implemented in INTEGRATION;
Δt	=	Duration of time interval used to solve the ODE;
T_o	=	Duration of analysis period (h);
T	=	Driver reaction time (s);
r	=	Number of vehicles passing a point at any location "x" over the analysis period "T_0" ;
p	=	Number of vehicles observed along an analysis section "L" at any instant "t";
L	=	Length of roadway section under analysis (km);
L_n	=	Length of vehicle "n" (m);
α	=	Driver sensitivity factor (1/s);
α_1	=	Driver sensitivity factor for short distance headways (1/s);
α_2	=	Driver sensitivity factor for long distance headways (1/s);
α_0	=	Driver sensitivity factor in Greenberg traffic stream model or GM-5 model (with l = 1 and z = 0) (1/s);
$\alpha(l, z)$	=	Driver sensitivity factor for exponents "l" and "z" (units dependent on the exponents "l" and "z");
l, z	=	Exponents of the following vehicle's speed and distance headway, respectively;
k	=	Traffic stream density (veh/km);
k_j	=	Jam density (veh/m);
kc	=	Traffic stream density at capacity (veh/km);
h_j	=	Jam density headway (m/veh);
u_f	=	Roadway free-speed (m/s);
u_c	=	Speed at capacity (m/s);
$\bar{u}$	=	Space-mean-speed (m/s);
q	=	Flow rate (veh/h);
q_c	=	Capacity of roadway (veh/h);
u	=	Vehicle speed (km/h);
u'	=	Partial derivative of speed with respect to density (km^2/veh-hr);
$u(t_i)$	=	Vehicle speed at instant "t_i" (km/h);
u_o	=	Speed at which vehicle attains maximum power (km/h);
$u_n(t)$	=	Speed of vehicle "n" at instant "t";
$\tilde{u}_n(t)$	=	Desired speed of vehicle "n" at instant "t" using a car-following model;
$\hat{u}_n(t)$	=	Maximum speed of vehicle "n" at instant "t" allowed by vehicle dynamics;
$\breve{u}_n(t)$	=	Maximum speed of vehicle "n" at instant "t" allowed by collision avoidance

constraint;

$a_n(t)$ = Acceleration of vehicle "n" at instant "t" (m/s^2);

$\hat{a}_n(t)$ = Maximum acceleration of vehicle "n" at instant "t" allowed by vehicle dynamics (m/s^2);

$\breve{a}_n(t)$ = Maximum deceleration of vehicle "n" at instant "t" allowed by collision avoidance constraint (m/s^2);

$x_n(t)$ = Position of vehicle "n" at instant "t";

x = Distance traveled by a vehicle (km);

$\dot{x}$ = First derivative of distance: speed (km/h);

$\ddot{x}$ = Second derivative of distance: acceleration (m/s^2);

$d_n(t)$ = Distance by which the LV is moved prior to applying the car-following logic;

$\tilde{d}_{n+1}(t)$ = Projected position of FV at instant "t";

n = Exponent of proportionality in Drew's generalized model;

c = Fluid compressibility;

c_1 = Fixed distance headway constant in Van Aerde model (km/veh);

c_2 = First variable distance headway constant in Van Aerde model (km^2/veh-h);

c_3 = Second variable distance headway constant in Van Aerde model (h/veh);

m = Constant used to solve the three headway constants in Van Aerde model (h/km);

$F_n(t)$ = Tractive effort of vehicle "n" at instant "t" (N);

$R_n(t)$ = Total resistance force , which is the sum of aerodynamic, rolling and grade resistance forces, on vehicle "n" at instant "t" (N);

M = Vehicle mass (kg);

M_{ta} = Vehicle mass on tractive axle (kg);

P = Engine power (kW);

η_d = Transmission efficiency;

β = Variable power factor;

μ = Coefficient of friction between tires and pavement;

w = Vehicle weight-to-power ratio (kg/kW);

G = Percentage grade (m/100m);

γ = Maximum acceleration factor to characterize typical acceleration behavior of drivers;

A_f = Vehicle frontal area (m^2);

C_d = Vehicle drag coefficient;

C_h = Altitude coefficient;

C_r = Rolling coefficient;

c_7 = A constant (0.047285);

c_8, c_9 = Rolling resistance coefficients;

CHAPTER ONE:

INTRODUCTION

1.1 Background

Microscopic simulation software use car-following models to capture the interaction of a vehicle and the preceding vehicle traveling in the same lane. The process of car-following should be modeled as an equation of motion under steady-state conditions plus a number of constraints that govern the behavior of vehicles while moving from one steady state to another (decelerating and accelerating). The first constraint governs the vehicle acceleration behavior, which is typically a function of the vehicle dynamics. The second and final constraint ensures that vehicles maintain a safe position relative to the lead vehicle in order to ensure asymptotic stability within the traffic stream.

Consequently, the calibration of the car-following behavior within microscopic simulation software can be viewed as a two-step process. In the first step, the steady-state behavior is calibrated followed by a calibration of the non-steady state behavior.

1.2 Problem Definition

In literature, much research has been carried out in the field of car-following and traffic stream modeling. Microscopic car-following models have been characterized by using the relationship between a vehicle's desired speed and the distance headway (h) between the lead and follower vehicles. Alternatively, the more common representation of car-following behavior has been to characterize the vehicle's desired acceleration and the speed differential between the lead and following vehicles. Though much work has been done in the formulation of these models, little effort has been paid to illustrate the advantages (or disadvantages) of using each approach, specifically speed or acceleration as a control variable.

Further, the question of whether a capacity drop occurs after the formation of a queue has been the subject of much debate. Many researchers have tried to address this issue by collecting data from interchanges using loop detectors and analyzing whether a reduction in capacity occurs after a queue forms. But little work has been done to tackle this issue by comparing the results from car-following models.

1.3 Thesis Objectives

The first objective of this thesis is to present the formulation and practical issues to be considered while modeling a car-following behavior. Specifically, the aim is to demonstrate and compare the two possible car-following formulations – speed and

acceleration approaches. In addition, a new approach for the acceleration form of car-following modeling is proposed.
The second objective is to address the issue of capacity drop using the car-following models used in simulation software. Thirdly, this thesis aims to study the behavior of discharge headways of a platoon of vehicles under various scenarios.

1.4 Thesis Contributions

The thesis has the following significant contributions:

- Firstly, it demonstrates the common drawbacks of state-of-the art car-following models and how they can be addressed.
- Secondly, the thesis presents a detailed description of the two possible car-following formulations – speed and acceleration as control variables. A new acceleration form of approach to car-following is proposed in the lines of Greenberg's model. The approaches are formulated for four selected state-of-the art models and a comparison of each approach is presented.
- Thirdly, the thesis demonstrates how the system of car-following behavior can be implemented within simulation software and the practical considerations that are to be considered to successfully implement them within microscopic traffic simulation software
- Fourthly, the thesis addresses the much debated question of capacity drop by using the method of car-following instead of analyzing the data collected using loop detectors.
- Finally, the thesis compares how the discharge headways vary for various considered scenarios for the selected state-of-the art car-following models used in traffic simulation software.

1.5 Thesis Layout and Approach

The Thesis contains five chapters. It starts with the description of literature review followed by a review of the four selected car-following models. Subsequently, formulation and practical issues to be considered in simulation are described. Then, to illustrate the significance of transition from one steady-state to another, the problem of capacity drop at signalized intersections is studied. Finally, the discharge headways of a platoon of vehicles leaving an intersection are compared for different car-following models.

Chapter 2 presents a historical review of the work done in the field of car-following and traffic stream models. It also discusses the details of the work done by researchers on the issue of capacity drop after queue formation.

Chapter 3 starts with a presentation of the link between car-following and traffic stream models. A detailed overview of four selected car-following models is discussed along

with the derivation of their corresponding traffic stream formulations. Then the chapter demonstrates the common drawbacks of these state-of-the art models and how they can be addressed. The next part of the chapter deals with the formulation and practical issues to be considered in modeling car-following models. Specifically, two possible approaches to car-following – speed and acceleration as control variables – are presented including a new fluid acceleration approach

Chapter 4 discusses how the three car-following formulations presented in the previous chapter compare with each other under different scenarios. Further, the question of capacity drop when queue forms on freeways and arterials is also addressed. For this purpose, five models - four car-following models selected in Chapter 3 and another model used in TRANSIMS (Cellular Automata) – are compared to find out whether a drop in capacity occurs when a queue forms at a signalized intersection. It also analyzes the effect of different scenarios on the discharge headway of vehicles leaving the intersection.

Finally, Chapter 5 presents a summary and conclusion of the findings in the thesis.

CHAPTER TWO:

LITERATURE REVIEW

2.1 Introduction

The importance of transportation in the present day need hardly be emphasized. Today's highway system carries significantly more vehicle miles of travel than ever before. The demands on the transportation system continue to grow faster than improvements can be made. Consequently, the ability to understand and apply the traffic flow fundamentals is very essential towards improving the transportation system. Traffic flow theories seek to describe in a precise mathematical way, the interactions between the vehicles and their operators and the infrastructure.

The scientific study of traffic flow had its beginnings in the 1930's with the application of probability theory to the description of road traffic and the pioneering studies conducted by Bruce D. Greenshields at the Yale Bureau of Highway Traffic. After World War II, with tremendous increase in use of automobiles and the expansion of the highway systems, there was also a surge in the study of various traffic characteristics. The 1950's saw theoretical developments based on a variety of approaches – car-following, traffic waves and queuing theories. By the 1970's the field of traffic flow and transportation has become so diffuse that it can no longer be covered under the same heading. Further research continues till date, improving/altering the previously held notions and formulating new theories that describe traffic variables more realistically.

The following sections describe the existing models in the areas of car-following and traffic stream modeling and issues in capacity and discharge headways at signalized intersections. The sections trace historically the development of concepts and ideas in the above mentioned fields.

2.2 Traffic Stream (Continuum Flow) Models

Traffic stream models describe the motion of a traffic stream by approximating for the flow of a continuous compressible fluid. These models relate three traffic stream variables, namely: the traffic stream flow rate, traffic stream density, and traffic stream space-mean-speed.

Since there are three traffic variables, three relationships must be established among them in order to compute the magnitude of these variables. The first relationship among flow (q), density (k) and speed (u) is inherent in the quantity definition:

$$q = ku \qquad [2\text{-}1]$$

The second relationship, the continuity of vehicles, is expressed as follows:

$$\frac{\partial k}{\partial t} + \frac{\partial q}{\partial x} = S(x,t) \qquad [2\text{-}2]$$

Where $S(x,t)$ = Generation (dissipation) rate of vehicles per time per unit length.

Solution of the continuity equation as it applies to traffic flow was first proposed by Lighthill and Whitham (1955). Both of the above relationships are true for all fluids, including traffic and there is no controversy as to their validity. However, it is the controversy about the third equation that gives a one-to-one relationship between speed and density or between flow and density, which has led to the development of many continuum flow (traffic stream) models.

2.2.1 Simple Continuum Models

These models use a deterministic form of speed-density relationship as the third equation. They state that the average traffic speed is a function of traffic density. The models of this type were developed in the earlier times and assumed a single regime phenomenon over the complete range of flow conditions including free-flow and congested regimes. Later models attempted to improve on the earlier ones by considering two separate regimes. Many such relationships have been mentioned in the literature and the important ones among them are mentioned below.

Single-Regime Models

The first single-regime model was developed by Greenshields in 1935, based on observing speed-density measurements obtained from an aerial photographic study. His conclusion was that, speed (u) is a linear function of density (k) and can be expressed mathematically as

$$u = u_f\left(1 - \frac{k}{k_j}\right) \qquad [2\text{-}3]$$

Where u_f = Free-flow speed;
k_j = Jam density.

Greenberg (1958) developed the second single regime model by treating the traffic stream as a continuous fluid. He utilized the theory developed by Lighthill and Whitham (1955) for his model. Starting with the equation of motion of a one-dimensional fluid:

$$\frac{du}{dt} = -\frac{c^2}{k}\frac{\partial k}{\partial x} \qquad [2\text{-}4]$$

and the two equations 2-1 and 2-2, the basic equation of traffic flow and the equation of continuity, he developed a model of the form:

$$u = u_c \ln\left(\frac{k_j}{k}\right) \qquad [2\text{-}5]$$

Where u_c = Speed at maximum flow (Optimal Speed).

The important consequence of this model was the discovery of the bridge between macroscopic and microscopic models in the work by Gazis et al a year later.

The third model was proposed by Underwood (1961) as a result of traffic studies on Merritt Parkway in Connecticut. He proposed this new model mainly to overcome the deficiency in the Greenberg model – values of speed going to infinity at very low density values. Hence, his model was of the form,

$$u = u_f e^{-k/k_o} \qquad [2\text{-}6]$$

Where k_o = Density at maximum flow (Optimal density).

But this model has shortcomings in that it requires the knowledge of k_o which is difficult to observe and that it does not represent zero speed at high densities.

A fourth model was proposed by a group of researchers at Northwestern University (1965) when they observed that most speed-density curves appear as S-shaped curves. The group proposed the following equation:

$$u = u_f e^{-\frac{1}{2}\left(\frac{k}{k_o}\right)^2} \qquad [2\text{-}7]$$

This formulation is related to the Underwood model in that knowledge of the free-flow speed and optimum density are required and also, speed does not go to zero when density goes to jam density.

Utilizing the bridge between the microscopic and macroscopic models developed by Gazis et al, and using the generalized equation of car-following (GHR model, described later), a whole family of traffic stream models were generated. Details of these are given later on. The emphasis on the research in this aspect was the conversion of car-following models to traffic stream models.

Further development of single regime models was directed toward the introduction of a parameter in the formulation which would provide for a more generalized modeling approach. For example, Pipes (1967) proposed a generalized form of Greenshields' model by introducing the additional parameter, n.

$$u = u_f \left[1 - \left(\frac{k}{k_j}\right)^n\right] \qquad [2\text{-}8]$$

He argued that this new addition might represent the behavior of drivers that leave little separation distance between themselves and the car that they are following. Drew (1968) proposed a formulation based on Greenberg's fluid flow approach. He started with the generalized equation motion:

$$\frac{du}{dt} = -c^2 k^n \frac{\partial k}{\partial x} \qquad [2\text{-}9]$$

and ended up with the following equation relating traffic stream and traffic density:

$$u = u_f \left[1 - \left(\frac{k}{k_j} \right)^{(n+1)/2} \right] \qquad [2\text{-}10]$$

Drew suggested varying n from -1 to +1 and called these models a linear model (n= +1), a parabolic model (n = 0) and an exponential model (n= -1).

Further research on each of the above single regime models showed that they had deficiencies over some portion of the density range. The most disconcerting feature of these models is their inability to track faithfully the measured field data near capacity conditions (May, 1990). This led several researchers to propose two-regime models with separate formulations for the free-flow and congested-flow regimes.

Multi-regime Models

Edie first proposed the idea of two-regime models in 1961 because of reservations of using car-following based models under free-flow conditions. More specifically, Edie proposed the use of the Underwood model for the free-flow regime and the Greenberg model for the congested-flow regime.

Supporting the idea of the use of multi-regime models, a Northwestern University research team (Drake et al, 1967) proposed three additional model formulations. The first was the use of the Greenshields-type model for the free-flow regime and the congested-flow regime separately. The second model suggested a constant speed model for the free-flow regime and a Greenberg model for the congested-flow regime. The last proposed multi-regime model suggested a three-regime model with the free-flow, transitional-flow and congested-flow regimes each being represented by the Greenshields formulation.

The development of simple continuum models has led to the understanding of the formation and propagation of shockwaves and also to the analytical queuing analysis at intersections. However, the research conducted on these models was unable to explain the dynamic effects associated with traffic flow. To explain these findings, higher order continuum flow models were proposed.

2.2.2 High-Order Continuum Models

The characteristic of these models is the use of another equation called the momentum equation for the required third relationship. This momentum equation accounts for the acceleration and inertia characteristics of the traffic mass.

Prigogine and Herman (1971) hypothesized that actual speeds in a traffic stream relax to an equilibrium speed, which is a function of density. Based on extensive theoretical calculations, they proposed their momentum equation to be of the following form:

$$\frac{du}{dt} = \frac{\partial u}{\partial t} + u\frac{\partial u}{\partial x} = \frac{1}{T}\{u_e(k) - u\} \quad [2\text{-}11]$$

Where T = Relaxation time,
$u_e(k)$ = Equilibrium speed.

Payne (1971) proposed a modification to the above form of model. He introduced an anticipation term in the momentum equation. The net effect of this modification was that the traffic tends to accelerate when it anticipates lower density ahead. His model is as follows:

$$\frac{du}{dt} = \frac{\partial u}{\partial t} + u\frac{\partial u}{\partial x} = \frac{1}{T}\left\{u_e(k) - u - \frac{g'}{k}\frac{\partial k}{\partial x}\right\} \quad [2\text{-}12]$$

Where g' = Anticipation coefficient

$$= -\frac{1}{2}\frac{du_e}{dk}$$

Papageorgiou (1989) proposed a further modification to the above formulation. In order to improve the computational effect of Payne's model, φ was added to the third term on right hand side to keep it limited when density becomes small; ζ was added only for the numerical computation of the model:

$$\frac{du}{dt} = \frac{\partial u}{\partial t} + u\zeta\frac{\partial u}{\partial x} = \frac{1}{T}\left\{u_e(k) - u - \frac{g'}{k+\varphi}\frac{\partial k}{\partial x}\right\} \quad [2\text{-}13]$$

Ross (1988) in his study claimed that all the deterministic and equilibrium traffic formulations that were listed above are all grossly unrealistic. He argued that deterministic relationships (simple continuum models) between traffic speed and density do not allow for observed scatter and imply that traffic can lock up spontaneously. Further, equilibrium relationships (Payne's model, etc) between speed and density allow impossibly high traffic densities and provide unrealistically slow responses to changes in roadway and traffic conditions. In order to overcome these problems, he proposed that traffic speed "relaxes" to the free-flow speed of the roadway, independent of density except that volume cannot exceed roadway capacity and flow is incompressible when traffic density is equal to the jam density. The form of momentum equation for his model is:

$$\frac{du}{dt} = \frac{\partial u}{\partial t} + u\frac{\partial u}{\partial x} = \frac{1}{T}\{u_f - u\} \quad [2\text{-}14]$$

Research has been going on in this area in recent years with major work done by Michalopoulos, Lyrintzis and others. However, many of these higher order models are not tested. It is unknown whether in practice high-order continuum models produce better results than those of the simple continuum model.

A main factor which affects the accuracy of the higher order models is the numerical solution by finite-element methods. The importance of the proper choice of the finite difference method was not addressed properly in the earlier literature and as a result improper results have been deduced (Nelson, 1995). Although the implicit first-order upwind scheme is strongly recommended for the simple continuum model, it is not clear which finite-difference method should be used with the high-order continuum models to achieve a higher computational accuracy (Michalopoulos et al, 1994).

2.3 Car-Following Theories

Theories describing how one vehicle follows another vehicle have been studied for almost half a century. These car-following theories, referred to as microscopic models, consider spacing between and speed of individual vehicles. In other words, this approach considers the discrete nature of the traffic. Alternatively, the more common representation of car-following behavior is to express the vehicle's desired acceleration as function of the speed differential between the lead and following vehicles. Specifically, Drew (1968) suggests "the car-following laws are simplified descriptions of a very complicated response to the world of stimuli that confronts a driver".

2.3.1 Gazis – Herman – Rothery (GHR) Model

The GHR model, also known as General Motors's model, was the most investigated and well-known model and dates from the late fifties and early sixties. The research was mainly conducted by a research group at General Motors Corp and later on carried by many other independent investigators.

The first Highway Capacity Manual (1950) lists many observational studies that were directed at identifying an operative speed (u) – spacing (D) relationship. The relation obtained from these studies is represented by:

$$D = \alpha + \beta u + \gamma u^2 \qquad [2\text{-}15]$$

These kind of models are applicable to cases where each vehicle in the traffic stream maintains the same or nearly the same constant speed and each vehicle is attempting to maintain the same spacing (i.e., a steady state condition). Through the work of Pipes (1953), the dynamical elements of a line of vehicles were introduced. In his work the focus was on the dynamical behavior of a stream of vehicles as they accelerate or decelerate and each driver-vehicle pair attempts to follow one another. Pipes formulated the phenomena of the motion of pairs of vehicles following each other by the expression:

$$x_n(t) - x_{n+1}(t) = b + S.\dot{x}_{n+1}(t) \qquad [2\text{-}16]$$

Where, $x_n(t)$ = position of n^{th} vehicle at time t;

b = distance headway at standstill;

S = sensitivity constant with units of time.

This model was developed based on the rule in California Motor Vehicle Code, namely, "a good rule for following another vehicle at a safe distance is to allow yourself the length of a car for every ten miles an hour you are traveling." The assumption made here was that responses are immediate and that no inertial effects exist in the vehicles or response lags in the drivers. Differentiation of Equation 2-1 gives the basic equation of car-following:

$$\ddot{x}_{n+1}(t) = \frac{1}{S}\left[\dot{x}_n - \dot{x}_{n+1}\right] \qquad [2\text{-}17]$$

Equation 2-2 is the basic stimulus-response relation which has been further investigated by many researchers over three decades. The response has been taken as the acceleration of the vehicle, since a driver has a direct control of this quantity through the gas and brake pedals. The researchers also observed that there is a high correlation between the response of a driver and the relative speed of his car and the one ahead. The stimulus was therefore selected as this relative speed. It was the question of sensitivity that the researchers focused on and this led to the development of a series of theories – each new one improving/modifying the previous one.

$$response = sensitivity \times stimulus \qquad [2\text{-}18]$$

Chandler, Herman and Montroll (1958) studied the traffic flow through the application of the theory of servomechanisms and network analysis. This analysis considers the role and interaction of the three components of the traffic system – road topology, vehicle characteristics and operator's behavior. Based on the experimental data available, they proposed that the acceleration at time t of a car which is attempting to follow a leader is proportional to the difference in velocity of the two cars at time (t – Δ).

$$\ddot{x}_{n+1}(t+\Delta) = \lambda[\dot{x}_n(t) - \dot{x}_{n+1}(t)] \qquad [2\text{-}19]$$

Their research yielded a value of about 1.5 sec for Δ, the time lag of the driver-car system and a value of about 0.37 sec^{-1} for the constant of proportionality. Thus they considered a constant sensitivity factor in their model. Further, they developed the conditions for stability of a traffic stream of vehicles following their proposed model.

Gazis, Herman and Potts (1959) subsequently attempted to derive Greenberg's macroscopic relationship describing speed and flow using the microscopic equation 2-19 as a starting point. The mismatch between the macroscopic relationship they obtained from the microscopic equation, and Greenberg's relationship, led to the hypothesis that the sensitivity term should be modified. In order to avoid the disparity, they proposed a sensitivity term which is inversely proportional to the distance headway.

$$\ddot{x}_{n+1}(t+\Delta) = \frac{\lambda_1}{\left[x_n(t) - x_{n+1}(t)\right]}[\dot{x}_n(t) - \dot{x}_{n+1}(t)] \qquad [2\text{-}20]$$

Field experiments were conducted to obtain the parameter values for λ_1 and Δ for test drivers on the General Motors test track. The significance of their research was that they established a bridge between the microscopic and macroscopic approaches.

Edie (1961) observed that although the models previously developed show a good fit to the experimental data, they become less and less realistic as the traffic becomes less and less dense. He explained this loss of realism to be because of the lack of an upper limit on stream velocity. In order to overcome this problem, he proposed a further refinement to the previous car-following model. It states that the sensitivity of a driver varies with his absolute velocity; the faster he is going, the greater is his sensitivity.

$$\ddot{x}_{n+1}(t+\Delta) = \frac{\lambda_2 . \dot{x}_{n+1}(t+\Delta)}{\left[x_n(t) - x_{n+1}(t)\right]^2}\left[\dot{x}_n(t) - \dot{x}_{n+1}(t)\right] \qquad [2\text{-}21]$$

This investigation by Edie was the first to propose that two separate relationships could be used in the description of traffic flow, one for non-congested (less density), and one for congested traffic (high density).

Closely analyzing the stimulus – response type of car-following theories developed till that time, Gazis, Herman and Rothery (1961) observed that the various sensitivity terms could be generalized with scaling factors for speed and distance headway. Thus, the car-following model, referred to as the GHR model, evolved into a non-linear form as below:

$$\ddot{x}_{n+1}(t+\Delta) = a\frac{\dot{x}^m_{n+1}(t+\Delta)}{\left[x_n(t) - x_{n+1}(t)\right]^l}\left[\dot{x}_n(t) - \dot{x}_{n+1}(t)\right] \qquad [2\text{-}22]$$

Utilizing the bridge between microscopic and macroscopic approaches, they derived the following macroscopic equation relating the steady-state speed of a traffic stream, *u* and the density, *k* by integrating Equation 2-22:

$$f_m(u) = cf_l(k) + c' \qquad [2\text{-}23]$$

Where, $f_p(x) = x^{1-p}$ $(p = m \text{ or } l \neq 1)$;

$f_p(x) = \ln x$ $(p = m \text{ or } l = 1)$;

c and c' = appropriate constants consistent with physical restrictions.

But, Nelson (1995) criticized the above deterministic development of traffic stream models from car-following models. He states that in traffic stream models, the three variables – speed, density and flow – are meaningful only if they are expressed as *mean* values relative to some distribution. "*Nonetheless, in the traffic flow literature there exist a number of developments of traffic stream models from car-following models, without any averaging process intervening between the deterministic car-following model and the supposedly resulting traffic stream model*". He justifies his statement on the basis that "the evaluation of the constant of integration for initial conditions corresponding to speed zero and headway equal to the reciprocal of jam density ignores large numbers of possibly relevant solutions of the underlying car-following model".

The study made by Newell (1961) differs from other previous models in that he lumped together the sensitivity and stimulus into a single function. He postulated that the velocity of n+1th car at time t, $u_{n+1}(t)$ is some non-linear function of the headway at time (t – Δ). He chose the non-linear function in such a way that it has the virtues of being physically reasonable and also of giving differential equations that can be solved explicitly at least

for $\Delta = 0$ as shown in Equation 2-24. He also showed that the selected model gives all results of the linear car-following theories in certain limiting cases and all the features of non-linear continuum theories in other cases. For example, an exact solution of the equation showed that a small amplitude disturbance propagates through a series of cars in the manner described by linear theories. Newell also noted that his theory had a number of serious deficiencies. It contains the implication that drivers follow one another under non-stationary conditions by adhering to the same velocity-headway relation they would choose under steady conditions. It had been found, for example, that if a lead driver travels at a constant velocity, then performs some maneuver, and returns to his original speed, a follower will not always reacquire the same headway that it had initially. Thus the relation between velocity and headway is not unique.

$$u_{n+1}(t) = u_f - u_f . e^{-\frac{\lambda_{n+1}\left[x_n(t-\Delta) - x_{n+1}(t-\Delta) - h_j\right]}{u_f}} \qquad [2\text{-}24]$$

Several investigations occurred during the following 20 years, in an attempt to define the 'best' combination of m and l in the GHR model. Among these the most notable are the following:

a) May and Keller (1967), using new data sets, found both optimal integer (m = 1, l = 3) and non-integer (m = 0.8, l = 2.8) solutions. The evaluation was based on minimizing the mean deviations of the data points from the determined regression curve. He explained that the introduction of non-integer exponents, m and l gives a more flexible adjustment to the evaluation criteria.

b) Heyes and Ashworth (1972) attempted to relate the generalized car-following (GHR) equation 2-22 to the perceptual models investigated by Michaels and Pipes (1967). They used the rate of change of visual angle as the trailing driver's stimulus instead of the relative speed between the lead and following vehicles. The sensitivity term was generalized to a function of time headway.

$$\ddot{x}_{n+1}(t+\Delta) = C\left[\frac{\dot{x}_{n+1}(t)}{x_n(t) - x_{n+1}(t)}\right]^P \left[\frac{\dot{x}_n(t) - \dot{x}_{n+1}(t)}{(x_n(t) - x_{n+1}(t))^2}\right] \qquad [2\text{-}25]$$

He deduced that the limiting values of the exponent P are 0 and 1. Using the data from the Mersey tunnel in UK, he evaluated the value of P to be 0.8.

c) Ceder and May (1976), using a far larger number of data sets than ever before, found an optimum of m = 0.6 and l = 2.4. However, their main advance was in acknowledging the 'two regime' approach that fitted the observed data better than using a single relationship. These relationships described behavior in the uncongested regime by the use of m = 0 and l = 3, and in congested conditions by m = 0 and l = 0 to 1.

d) Ceder (1976, 1978) proposed yet another modification to the GHR model. He felt that the sensitivity term in that equation is very complicated which makes it very

difficult to make a stability analysis. In order to overcome this problem, he proposed a new sensitivity function for the two-regimes.

$$\ddot{x}_{n+1}(t+\Delta) = \alpha \frac{A^{-\frac{h_j}{h_{n+1}(t)}}}{h_{n+1}^2(t)}\left[\dot{x}_n(t) - \dot{x}_{n+1}(t)\right] \qquad [2\text{-}26]$$

Where, A = non-dimensional weighing factor
= approximately 0 for free-flow;
= between 1 – 10 for congested conditions.
α = constant depending on A and h_j.

As it can be seen, a great deal of work has been performed on the calibration and validation of the generalized car-following equation 2-7. However, since the late 70's it has been investigated less and less frequently. This was attributed to the large number of contradictory findings as to the correct values of *m* and *l*.

2.3.2 Linear Models

In linear car-following theories, the acceleration of following vehicle is usually represented as a linear function of relative speed and/or spacing between lead and following vehicles. The model proposed by Chandler, Herman and Montroll, Equation 2-19, is of the linear form.

The linear form of models is usually attributed to Helly (1959). He proposed that the driver of the following vehicle will seek to minimize both the velocity difference, $(\dot{x}_n - \dot{x}_{n+1})$ and the difference between his actual headway and his desired headway (D), $(x_n - x_{n+1} - D)$. He also proposed to include additional terms for the adaptation of the acceleration according to whether the vehicle in front (and the vehicle two in front) was braking. He calibrated the constants using the data collected from 14 drivers. The combined control equation according him is:

$$\ddot{x}_{n+1}(t+\Delta) = C_1\left[\dot{x}_n(t) - \dot{x}_{n+1}(t)\right] + C_2\left[x_n(t) - x_{n+1}(t) - D_{n+1}(t)\right] + C_3 B_n + C_4 B_{n-1} \qquad \ldots. \quad [2\text{-}27]$$

Where, $D_{n+1}(t)$ = desired headway for vehicle $n+1$
$= \alpha + \beta\dot{x}_{n+1}(t) + \gamma\ddot{x}_{n+1}(t)$ for constants α, β and γ.
C_1, C_2, C_3 and C_4 = corresponding control parameters;
$B_p = 0$ if vehicle p if not braking
= 1 otherwise.

Lee (1966) proposed a generalized a linear car-following theory, in which he introduced a memory function to describe the relative speeds. He argued that the response of the follower vehicle depends not on what the relative speed was at a certain earlier instant, but rather on its time history. This, he mathematically represented as:

$$\ddot{x}_{n+1}(t) = \int_0^t M(t-t')\left[\dot{x}_{n-1}(t') - \dot{x}_n(t')\right]dt' \qquad [2\text{-}28]$$

Where, *M(t)* = Memory function.

Several examples of possible memory functions – Dirac-delta, decaying exponential, unitary square wave – were worked out. He showed that the linear form of models that were already developed were a special case of his generalized model.

Another linear model was proposed by Bekey, Burnham and Seo (1977) who attempted to derive a car-following model using traditional methods from the design of optimal control systems. Calibration was performed based on Ohio state aerial data.

2.3.3 Collision Avoidance models

With the increasing simplicity of usage of computers, simulation software packages have found widespread use in the traffic engineering community. In these packages, many realistic features have been added to the existing and newly developed models. These features include additional constraints on acceleration or deceleration of the vehicle to get practical results. Research in this direction began in the late fifties by Kometani et al. and later continued by Gipps and others.

Kometani and Sasaki (1959) proposed a car-following model in which the following vehicle driver seeks to maintain a safe following distance behind the lead vehicle. This safe distance would enable the following vehicle to avoid a collision with the lead vehicle if the driver of the vehicle in front were to act 'unpredictably'. Data for calibration of the proposed model were collected and the values for the parameters for which the best fit was obtained were fixed.

$$x_n(t-\Delta) - x_{n+1}(t-\Delta) = \alpha' u_n^2(t-\Delta) + \beta_l u_{n+1}^2(t) + \beta u_n(t) + b_0 \qquad [2\text{-}29]$$

The next major development of this model was made by Gipps (1981). He modeled the response of the following vehicle based on the assumption that each driver sets limits to his desired braking and acceleration rates. These limits enable the model to calculate a safe speed for the follower vehicle so that it can come to a safe stop if the vehicle ahead stops suddenly. The factors which he considered in the model are the 'safety' reaction time, maximum braking rate of lead vehicle and the maximum braking rate of the lead vehicle that the driver of the following vehicle believes is likely to be used. His model was of the following form:

$u_{n+1}(t+\Delta)$ = *min (desired speed constrained by the limit on acceleration, speed limited by braking to maintain a safe headway)* [2-30]

All the simulation models at present model the car following as an equation of motion under steady state conditions plus a number of constraints that govern the behavior of vehicles while moving from one steady state to another (decelerating and accelerating).

Various collision constraint models that are being implemented in simulation models are outlined in literature (Khan et al, 2000) and are listed below.

The collision constraint model of FRESIM assumes that the lead vehicle may decelerate to a stop at its maximum rate at the end of a time interval. After a reaction time, the follower vehicle may decelerate at a rate within the maximum deceleration rate (same as that of lead vehicle) so as to maintain a critical safe gap. This model assumes a constant velocity for the follower vehicle during the reaction time, thus making it inconsequential. Further, the critical safe gap used here does not contain a buffer distance.

The second drawback mentioned above was overcome in the CARSIM model where two specific constraints are used. The first ensures that a minimum separation distance is maintained during reaction time. The second constraint is the same as the one used in FRESIM, and hence ignores the reaction time.

A different kind of approach is used in INTELSIM. Here, a collision constraint is applied only if the lead vehicle is in deceleration and if the following vehicle's time to reach steady state is greater than the time it would take the lead vehicle to come to a complete stop. Thus in this model a safe distance may not be maintained.

In order to overcome the drawbacks of the above models, Khan et al proposed a correction. Instead of keeping the velocity of follower vehicle constant during the reaction time, they suggested to include a change in the velocity.

2.3.4 Other Models

Tolle (1974) developed a composite form of car-following model by combining four previously developed models. First he used the data collected by aerial photography to compare the four models – Chandler, Greenshields, Greenberg and Edie – and observed that Chandler and Greenberg models represent congested state better and the other two the non-congested state. Then, by using the inverse tangent function, he constructed models for congested and non-congested states separately. Chi-square tests were performed on these models but no good fits were obtained.

A distinct stage in the development of car-following models started with the use of fuzzy logic. Kikuchi and Chakroborty (1992) attempted to 'fuzzify' the traditional GHR model using Δx, Δv and a_{n-1} as inputs, and grouping these into 6,6, and 12 natural language based sets respectively. Each of these sets was taken to be triangular and the Δx set was scaled according to v_{n-1} in order to incorporate a measure of time headway. The consequence of their rule base is that vehicle 'n' will accelerate at the same rate as n-1, plus a small term to account for Δv and Δx. Each term from the fuzzy inference is of the form:

$$\text{IF } \Delta x = \text{'ADEQUATE' THEN } a_{n,i} = \frac{\Delta v_i + a_{n-1,i} xT}{\gamma} \qquad [2\text{-}31a]$$

Where,

T (=1) = reaction time;
γ (=2.5) = time in which the driver wishes to 'catch up' with vehicle n-1.

If $\Delta x \neq$ 'ADEQUATE', then the response is altered by sliding the membership function according to the degree of deviation from ADEQUATE. Thus,

$$a_{n,i} = \frac{\Delta v_i + a_{n-1,i} xT}{\gamma} + 0.3_{\Delta x} \quad [2\text{-}31b]$$

Van Aerde (1995) and Van Aerde and Rakha (1995) proposed a new model by amalgamating the car-following model that evolves from the Greenshields traffic stream model and the Pipes model into a four-parameter model:

$$h = c_1 + c_3 u + \frac{c_2}{u_f - u} \quad [2\text{-}32]$$

The first two parameters in the above equation provide the linear increase in vehicle speed as a function of the distance headway, while the third parameter introduces curvature to the model and ensures that the vehicle speed does not exceed the free speed. The variables c_1, c_2 and c_3 were related to the four traffic parameters – free speed (u_f), speed-at-capacity (u_c), capacity (q_c) and jam density (k_j) – by utilizing the various boundary conditions as follows:

$$c_1 = \frac{1}{k_j} - \frac{c_2}{u_f} \quad [2\text{-}32a]$$

$$c_2 = \frac{1}{k_j (m + \frac{1}{u_f})} \quad [2\text{-}32b]$$

$$c_3 = \frac{-c_1 + \frac{u_c}{q_c} - \frac{c_2}{u_f - u_c}}{u_c} \quad [2\text{-}32c]$$

$$\text{Where, } m = \frac{2u_c - u_f}{(u_f - u_c)^2} \quad [2\text{-}32d]$$

In an effort to achieve continuous acceleration profiles, Aycin and Benekohal (1998) proposed a linear acceleration car-following model. They introduced the use of preferred time headway to determine the separation during car-following. The model was validated at microscopic and macroscopic levels by using field data.

Cohen (2002) provided two modifications for the Pitt car-following model, which is a modified form of Pipes model which is implemented in FRESIM model. He studied the reaction time in the model and eliminated the requirement that it be less than the simulation time step. Through the second modification, he introduced a multiplicative factor that addresses the issues relating to over damping and dead band. He also

addressed the asynchronous nature in leader-follower relationship when applied to simulation models.

The other major area of work done in the area of car-following is the control theory based studies. These control theory based models include manual car-following laws which were explained in detail earlier, and automatic vehicle headway control laws in the recent ITS studies. Although having different objectives, both the manual car-following control and automatic vehicle headway control studies concentrate on the behavior of a following vehicle with respect to the changes of position and velocity of the vehicle ahead, accelerating to reach a desired speed or breaking to avoid collision.

The study of automatic headway control started in the 1970's and has been increasing rapidly in recent years, as the congestion and safety problems on highways nationwide are worsening year after year. Various automatic control laws were developed, which give different control strategies – from vehicle based control to infrastructure based control. The vehicle based control system uses the differences between the state of each vehicle and the state of its predecessor as the error signals for regulation. The infrastructure based control system uses the differences between the position and/or velocity of each vehicle and the corresponding position and/or velocity of a virtual reference point that moves along the roadway as its error signals.

Depending on the assumptions made regarding the key factors in the vehicle-roadway system, deterministic and stochastic headway control technologies have been proposed. These control models describe vehicle control process through the vehicle dynamic characteristics. Generally, they take a vehicle as an independent system or a platoon as an independent system and each vehicle within the platoon as a subsystem. The inputs of the system (or subsystem) are usually the speed and acceleration of the leading vehicle or the vehicle ahead, and the relative distance of a vehicle from the leading vehicle. The most likely outputs of the system are the speed and acceleration of the vehicle and its distance from the vehicle ahead. These usually form the feedback system, and the information used to feedback usually comes from the deviation of the desired distance and speed.

Two significant deterministic headway control models developed over the years are the PATH program and Multiple-Mode Vehicle Headway Control Model (MVHC Model). The PATH program, which is a vehicle based control system, assumes a platoon of *N* vehicles. Each vehicle within the platoon gets input only from the vehicle ahead of it. The general control law of the model is described briefly below.

Let Δ_i be the deviation of the i^{th} vehicle from its assigned position:

$$\Delta_i = x_{i-1} - x_i - L$$

Where, x_i is the position of the i^{th} vehicle and L is the average length of a vehicle.

The control laws for the linearized vehicle model were developed as :

$$c_i = c_p \Delta_i(t) + c_v \dot{\Delta}_i(t) + c_a \ddot{\Delta}_i(t) + k_v \left[v_{i-1}(t) - v_{i-1}(0) \right] + k_a a_{i-1}(t) \qquad [2\text{-}33]$$

Where, $v_{i-1}(0)$ denotes the initial state value of the (i-1)th vehicle's velocity and c_p, c_v, c_a, k_v and k_a are design constants. Then, using the Laplace transforms, the transfer functions of the control system used to describe the relationship between the input and output are obtained as follows:

$$h(s) = \frac{s^2 - k_a s - k_v}{s^3 + c_a s^2 + c_v s + c_p} \quad [2\text{-}34a]$$

$$g(s) = \frac{(c_a + k_a)s^2 + (c_v + k_v)s + c_p}{s^3 + c_a s^2 + c_v s + c_p} \quad [2\text{-}34b]$$

The design of the control system is to select a set of parameters to get a stable response curve for the system.

The Multiple-Mode Vehicle Headway Control Model (MVHC Model) is set up based on the work of manual driving process simulation. The model incorporates vehicle dynamics and roadway conditions in the control algorithms, and is suitable for mixed traffic flow on a rural highway. This model is established based on the following descriptions. A platoon consisting of *n* vehicles assumed to be traveling on an automated highway, which has a design speed, DS. A safety distance with respect to the vehicle ahead is assigned to each vehicle at any moment of its traveling, which is a function of the speed and deceleration capacity of the vehicle. For the sake of safety, a vehicle must keep sensoring the state changes of the vehicle ahead and comparing its control mode thresholds with the relative speed and relative distance with respect to the vehicle ahead. There are five control modes in the MVHC model – cruise control mode, following control mode, rapid deceleration mode, slowly deceleration mode and emergency braking mode. A vehicle will travel at the design speed if the spacing with respect to the vehicle ahead is equal to or greater than a first safe spacing threshold. If the spacing is less than the first safe spacing threshold, the controller will check with second threshold, relative speed and operating status of the vehicle ahead, and switch the control mode to another mode correspondingly.

2.4 Capacity and Discharge Headway at Signalized Intersections

In literature, car-following behavior has been viewed as a two-step process. In the first step, the steady-state behavior is calibrated followed by a calibration of the non-steady state behavior. The calibration of the steady-state behavior is critical because it dictates the maximum roadway throughput (capacity), the speed at which vehicles travel at different levels of congestion (traffic stream behavior), and the spatial extent of queues when fully stopped (jam density). Alternatively, the calibration of the non-steady state behavior, which in most cases is less critical, influences how vehicles move from one steady state to another. In rare instances, non-steady state behavior can dominate steady-state behavior. For example, vehicle dynamics may prevent a vehicle from attaining steady-state conditions. A typical example of such a case is the motion of a truck along a

significant upgrade section. In this case, the actual speed of the truck is less than the desired steady-state speed because the vehicle dynamics does not permit the vehicle from attaining its desired speed.

Such non-steady state conditions can be observed downstream of bottlenecks – such as at intersections and lane drops. Several different studies have been conducted to analyze the traffic flow at such bottleneck regions. Two such studies which are considered for further analysis in this thesis are capacity and discharge headway. The literature concerning these two topics is described below.

2.4.1 Capacity Drop

The question of whether or not the flow downstream of a freeway bottleneck decreases when congestion sets in has been the subject of much discussion and debate over the past several decades. Wattleworth (1963) put forward two conflicting theories about this capacity drop – one supporting it and another opposing. Several researchers felt that the reason for such state of affairs is the dearth of data. But even with additional data collected over years, the debate still rages on.

Many researchers like Edie (1961), Ceder and May (1976) and Payne (1984) tried to provide a justification for the capacity drop based on their findings of the flow-density curves obtained from their respective car-following models. According to them, congestion reduces capacity. This is represented by a parabolic flow-density curve, the upper left-hand portion showing operations under free-flow conditions and the negatively sloped lower part of the curve representing congested conditions.

An issue arising from the discussion on capacity drop is the lack of clarity about the place to look for capacity. HCM states that capacity should be measured where there is the existence of 'sufficient demand', but this qualification is not very clear. Sufficient demand may be possible in the presence or absence of a queue. Earlier capacity studies which did not take this into consideration are likely to be unreliable (Agyemang-Duah and Hall, 1991). Despite the fact that the place to take the measurement is critical for capacity analysis, very little attention has been given to it in published work.

Agyemang-Duah and Hall (1991) collected fifty-two days of data on peak period traffic volume, occupancy and speed from a section of the Queen Elizabeth Way (QEW) in Ontario to investigate the possibility of a drop in capacity as a queue forms. They selected the site for capacity estimation in such a way that it was outside the influence of any ramps and/or weaving maneuvers and that a sufficient demand exists upstream of the bottleneck. Based on their study, they reported a drop of about 5% in capacity after the queue formed. Interestingly, Hall and Hall (1990) based on the study of the same bottleneck at QEW, concluded that queue formations had no effect on the flow rates but did affect observed speeds.

Banks (1990, 1991) studied the flow processes in the vicinity of a high-volume bottleneck on I-8 near Lake Murray Blvd.-70th S. interchange. Based on the data, he

supported the hypothesis that maximum flow rates decrease when queues form. But simultaneously, he left the question of why queue formation leads to reduction in maximum flow rate unanswered. He thought that this phenomenon might be related to the lag times in traffic flows usually incorporated by car-following models.

To put to rest all the questions about the capacity issue, Cassidy and Bertini (1999) observed data from two freeway bottlenecks in and near Toronto, Canada. They argued that the methods used to process measured data by earlier researchers were flawed in that they used a time-series plots of flow, which do not always reveal important traffic features. Their results showed that the discharge flows from the bottlenecks always followed a particular order – a period of low flow, followed by a high discharge flow, always accompanied by the onset of upstream queues. However, the average of such discharge flows was 'nearly' constant in their studies. In addition, they observed that this average discharge flow was roughly 10% lower than the flow measured prior to the queue's formation.

Many other researchers like Newman, Persaud and Hurdle also conducted studies on this issue. But, even with so many studies and analysis, the issue of capacity drop still remains a contentious one. Perhaps, the whole problem may be summed up in a statement by Wattleworth (1963): "Perhaps, the question did not have a simple yes or no answer".

2.4.2 Discharge Headway

The discharge or entering headway, that is, the time between successive stopped vehicles entering a signalized intersection after the signal turns green, is of fundamental importance to traffic engineers. The values of several important parameters regarding signalized intersection operation – such as saturation flow rate, starting delay and lost time – are often derivatives of measurements of the entering headway. Many studies have been conducted to understand the nature of discharge headways which date back to late forties.
Greenshields et al. (1947) used a camera to study the traffic flow behavior at intersections in New York City and Connecticut. Theirs was one of the earliest efforts to quantify to quantify discharge headway on intersection approaches. Their data indicated that an average of 3.8 sec was necessary for the first stopped vehicle to enter the intersection after the traffic signal turned green. The successive mean headways for the following vehicles were found to be 3.1, 2.7, 2.4, 2.2 and 2.1 sec.

Similar studies were carried out by Gerlough and Wanger (1967), Carstens (1971) and many others. Their results were also similar to the ones obtained by Greenshields. The common thread among all these studies was that the discharge headways are initially large but eventually they converge to a minimum discharge headway. This basic trend of convergence to a constant value was recognized in the 1985 Highway Capacity Manual (HCM), which suggested that the constant headway is reached by the fifth queue position.

Lee and Chen (1986) conducted studies in Lawrence, Kansas with an aim to measure discharge headways in a small city. They studied the effect of following six factors on the discharge headways – signal type, time of day, vehicles in inside and outside lanes, vehicles approaching intersection with lower speeds, vehicles entering intersection from smaller roads and longer queue lengths. However, they concluded that because of data limitations, their findings can be viewed only as preliminary.

Bonneson (1992) proposed a deterministic model to describe the discharge headways at signalized intersections. The model was based on vehicle and driver capabilities, including driver reaction time, driver acceleration and vehicle speed. His proposed model has the following form:

$$h_n = \tau \times N_1 + T + \frac{d}{V_{\max}} + \frac{V_{s1(n)} - V_{s1(n-1)}}{A_{\max}} \qquad [2\text{-}35]$$

Where, h_n = headway of the n^{th} queued vehicle,
T = driver starting response time,
τ = additional response time of the first queued driver,
N_1= 1 if n = 1 or 0 if n > 1,
d = distance between vehicles in a stopped queue,
$V_{s1(n)}$ = stop line speed of n^{th} queued vehicle,
V_{max} = maximum speed,
A_{max} = maximum acceleration.

The first two terms in the above equation represent the time increment measured from the beginning of the signal phase to the instant when the driver first begins motion. The next two terms represent the time needed to accelerate over the distance between the stopped vehicle and the stop line. This model was calibrated using data from signalized intersections. The results of this model show that the discharge headway becomes constant only after the eighth or higher queue position.

Cohen (2002), after suggesting two modifications to the existing Pitt car-following model (as described previously), applied the modified model in a spreadsheet simulation to see the effect on discharge headways. In order to assess the consequence of using a car-following model to describe the queue discharges, he considered several scenarios – variation of free-flow speed, increase the length of vehicle, introduction of a truck in different queue position, introduction of a turning vehicle in different queue position, etc. He concluded that the Pitt model has a far wider range of applicability than the simple equal headway model.

2.5 Conclusions

A study of the literature reveals that much work has been done in the fields of car-following and traffic stream modeling. But the research is lacking in a comparative analysis of different possible formulation – especially speed and acceleration as control

variables. The present work aims at achieving this goal and in doing so, encompasses the various practical issues that should be considered in simulation modeling.

Further, though an extensive study and analysis is going on for decades on the issue of capacity of a roadway after queue formation, no definite conclusion has been reached. Little effort has been paid to address this problem by using the car-following models used in simulation models. This research effort tries to tackle the issue using state-of-the-art car-following models and also analyzes the discharge headways of vehicles entering an intersection using the models.

CHAPTER THREE:

CAR FOLLOWING MODELS: FORMULATION ISSUES AND PRACTICAL CONSIDERATIONS

3.1 Introduction

Microscopic simulation software uses car-following models to capture the interaction of a vehicle and the preceding vehicle traveling in the same lane. The process of car-following should be modeled as an equation of motion under steady-state conditions plus a number of constraints that govern the behavior of vehicles while moving from one steady state to another (decelerating and accelerating). The first constraint governs the vehicle acceleration behavior, which is typically a function of the vehicle dynamics. The second and final constraint ensures that vehicles maintain a safe position relative to the lead vehicle in order to ensure asymptotic stability within the traffic stream. Consequently, the calibration of the car-following behavior within microscopic simulation software can be viewed as a two-step process. In the first step, the steady-state behavior is calibrated followed by a calibration of the non-steady state behavior.

Many different formulation and models have been presented in literature concerning the steady-state behavior of traffic. This chapter selects four of the models based on their great significance attached to them over the years. For each of these four models, two different possible formulations have been considered – speed and acceleration as control variable. It should be noted that the literature points out these approaches. But the significance of presenting them again in this chapter is to provide a smooth transition for presenting a new form of acceleration formulation. This formulation utilizes the fluid condition of traffic as considered by Greenberg.

The non-steady state behavior of traffic modeling is accomplished by using two constraints – acceleration and collision avoidance. This chapter puts together the approaches proposed in literature for these constraints and presents a comprehensive car-following behavior formulation. This formulation is used to compare the two approaches to car-following presented in this paper – speed and acceleration as control variables.

This chapter first presents the link between car-following and traffic stream modeling and utilizes this to present both the formulations for the four selected models. Then, the formulation and practical issues to be considered while modeling the car-following in simulation are described. Finally, the different approaches are compared and conclusions provided at the end.

3.1.1 Link between Car-following and Traffic Stream Models

Microscopic car-following models characterize the relationship between a vehicle's desired speed and the distance headway (h) between the lead and follower vehicles.

Alternatively, the more common representation of car-following behavior is to characterize the vehicle's desired acceleration and the speed differential between the lead and following vehicles. Specifically, Drew (1968) suggests *"the car-following laws are simplified descriptions of a very complicated response to the world of stimuli that confronts a driver. In fact, only two stimuli are considered: the relative speed between a vehicle and the one ahead and the spacing between the two vehicles. Obviously a driver considers more. Considerable realism can be achieved by including several vehicles ahead of and perhaps the vehicle immediately behind the driver. Most drivers are continually evaluating several gaps ahead and are extremely conscious of the proximity of the car behind."*

State-of-practice car-following models are typically modeled as a closed-loop control system, where the vehicle acceleration is the control variable, the speed differential between the lead and follower vehicle is the stimulus, and the driver sensitivity is a constant parameter or may vary as a function of the vehicle speed and the distance headway between the lead and following vehicle. This approach considers the discrete nature of traffic stream, as will be discussed later.

Alternatively, traffic stream models describe the motion of a traffic stream by approximating for the flow of a continuous compressible fluid. The traffic stream models relate three traffic stream variables, namely: the traffic stream flow rate, traffic stream density, and traffic stream space-mean-speed. Consequently, the macroscopic and microscopic traffic models can be related to each other by establishing the relationship between these microscopic and macroscopic parameters that feed into each of the respective models. Specifically, considering a relatively long analysis period (T_0), the duration of the analysis period can be approximated for the summation of the time headways of successive vehicles within the analysis period, as demonstrated in Equation 1. Consequently, the flow rate can be expressed as the inverse of the average vehicle time headway "$\bar{s}$." Similarly, the traffic density can be approximated for the inverse of the average distance headway "*h*" for all vehicles within a section of roadway of length "*L*," as demonstrated in Equation 2.

$$T_0 \approx \sum_{i=1}^{r} s_i$$
$$q^{-1} = \frac{T_0}{r} \approx \frac{1}{r}\sum_{i=1}^{r} s_i \qquad \Rightarrow \; q^{-1} \approx \bar{s} \qquad [3\text{-}1]$$

$$L \approx \sum_{i=1}^{p} h_i$$
$$k^{-1} = \frac{L}{p} \approx \frac{1}{p}\sum_{i=1}^{p} h_i \qquad \Rightarrow \; k^{-1} \approx \bar{h} \qquad [3\text{-}2]$$

Where:
T_0 = Duration of analysis period (h)
s_i = Time headway between vehicle "i" and vehicle "i-1" (h)
r = Number of vehicles passing a point at any location "x" over the analysis period "T_0"
L = Length of roadway section (km)

h_l = Distance headway between vehicle "l" and vehicle "l-1" (km)
p = Number of vehicles observed along the analysis section "L" and any instant "t"
q = Flow rate at location "x" over period "T_0" (veh/h)
k = Traffic stream density over a roadway section of length "L" (veh/km)
$\bar{s}, \bar{h}$ = Average time and distance headway between successive vehicles, respectively.

Drew (1968) related microscopic car-following and macroscopic traffic stream models as follows: "*The similarities in the macroscopic and microscopic approaches have been emphasized. The former solves a differential equation of stream motion and a differential equation of continuity, both expressed in terms of speed "u" and density "k" to obtain an equation of state (the equation of the fundamental q-u-k traffic surface). The latter combines the differential equation of motion for an individual vehicle together with the appropriate boundary conditions to obtain an equation of state*."

3.1.2 Standard Car-Following Notation

This section describes a comprehensive set of notations and definitions used to represent car-following between two vehicles. The notations are summarized in Figure 3-1. Two vehicles are moving from left to right with vehicle n as the lead vehicle and having a length of L_n and vehicle $n+1$ as the following vehicle and having a length of L_{n+1}. The distance positions, speeds and acceleration (or deceleration) rates are denoted as x, $\dot{x}$, $\ddot{x}$ respectively. Since the vehicles change positions, speeds and acceleration (or deceleration) rates over time, the subscript t is used to specify time.

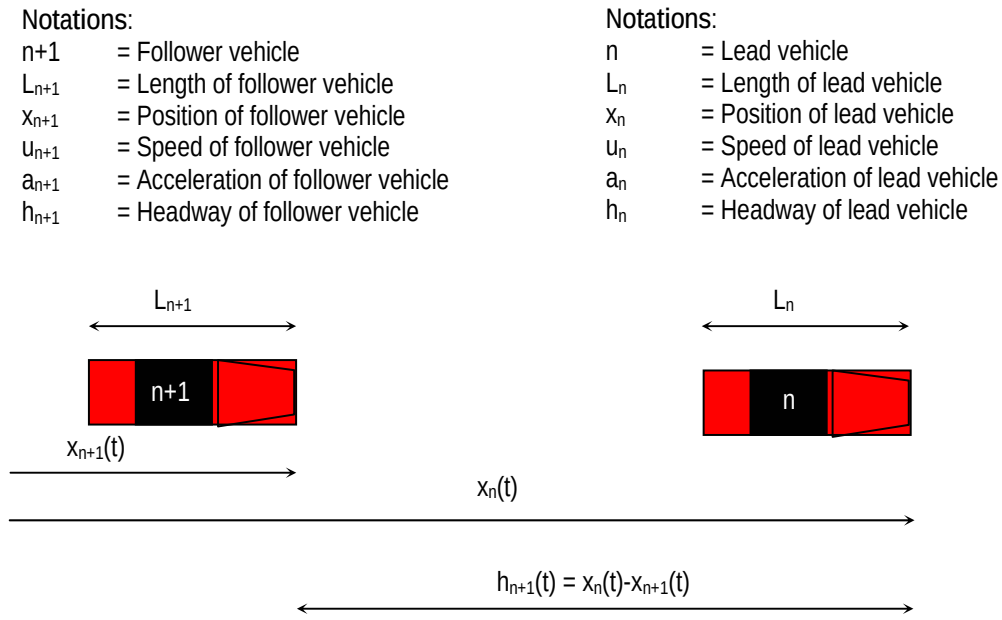

Figure 3-1: Car-Following Notations and Definitions

3.1.3 Illustrative Example

As has been already mentioned, this thesis compares the four selected car-following models along with demonstrating other things. In order to facilitate this comparison, a simple example illustration is considered using a lead vehicle profile, as illustrated in Figure 3-2.

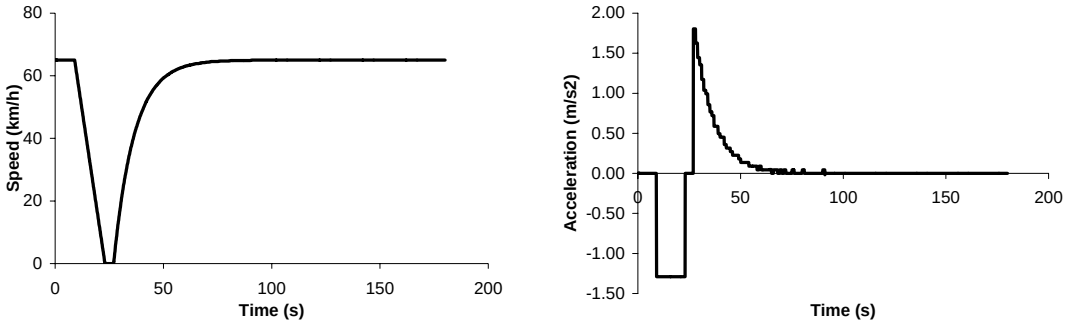

Figure 3-2: Example Lead Vehicle Speed and Acceleration Profile

3.2 Overview of Selected Models

As can be seen from Chapter 2, a number of car-following and traffic stream models have been proposed and described in the literature. Among the various models, those developed by researchers at General Motors Research Laboratory, Greenshields, Pipes and Greenberg have received the greatest attention over the years. Consequently, this thesis focuses on these specific car-following models in addition to a model proposed by Van Aerde (1995) and Van Aerde and Rakha (1995).

This section describes in detail, the four selected car-following models – Pipes, Greenshields, Greenberg and Van Aerde models. Utilizing the link between car-following and traffic stream models, as illustrated in section 3.1.1, the corresponding traffic stream formulations are developed for each of the four car-following models. Specifically, two car-following formulations – speed expressed as a function of distance headway and acceleration expressed as a function of the speed differential – for each of the four selected models are listed below as developed in the literature.

3.2.1 Pipes or GM – 1 Car Following Model

The car-following models developed by GM are stimulus-response models of car-following behavior that assume that the following vehicle responds to the relative speed (known as the stimulus) between it and the lead vehicle by accelerating or decelerating (response) depending on a driver sensitivity factor. All GM models assumed a time lag between the stimulus and the driver response, which is equal to the driver reaction time (T).

The first GM model (GM-1 model) assumed a constant driver sensitivity factor, as demonstrated in Equation 3. The equation characterized the driver response (acceleration at time "*t*") as the product of the driver sensitivity factor and the speed differential between the vehicle and the vehicle preceding it "*T*" seconds earlier (time *t-T*). Experiments were conducted on the GM test track in order to quantify typical driver reaction times and sensitivity factors. The studies estimated an average reaction time of 1.55 seconds that ranged from 1.0 to 2.2 seconds and an average driver sensitivity factor of 0.37 s^{-1} that ranged from 0.17 to 0.74, as presented in the literature (May, 1990).

By integrating Equation 3 and using the limiting condition that the vehicle speed is zero at jam density, Equation 4 can be derived. Equation 4 characterizes the motion of the following vehicle using the vehicle speed as the control variable and the distance headway as the stimulus. By imposing a constraint on the maximum vehicle speed, Equation 5 can be derived to reflect driver behavior more accurately. Equation 5 constitutes the Pipes car-following model, which is currently implemented as the steady-state car-following model in a number of simulation software, including the FRESIM and VISSIM models, as demonstrated by Rakha and Crowther (2002). By expanding Equation 5 to consider a stream of vehicles that maintain an average desired headway ($\bar{h}$), Equation 6 can be derived to reflect the traffic stream model that is associated with the Pipes car-following model.

$$a_{n+1}(t) = \lambda\left(u_n(t-T) - u_{n+1}(t-T)\right) \quad [3\text{-}3]$$

$$u_{n+1}(t) = \lambda\left(x_n(t-T) - x_{n+1}(t-T) - h_j\right) \quad [3\text{-}4]$$

$$u_{n+1}(t) = \min\left\{\lambda\left(x_n(t-T) - x_{n+1}(t-T) - h_j\right), u_f\right\} \quad [3\text{-}5]$$

$$\bar{h} = h_j + \frac{\bar{u}}{\lambda} = h_j + c_3\bar{u} \quad \Rightarrow k = \frac{1}{\frac{1}{k_j} + c_3\bar{u}} \quad [3\text{-}6]$$

Where:
T = Perception reaction time (s)
λ = Driver sensitivity factor (1/s)
c_3 = Constant which is the inverse of the driver sensitivity factor (s)
$a_n(t)$ = Vehicle "n" acceleration at instant "t" (m/s^2)
$u_n(t)$ = Vehicle "n" speed at instant "t" (m/s)
$x_n(t)$ = Vehicle "n" position at instant "t" (m)
u_f = Roadway free-speed (m/s)
h_j = Jam density headway (m)
k_j = Jam density (veh/m)

Figure 3-3a illustrates the car-following model that is associated with Equation 5 superimposed on field collected minimum driver headways that were extracted from the literature (May, 1990). The figure clearly demonstrates that the assumption of a constant driver sensitivity factor does not reflect differences in driver behavior in the short headway and long headway regimes.

Over the 1950's four more forms of GM models were developed by researchers. They are detailed in the literature review chapter. All these models have the same form of stimulus-response type relationship. The final model in this series – GM 5 Model, also known as GHR model – represents the generalized form of all the earlier developed GM models:

$$\ddot{x}_{n+1}(t+\Delta) = a\frac{\dot{x}_{n+1}^{m}(t+\Delta)}{\left[x_n(t)-x_{n+1}(t)\right]^{l}}\left[\dot{x}_n(t)-\dot{x}_{n+1}(t)\right] \qquad [3\text{-}7]$$

Where:
l = FV – LV headway exponent;
m = FV speed exponent.

(a)

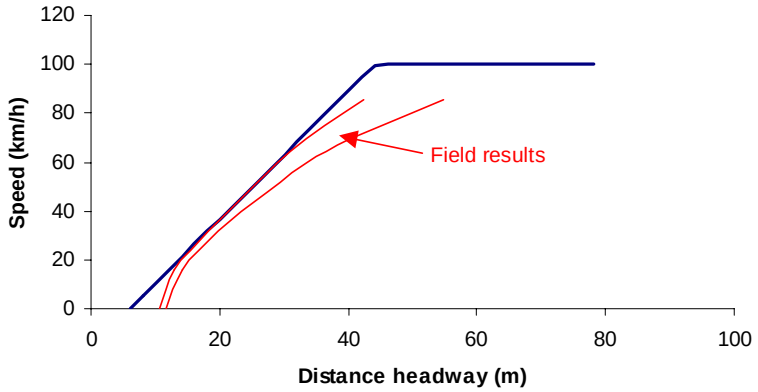

(b)

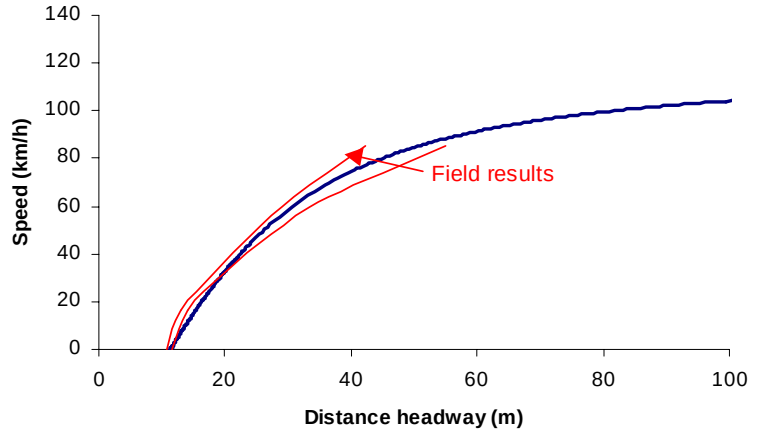

Figure 3-3: Typical Minimum Distance Headways (a) Pipes Model (b) Van Aerde Model

3.2.2 Greenshields Model

The first and most famous single-regime traffic stream model is the Greenshields model (Greenshields, 1935) that was developed in 1934 based on observations of speed-density measurements obtained from an aerial photographic study (May, 1990). Using these data, Greenshields concluded that the relationship between space-mean-speed ($\bar{u}$) and traffic density (k) is linear, as shown in Equation 8. Using the linear speed-density relationship together with the basic traffic stream model presented in Equation 9, the speed-flow relationship is represented as a parabolic relationship, as demonstrated in Equation 10. Equation 11 shows the speed-at-capacity that can be computed by taking the derivative of flow with respect to speed and setting it to zero, which is equal to half the free-speed. It should be noted that the calibration of the Greenshields model requires the estimation of two parameters, namely, the free-speed and either the roadway jam density or capacity.

$$\bar{u} = u_f - \frac{u_f}{k_j} k \qquad [3\text{-}8]$$

$$q = k\bar{u} \qquad [3\text{-}9]$$

$$q = \frac{k_j}{u_f}\left(u_f - \bar{u}\right)\bar{u} = k_j\left(\bar{u} - \frac{\bar{u}^2}{u_f}\right) \qquad [3\text{-}10]$$

$$\left.\frac{\partial q}{\partial u}\right|_{u_c} = 1 - \frac{2u_c}{u_f} = 0 \qquad \Rightarrow \quad u_c = \frac{u_f}{2} \qquad [3\text{-}11]$$

Using the basic Greenshields traffic stream model of Equation 8 and differentiating with respect to time, the vehicle acceleration can be derived, as demonstrated in Equation 12. Consequently, it can be observed that Equation 12 is a GM-5 car-following model with the FV speed exponent equal to 0 ($m = 0$) and the FV-LV headway exponent equal to 2 ($l = 2$). This derivation assumes that the various vehicles within the traffic stream can be assumed to travel at the space-mean-speed and considers the discrete, as opposed to the continuous nature of vehicles traveling within a traffic stream.

$$u = u_f\left[1 - \left(\frac{k}{k_j}\right)\right] = u_f\left[1 - \left(\frac{h_j}{\bar{h}}\right)\right]$$

$$\frac{du_{n+1}(t)}{dt} = -u_f \frac{d}{dt}\left(\frac{h_j}{\bar{h}}\right) = -u_f h_j \frac{d}{dt}\left(\frac{1}{x_n - x_{n+1}}\right) = u_f h_j \frac{u_n(t-T) - u_{n+1}(t-T)}{\left[x_n(t-T) - x_{n+1}(t-T)\right]^2} \qquad [3\text{-}12]$$

$$a_{n+1}(t) = \frac{u_f h_j}{h_{n+1}(t-T)^2}\left[u_n(t-T) - u_{n+1}(t-T)\right] = \frac{\alpha u_{n+1}(t)^0}{h_{n+1}(t-T)^2}\left[u_n - u_{n+1}\right]$$

$$a_{n+1}(t) = \left\{\frac{\alpha(2,0)\cdot u_{n+1}(t)^0}{h_{n+1}(t-T)^2}\right\}\cdot\left[u_n(t-T) - u_{n+1}(t-T)\right]$$

3.2.3 Greenberg Model

Greenberg (1959) used hydrodynamic analogy combining the equation of motion for a one-dimensional compressible fluid with a concentration "*k*" and a fluid velocity "*u*" (Equation 13) with the flow continuity equation (Equation 14) to derive a traffic stream model, as demonstrated in Equation 15. The details of how this traffic stream model was derived is described in depth because it serves as an initial step in deriving a generalized procedure for relating microscopic car-following and macroscopic traffic stream models as will be derived later.

$$\frac{du}{dt} = -\frac{c^2}{k}\frac{\partial k}{\partial x} \qquad [3\text{-}13]$$

$$\frac{\partial k}{\partial t} + \frac{\partial q}{\partial x} = 0 \qquad [3\text{-}14]$$

$$u = u_c \ln\left(\frac{k_j}{k}\right) \qquad [3\text{-}15]$$

Solving the equation of motion for a one-dimensional compressible fluid (Equation 13) together with the total derivative of speed (*u(x,t)*) assuming that the traffic flow is continuous in *x* and *t* (Equation 16), Equation 17 is derived. Given that the traffic stream speed is a function of the traffic stream density, Equations 18 and 19 can be derived where *u*' is the partial derivative of speed with respect to density. Substituting Equations 18 and 19 in Equation 17, Equation 20 can be derived.

$$\frac{du}{dt} = \frac{\partial u}{\partial x}\frac{dx}{dt} + \frac{\partial u}{\partial t}\frac{dt}{dt} \qquad [3\text{-}16]$$

$$\frac{\partial u}{\partial x}u + \frac{\partial u}{\partial t} + \frac{c^2}{k}\frac{\partial k}{\partial x} = 0 \qquad [3\text{-}17]$$

$$\frac{\partial u}{\partial x} = u'\frac{\partial k}{\partial x} \qquad [3\text{-}18]$$

$$\frac{\partial u}{\partial t} = u'\frac{\partial k}{\partial t} \qquad [3\text{-}19]$$

$$\frac{\partial k}{\partial t} + \left(u + \frac{c^2}{ku'}\right)\frac{\partial k}{\partial x} = 0 \qquad [3\text{-}20]$$

Alternatively, using the flow continuity equation (Equation 14) and the basic traffic stream equation (Equation 9), Equation 21 can be derived.

$$\frac{\partial k}{\partial t} + \left(u + ku'\right)\frac{\partial k}{\partial x} = 0 \qquad [3\text{-}21]$$

Solving Equations 20 and 21 simultaneously and assuming $\partial k/\partial x \neq 0$, Equation 22 is derived. Two solutions are possible for Equation 22, as demonstrated in Equation 23. The

negative solution is selected because it ensures that traffic stream speeds are positive in magnitude.

$$u + \frac{c^2}{ku'} = u + ku', \quad (\text{assuming } \partial k/\partial x \neq 0) \qquad [3\text{-}22]$$

$$u' = \frac{du}{dk} = \pm\frac{c}{k} \qquad [3\text{-}23]$$

Solving the Differential Equation (DE) and using the limiting condition that the traffic stream speed is zero at jam density (u=0 at k=k_j), Equation 24 is derived. Furthermore, multiplying both sides of Equation 24 by the traffic stream density, Equation 25 provides the macroscopic traffic stream relationship between flow and density. Using the limiting condition that at capacity the partial derivative of flow with respect to density is zero (at k=k_c and $\partial q/\partial k$=0), the constant "c" is computed to equal the speed-at-capacity (u_c), as demonstrated in Equation 26. Finally, the macroscopic equation of traffic stream motion can be derived, as demonstrated earlier in Equation 15.

$$u = c\ln\left(\frac{k_j}{k}\right) \qquad [3\text{-}24]$$

$$q = kc\ln\left(\frac{k_j}{k}\right) \qquad [3\text{-}25]$$

$$\begin{aligned} 0 &= c\ln\left(\frac{k_j}{k_c}\right) + k_c c\left(\frac{k_c}{k_j}\left(-\frac{k_j}{k_c^2}\right)\right) \quad \Rightarrow k_c = \frac{k_j}{\exp(1)} = \frac{k_j}{e} \\ u_c &= c\ln\left(\frac{k_j}{k_c}\right) = c\ln(e) = c \end{aligned} \qquad [3\text{-}26]$$

The derivation of this relationship is presented here, because this derivation will be expanded to cover a wider range of traffic stream models, as will be demonstrated in the subsequent sections. Following same line of analysis as in Equation 12, a car-following model corresponding to the Greenberg traffic stream model can be derived as in Equation 27.

$$\begin{aligned} u &= u_c\ln\left(\frac{k_j}{k}\right) = u_c\ln\left(\frac{\bar{h}}{h_j}\right) \\ \frac{du_{n+1}(t)}{dt} &= u_c\frac{d}{dt}\left(\ln\left(\frac{\bar{h}}{h_j}\right)\right) = \frac{u_c}{h_j}\frac{d}{dt}\left(\ln\left(x_n - x_{n+1}\right)\right) = \frac{u_c}{h_j}\frac{u_n(t-T) - u_{n+1}(t-T)}{\left[x_n(t-T) - x_{n+1}(t-T)\right]} \\ a_{n+1}(t) &= \frac{u_c/h_j}{h_{n+1}(t-T)}\left[u_n(t-T) - u_{n+1}(t-T)\right] \\ a_{n+1}(t) &= \left\{\frac{\alpha(1,0)\cdot u_{n+1}(t)^0}{h_{n+1}(t-T)}\right\}\cdot\left[u_n(t-T) - u_{n+1}(t-T)\right] \end{aligned} \qquad [3\text{-}27]$$

Thus it can be demonstrated that the Greenberg traffic stream model was indeed a GM car-following model with l=1 and m=0 (GM-3 model).

3.2.4 Van Aerde Model

The functional form of the Van Aerde model (Van Aerde, 1995; Van Aerde and Rakha, 1995) combines the Greenshields and the GM-1 model (Pipes car-following model), as demonstrated in Equation 28 (Rakha and Crowther, 2002). This combination provides the functional form with four degrees of freedom as opposed to two degrees of freedom in the case of the Greenshields model and three degrees of freedom in the case of the Pipes model. Specifically, the first two parameters provide the linear increase in vehicle speed as a function of the distance headway, while the third parameter introduces curvature to the model and ensures that the vehicle speed does not exceed the free-speed. The Van Aerde single-regime model overcomes the main flaws of the Pipes and Greenshields models. Specifically, the model overcomes the shortcoming of the Pipes model, which assumes that vehicle speeds are insensitive to traffic density in the uncongested regime and does not reflect the variability in driver sensitivity factor as a function of the distance headway, as demonstrated in Figure 3-3. Alternatively, the model overcomes the main shortcoming of the Greenshields model, which assumes that the speed-flow relationship is parabolic and again is inconsistent with field data from a variety of facility types (Rakha and Crowther, 2002). Figure 3-3 demonstrates a close match between the model behavior and field data, thus demonstrating the ability of the model to reflect actual driving behavior.

$$h_{n+1}(t-T) = c_1 + c_3 u_{n+1}(t) + \frac{c_2}{u_f - u_{n+1}(t)} \qquad [3\text{-}28]$$

Where:
c_1 = fixed distance headway constant (km/veh),
c_2 = first variable distance headway constant (km^2/h-veh),
c_3 = second variable distance headway constant (h/veh), and
u_f = free-speed (km/h),

The traffic stream model associated with the Van Aerde car-following model can be derived by considering that the traffic stream density is approximately equal to the inverse of the average vehicle distance headway, as demonstrated earlier in Equation 2. Consequently, the traffic stream model is derived by substituting the density for the inverse of the mean distance headway and the space-mean-speed ($\bar{u}$) for the FV speed, as demonstrated in Equation 29. Furthermore, the speed-flow relationship can be derived by substituting the traffic density for the flow divided by the space-mean-speed, as demonstrated in Equation 30. The functional form is also constrained to ensure that the traffic stream density at any speed is less than or equal to the jam density (k_j), as demonstrated in Equation 31. This ensures that there are no inflection points in the traffic stream model.

$$k = \frac{1}{c_1 + \frac{c_2}{u_f - \overline{u}} + c_3\overline{u}} \quad [3\text{-}29]$$

$$q = \frac{\overline{u}}{c_1 + \frac{c_2}{u_f - \overline{u}} + c_3\overline{u}} \quad [3\text{-}30]$$

$$k \le k_j \quad [3\text{-}31]$$

Two boundary conditions exist. The first boundary condition is that the maximum flow rate (capacity) occurs at the speed-at-capacity when the derivative of the flow rate (q) with respect to the space-mean-speed ($\overline{u}$) is equal to zero. The second boundary condition is that at jam density, the traffic stream space-mean-speed is zero. Using these two boundary conditions, the model constants can be related to the four traffic stream parameters, namely, the free-speed (u_f), the speed-at-capacity (u_c), the capacity (q_c), and the jam density (k_j), as demonstrated in Equations 32 through 35.

$$c_1 = \frac{1}{k_j} - \frac{c_2}{u_f} \quad [3\text{-}32]$$

$$c_2 = \frac{1}{k_j\left(m + \frac{1}{u_f}\right)} \quad [3\text{-}33]$$

$$m = \frac{2u_c - u_f}{\left(u_f - u_c\right)^2} \quad [3\text{-}34]$$

$$c_3 = \frac{-c_1 + \frac{u_c}{q_c} - \frac{c_2}{u_f - u_c}}{u_c} \quad [3\text{-}35]$$

Where:
u_f = free-speed (km/h),
u_c = speed at capacity (km/h),
q_c = flow at capacity (veh/h),
k_j = jam density (veh/km), and
m = is a constant used to solve for the three headway constants (h/km).

Similar to what was done for the Greenshields, Greenberg, and Pipes models, the acceleration of the FV can be derived from the speed formulation, as demonstrated in Equation 36. Equation 36 demonstrates that the sensitivity factor within the Van Aerde model is inversely proportional to the distance headway between the LV and FV and is a function of the vehicle's speed. Furthermore, the sensitivity factor is a function of the facility traffic stream parameters, namely, the free-speed, speed-at-capacity, capacity, and

jam density. A comparison of the various car-following acceleration formulations will be discussed in further detail in the forthcoming section.

$$h_{n+1}(t-T) = c_1 + \frac{c_2}{u_f - u_{n+1}(t)} + c_3 u_{n+1}(t)$$

$$\frac{dh_{n+1}(t-T)}{dt} = u_n(t-T) - u_{n+1}(t-T) = \left[c_3 + \frac{c_2}{\left(u_f - u_{n+1}(t)\right)^2} \right] \frac{du_{n+1}(t)}{dt}$$

$$a_{n+1}(t) = \frac{1}{\left[c_3 + \frac{c_2}{\left(u_f - u_{n+1}(t)\right)^2} \right]} \left[u_n(t-T) - u_{n+1}(t-T) \right] \qquad [3\text{-}36]$$

$$a_{n+1}(t) = \left\{ \frac{u_f - u_{n+1}(t)}{c_3 (u_f - 2u_{n+1}(t)) - c_1 + h_{n+1}(t-T)} \right\} \cdot \left[u_n(t-T) - u_{n+1}(t-T) \right]$$

3.3 Formulation Issues

This section describes the two possible formulations of car following behavior. The first formulation considers the vehicle acceleration as the control variable (most commonly documented in the literature), while the second formulation considers the vehicle speed as the control variable. Both formulations are described in detail and the practical considerations that are required to successfully implement these formulations are discussed in the next section.

The description of car-following models in the literature tends to ignore that simulation software move vehicles at discrete time steps (Δt), which are typically set at a deci-second or a second level of resolution. In order to account for this effect, predicted headway, $\tilde{h}$ is used instead of the headway term, h. As explained in the next section, the predicted headway $\tilde{h}$ is computed from Equation 37:

$$\tilde{h}_{n+1}(t-T) = h_{n+1}(t-T-\Delta t) + \left[u_n(t-T) - u_{n+1}(t-T-\Delta t) \right] \Delta t + 0.5 a_n(t-T) \Delta t^2 \qquad [3\text{-}37]$$

3.3.1 Speed Formulation

A number of car-following formulations consider the vehicle speed as the control variable and the distance headway as the stimulus. In some instances, the speed differential is also considered as a stimulus as will be described later.

Van Aerde Model

Using Equation 37 to estimate the distance headway at instant (*t-T*) the vehicle's desired speed can be estimated using the Van Aerde car-following functional form. This section describes how the vehicle speed is computed using the Van Aerde model that was demonstrated earlier and repeated again in Equation 38 incorporating the estimated distance headway of Equation 37. It should be noted that because the Van Aerde car-following model is not a linear function of the vehicle speed, the solution for the vehicle speed requires solving a quadratic equation, as demonstrated in Equations 39 and 40. It should be noted that only one of the roots is used, namely, the root that results in a vehicle speed less than the free-speed. As mentioned earlier, the calibration of the Van Aerde model requires estimating four facility specific parameters, namely, the free-speed (u_f), the speed-at-capacity (u_c), the capacity (q_c), and the jam density (k_j). It should be noted that the formulation that is presented in Equation 40 is implemented within the INTEGRATION software (Rakha and Ahn, 2003; Van Aerde & Assoc., Ltd 2003a and 2003b).

$$\tilde{h}_{n+1}(t-T) = c_1 + \frac{c_2}{u_f - \tilde{u}_{n+1}(t)} + c_3\tilde{u}_{n+1}(t) \quad [3\text{-}38]$$

$$c_3\tilde{u}^2_{n+1}(t) + \left[c_1 - c_3u_f - \tilde{h}_{n+1}(t-T)\right]\tilde{u}_{n+1}(t) + \left[\tilde{h}_{n+1}(t-T)u_f - c_1u_f - c_2\right] = 0 \quad [3\text{-}39]$$

$$\tilde{u}_{n+1}(t) = \frac{-c_1 + c_3u_f + \tilde{h}_{n+1}(t-T) - \sqrt{\left[c_1 - c_3u_f - \tilde{h}_{n+1}(t-T)\right]^2 - 4c_3\left[\tilde{h}_{n+1}(t-T)u_f - c_1u_f - c_2\right]}}{2c_3} \quad [3\text{-}40]$$

Greenshields, Greenberg, and Pipes Models

The solution for the vehicle speed using the Greenshields model requires a simple mathematical manipulation of the basic car-following model (Equation 41) to derive the control variable (speed) as a function of the vehicle's distance headway, as demonstrated in Equation 42. The calibration of the Greenshields model requires estimating two parameters, the free-speed and the constant c_2. The constant c_2 can be calibrated by estimating either the roadway jam density (k_j) or the roadway capacity (q_c), as demonstrated in Equation 43.

$$\tilde{h}_{n+1}(t-T) = \frac{c_2}{u_f - \tilde{u}_{n+1}(t)} \quad [3\text{-}41]$$

$$\tilde{u}_{n+1}(t) = u_f - \frac{c_2}{\tilde{h}_{n+1}(t-T)} \quad [3\text{-}42]$$

$$c_2 = h_ju_f = \frac{u_f}{k_j} = \frac{u_f^2}{4q_c} \quad [3\text{-}43]$$

Similarly, the Greenberg car-following model can be derived, as demonstrated in Equation 44, if we replace the vehicle headway for the inverse of traffic density in the Greenberg traffic stream model. Consequently, the calibration of the Greenberg model requires the estimation of two roadway specific parameters, namely, the speed-at-capacity (u_c) and the jam density (k_j).

$$\widetilde{u}_{n+1}(t) = u_c \ln\left(\frac{\widetilde{h}_{n+1}(t-T)}{h_j}\right) = u_c \ln\left(k_j \cdot \widetilde{h}_{n+1}(t-T)\right) \quad [3\text{-}44]$$

Finally, the Pipes car-following model can be derived from the basic formulation of Equation 45 to be represented by Equation 46 by solving for the boundary condition that at jam density (headway = h_j) the vehicle speed is zero. It should be noted that Equation 46 ensures that the vehicle speed does not exceed the roadway free-speed. The derivation of the constant (c_3) was derived by Rakha and Crowther (2003) and is a function of three parameters, namely, the facility free-speed (u_f), jam density (k_j), and capacity (q_c), as demonstrated in Equation 47.

$$\widetilde{h}_{n+1}(t-T) = c_1 + c_3 \widetilde{u}_{n+1}(t) \quad [3\text{-}45]$$

$$\widetilde{u}_{n+1}(t) = \min\left\{\frac{1}{c_3}\cdot\left[\widetilde{h}_{n+1}(t-T) - h_j\right], u_f\right\} \quad [3\text{-}46]$$

$$c_3 = \frac{1}{q_c} - \frac{h_j}{u_f} = \frac{1}{q_c} - \frac{1}{k_j u_f} \quad [3\text{-}47]$$

In summary, the Van Aerde model requires the calibration of four facility-specific parameters (u_f, u_c, q_c and k_j), the Greenshields model requires the calibration of two parameters (u_f & k_j or u_f and q_c), the Greenberg model requires the calibration of two parameters (u_c and k_j), and the Pipes model requires the calibration of three parameters (u_f, k_j and q_c).

Range of Validity for Van Aerde Model

In the speed formulation of Van Aerde model, one has to evaluate a square root for solving the speed of the FV. The presence of this square root term in the speed formulation raises a question about the valid range for Van Aerde model. The aim of this section is to find out this valid range. The Van Aerde model will be invalid if the term under the square root becomes negative. Before proceeding to determine the valid range for Van Aerde model, first the term under square root, X is simplified as follows, in Equation 3-48.

$$\begin{aligned} X &= \left[c_1 - c_3 u_f - \widetilde{h}_{n+1}\right]^2 - 4c_3\left[\widetilde{h}_{n+1}u_f - c_1 u_f - c_2\right] \\ &= \left(c_1 - c_3 u_f\right)^2 + \widetilde{h}_{n+1}{}^2 - 2.(c_1 - c_3 u_f).\widetilde{h}_{n+1} - 4c_3 u_f.\widetilde{h}_{n+1} + 4c_1 c_3 u_f + 4c_2 c_3 \\ &= \widetilde{h}_{n+1}{}^2 + \widetilde{h}_{n+1}.\left[-2.c_1 + 2c_3 u_f - 4c_3 u_f\right] + c_1^2 + c_3^2 u_f^2 - 2c_1 c_3 u_f + 4c_1 c_3 u_f + 4c_2 c_3 \end{aligned}$$

$$= \widetilde{h}_{n+1}{}^2 + \widetilde{h}_{n+1}.\left[-2.c_1 - 2c_3u_f\right] + c_1^2 + c_3^2u_f^2 + 2c_1c_3u_f + 4c_2c_3$$
$$= \widetilde{h}_{n+1}{}^2 - 2.\widetilde{h}_{n+1}.\left[c_1 + c_3u_f\right] + \left(c_1 + c_3u_f\right)^2 + 4c_2c_3$$
$$= \left[\widetilde{h}_{n+1} - \left(c_1 + c_3u_f\right)\right]^2 + 4c_2c_3 \qquad [3\text{-}48]$$

In the above simplified form of *X*, the first term is perfect square and hence is always greater than or equal to zero. The other term, $4c_2c_3$ can be either positive or negative depending on the values of c_2 and c_3. So, X can be negative if

$$4c_2c_3 < 0 \text{ and } -4c_2c_3 > \left[\widetilde{h}_{n+1} - \left(c_1 + c_3u_f\right)\right]^2 \qquad [3\text{-}49]$$

If we express the values of c_1, c_2 and c_3 in terms of the four roadway parameters – u_f, u_c, k_j and q_c – a better analysis can be done to find out when they are negative. The next Equation 3-50 expresses c_1, c_2 and c_3 in such a manner. From that, we can see that c_2 is always positive whereas c_3 can turn out to be negative and hence $4c_2c_3$ can be negative if $\frac{1}{q_c} < \frac{u_f}{k_j.u_c^2}$.

$$c_1 = \frac{u_f}{k_j.u_c^2}.(2u_c - u_f)$$
$$c_2 = \frac{u_f}{k_j.u_c^2}.(u_f - u_c)^2 \qquad [3\text{-}50]$$
$$c_3 = \frac{1}{q_c} - \frac{u_f}{k_j.u_c^2}$$

So, it would be sufficient to do the analysis only for the range in which c_3 is negative. If c_3 is negative, in order for X to be still positive, the headway should not lie within a certain range. This is determined as follows in Equation 3-51.

If $c_3 < 0 \Rightarrow q_c > \frac{k_j u_c^2}{u_f}$; in order for $X \geq 0$,

$$\widetilde{h}_{n+1} \notin \left(c_1 + c_3u_f - \sqrt{-4c_2c_3}, c_1 + c_3u_f + \sqrt{-4c_2c_3}\right) \qquad [3\text{-}51]$$

Since $c_3 < 0$, let $c_4 = -c_3$

So,

$$\widetilde{h}_{n+1} \notin \left(c_1 - c_4u_f - \sqrt{4c_2c_4}, c_1 - c_4u_f + \sqrt{4c_2c_4}\right)$$

Next the aim is to find the maximum possible value of $Y = c_1 - c_4 u_f + \sqrt{4c_2 c_4}$ for all the possible values of roadway parameters. This can be performed by utilizing the concept of differential calculus. The maximum/minimum value of Y can be obtained by equating the first differential of Y with respect to c_4 to zero.

$$\frac{\partial Y}{\partial c_4} = 0 \Rightarrow -u_f + \sqrt{\frac{c_2}{c_4}} = 0$$

So, Y can have its maximum or minimum value at $c_4 = \frac{c_2}{u_f^2}$. Further, if the second differential of Y w.r.t. c_4 at the above calculated value of c_4 turns out to be negative, then Y has the maximum value at $c_4 = \frac{c_2}{u_f^2}$.

$\left.\frac{\partial^2 Y}{\partial^2 c_4}\right|_{c_4=\frac{c_2}{u_f^2}} = -\frac{1}{c_4}\sqrt{\frac{c_2}{c_4}}\Bigg|_{c_4=\frac{c_2}{u_f^2}} = -\frac{u_f^3}{c_2}$ is -ve. Hence Y has a maximum value at $c_4 = \frac{c_2}{u_f^2}$.

So,

$$Y_{\max} = c_1 - \frac{c_2}{u_f^2}u_f + \sqrt{4c_2 . \frac{c_2}{u_f^2}}$$

$$Y_{\max} = c_1 - \frac{c_2}{u_f} + 2\frac{c_2}{u_f} = c_1 + \frac{c_2}{u_f}$$

$$Y_{\max} = \frac{u_f}{k_j . u_c^2}.(2u_c - u_f) + \frac{1}{u_f}.\frac{u_f}{k_j . u_c^2}.(u_f - u_c)^2 \qquad [3\text{-}52]$$

$$Y_{\max} = \frac{1}{k_j . u_c^2}.\left[2u_c u_f - u_f^2 + (u_f - u_c)^2\right]$$

$$Y_{\max} = \frac{1}{k_j . u_c^2}.\left[u_c^2\right] = h_j$$

Using Equation 3-52, the Equation 3-51 turns out to be as follows:

If $c_3 < 0 \Rightarrow q_c > \frac{k_j u_c^2}{u_f}$; in order for $X \geq 0$,

$$\widetilde{h}_{n+1} \notin \left(c_1 + c_3 u_f - \sqrt{-4c_2 c_3}, h_j\right) \qquad [3\text{-}53]$$

Since $\tilde{h}_{n+1} \geq h_j$, $\tilde{h}_{n+1}$ will never lie in the range prescribed in Equation 3-53. So, X is always positive and hence the Van Aerde model is valid for all ranges of headways and speeds as long as $\tilde{h}_{n+1} \geq h_j$. So, in order to implement Van Aerde model in simulation software, the condition that $\tilde{h}_{n+1} \geq h_j$ should be checked at every simulation time step. This results in a lot of computational inefficiency. This can be overcome by rephrasing this condition as follows in Equation 3-54.

$$\tilde{h}_{n+1} \geq h_j$$

$$\Rightarrow c_1 + \frac{c_2}{u_f - \tilde{u}_{n+1}} + c_3\tilde{u}_{n+1} \geq c_1 + \frac{c_2}{u_f}$$

$$\Rightarrow c_3\tilde{u}_{n+1} \geq \frac{c_2}{u_f} - \frac{c_2}{u_f - \tilde{u}_{n+1}} \quad [3\text{-}54]$$

$$\Rightarrow c_3\tilde{u}_{n+1} \geq -\frac{c_2.\tilde{u}_{n+1}}{u_f.\left(u_f - \tilde{u}_{n+1}\right)}$$

$$\Rightarrow c_3 \geq -\frac{c_2}{u_f.\left(u_f - \tilde{u}_{n+1}\right)}$$

Since the speed of vehicles range from 0 to free-flow speed, the maximum value of RHS in the above equation will be obtained for the speed being zero.

$$\Rightarrow c_3 \geq -\frac{c_2}{u_f^2}$$

$$\Rightarrow \frac{1}{q_c} - \frac{u_f}{k_j.u_c^2} \geq -\frac{1}{u_f^2}.\frac{u_f}{k_j.u_c^2}.(u_f - u_c)^2 \quad [3\text{-}55]$$

$$\Rightarrow \frac{1}{q_c} \geq \frac{u_f}{k_j.u_c^2}.\left[1 - \frac{(u_f - u_c)^2}{u_f^2}\right]$$

So, if this above condition in Equation 3-55 is met, then the Van Aerde model is valid for all values of headways and speeds of FV.

3.3.2 Acceleration Formulation

The literature typically presents car-following models in a similar fashion to the GM model formulation, namely, a control variable (vehicle acceleration) equal to a driver sensitivity factor multiplied by a stimulus (speed differential between lead and follower

vehicles). The derivation of the acceleration formulation can be done using two approaches. The first approach considers the discrete nature of traffic and thus recognizes that the partial derivative of headway or density with respect to the vehicle position is not a continuous function. The second approach considers the flow of the traffic stream similar to the flow of a compressible fluid, thus the traffic density is a function of both time and location along the roadway (i.e. $k = k(x,t)$). This section describes how the acceleration formulation of car-following models can be derived using both approaches. Furthermore, both approaches are compared to demonstrate similarities and differences in the car-following behavior that result from both formulations.

Molecular Approach

Considering the discrete nature of traffic along the roadway, it is possible to replace the distance headway between two vehicles as the difference in vehicle positions i.e.

$$h_{n+1}(t) = x_n(t) - x_{n+1}(t) \qquad [3\text{-}56]$$

Specifically, Equation 36 derives the molecular acceleration formulation of the Van Aerde model. The formulation is presented again in Equation 57 except that the distance headway is replaced for the projected distance headway of Equation 37 in order to reflect the sequence of vehicle movements within a traffic simulation environment. Similarly, the molecular formulations for the Greenshields, Greenberg, and Pipes models are presented in Equations 58, 59, and 60, respectively. In all formulations, the stimulus term (speed differential between lead and following vehicles) is presented in brackets, while the driver sensitivity term is presented in braces. It is evident from Equation 57 through 60 that the Van Aerde model offers a much more sophisticated driver sensitivity factor that is not only dependent on the facility type but also on the speed of the FV and distance headway between the LV and FV.

$$a_{n+1}(t) = \left\{ \frac{u_f - u_{n+1}(t)}{c_3(u_f - 2u_{n+1}(t)) - c_1 + \tilde{h}_{n+1}(t-T)} \right\} \cdot \left[u_n(t-T) - u_{n+1}(t-T) \right] \qquad [3\text{-}57]$$

$$a_{n+1}(t) = \left\{ \frac{c_2}{\tilde{h}_{n+1}(t-T)^2} \right\} \cdot \left[u_n(t-T) - u_{n+1}(t-T) \right] \qquad [3\text{-}58]$$

$$a_{n+1}(t) = \left\{ \frac{u_c}{\tilde{h}_{n+1}(t-T)} \right\} \cdot \left[u_n(t-T) - u_{n+1}(t-T) \right] \qquad [3\text{-}59]$$

$$a_{n+1}(t) = \left\{ \frac{1}{c_3} \right\} \cdot \left[u_n(t-T) - u_{n+1}(t-T) \right] \qquad [3\text{-}60]$$

The variation in driver sensitivity factor for a number of facilities including freeway and arterial roadways were compared. Figure 3-4 and Figure 3-5 illustrate the speed-flow, speed-density, flow-density, and speed-headway relationships for a sample freeway and

arterial roadway section, respectively. Figure 3-4 demonstrates a flat speed-flow relationship for the uncongested regime in the case of the freeway facility. However, Figure 3-5 demonstrates that this relationship is not the case for the arterial facility.

Figure 3-6 illustrates the variation in driver sensitivity factor for all four models as a function of the speed of FV for four different facility types. It should be noted that in computing the driver sensitivity factor, the steady-state distance headway was considered for the projected distance headway. The figure shows that the driver sensitivity factors for

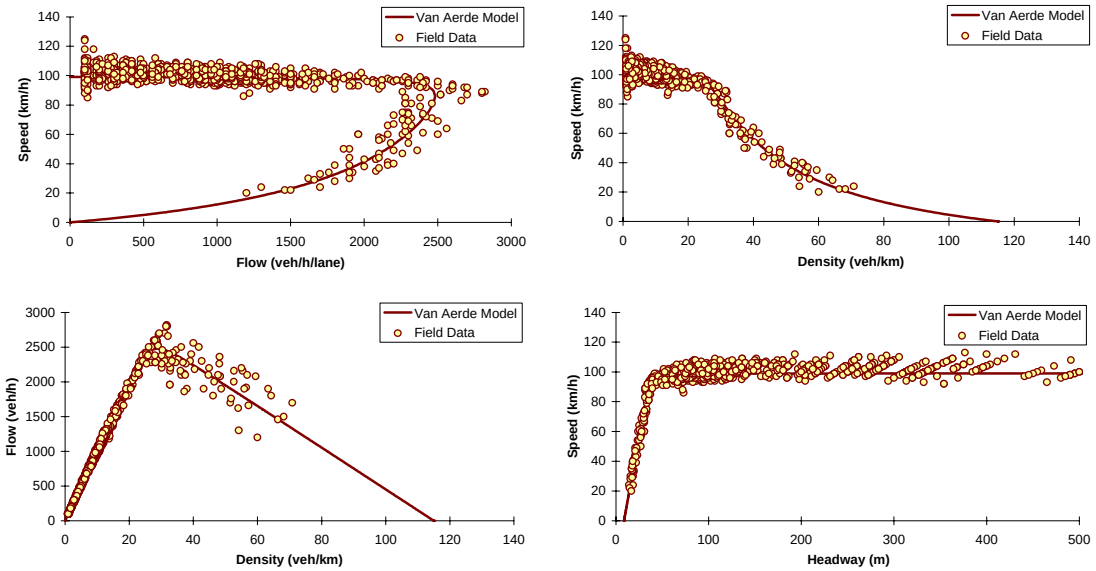

Figure 3-4: Example Illustration of Freeway Loop Data (Amsterdam Ring Road)

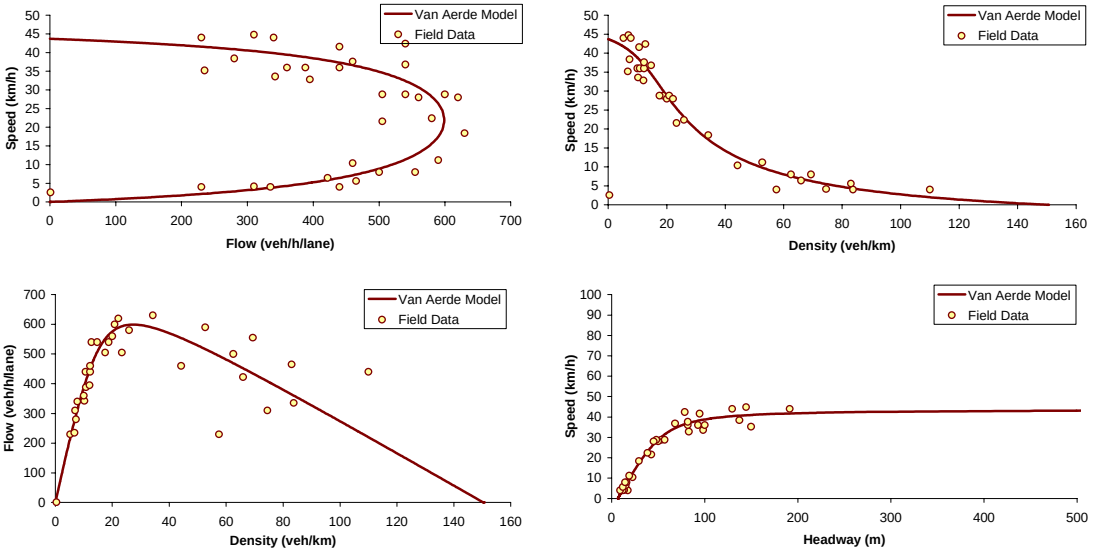

Figure 3-5: Example Illustration of Arterial Loop Data

Van Aerde and Greenshields models approach zero as the FV speed approaches the free speed, which means that for these two models, the FV acceleration tends to zero irrespective of the stimulus (speed differential). All models, except for the Pipes model, indicate that the FV is more sensitive to the speed differential stimulus at lower speeds versus higher speeds. The Van Aerde model demonstrates a relatively small variation in the FV sensitivity factor as a function of the vehicle speed in the case of a freeway facility with a speed limit (flat speed-flow relationship in the uncongested regime). Alternatively, the Greenshields and Greenberg models indicate a highly responsive sensitivity factor as a function of the FV speed. In the case of an arterial facility, the Van Aerde model demonstrates a more responsive sensitivity factor compared to a freeway facility.

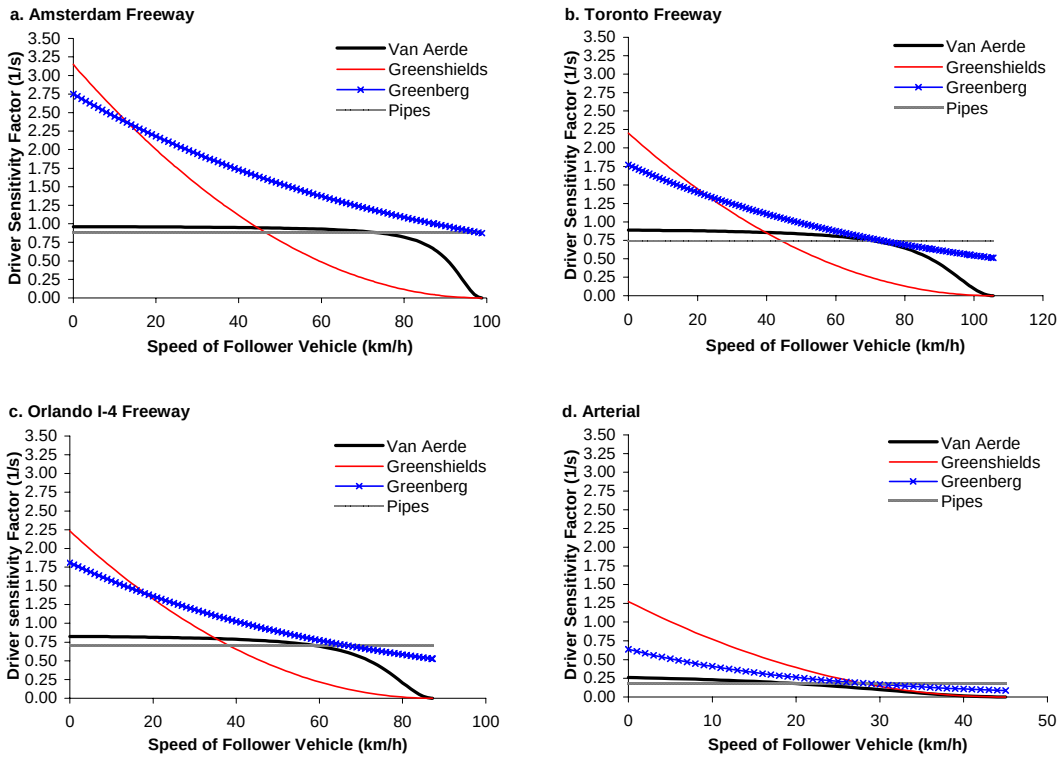

Figure 3-6: Comparison of Driver Sensitivity Factor in Molecular Acceleration Formulation

Fluid Approach

An alternative approach to estimating vehicle accelerations is developed in this paper. The approach extends the approach that was used by Greenberg in deriving his traffic stream model. Specifically, we propose replacing the vehicle speed for the traffic stream space-mean-speed and the distance headway for the average distance headway within the traffic stream, as demonstrated in Van Aerde's model in Equation 61. Recognizing that the average traffic stream headway and space-mean-speed varies both spatially and temporally, the derivative of these variables can be disaggregated into their respective partial derivatives, as demonstrated in Equations 62 and 63. It should be noted that

Equation 63 estimates the average acceleration within the traffic stream as opposed to specific vehicle acceleration as in Equations 57 through 60.

$$\bar{h} = c_1 + \frac{c_2}{u_f - \bar{u}} + c_3\bar{u} \quad [3\text{-}61]$$

$$\frac{d\bar{h}}{dt} = \left\{ \frac{c_2}{\left[u_f - \bar{u}\right)\right]^2} + c_3 \right\} \cdot \frac{d\bar{u}}{dt} \quad [3\text{-}62]$$

$$a = \left\{ \frac{1}{\frac{c_2}{\left[u_f - \bar{u}\right)\right]^2} + c_3} \right\} \cdot \left[\frac{\partial \bar{h}}{\partial t} + \bar{u}\frac{\partial \bar{h}}{\partial x} \right] \quad [3\text{-}63]$$

Equation 64 can be derived using the flow continuity equation that was presented earlier (Equation 10) and recognizing that the average distance headway ($\bar{h}$) is equal to the inverse of the traffic stream density (k) based on Equation 2. Taking the partial derivative of Equation 61 with respect to the spatial location (x), Equation 65 is derived. Finally, substituting Equation 65 into Equation 64, Equation 66 is derived.

$$q = \frac{\bar{u}}{\bar{h}} \quad \Rightarrow \frac{\partial q}{\partial x} = \frac{1}{\bar{h}}\frac{\partial \bar{u}}{\partial x} - \frac{\bar{u}}{\bar{h}^2}\frac{\partial \bar{h}}{\partial x} \quad [3\text{-}64]$$

$$\frac{\partial \bar{h}}{\partial x} = \left\{ \frac{c_2}{\left[u_f - \bar{u}\right)\right]^2} + c_3 \right\} \cdot \frac{\partial \bar{u}}{\partial x} \quad [3\text{-}65]$$

$$\frac{\partial q}{\partial x} = \left\{ \frac{1}{\bar{h}\left[\frac{c_2}{\left(u_f - \bar{u}\right)^2} + c_3 \right]} - \frac{\bar{u}}{\bar{h}^2} \right\} \cdot \frac{\partial \bar{h}}{\partial x} \quad [3\text{-}66]$$

Using the flow conservation equation (Equation 14) and substituting the average distance headway ($\bar{h}$) for the inverse of traffic stream density, Equation 67 is derived. Solving Equations 66 and 67 simultaneously, the relationship between the partial derivative of the average headway with respect to time ($\partial\bar{h}/\partial t$) can be related to the partial derivative of the average headway with respect to location ($\partial\bar{h}/\partial x$), as demonstrated in Equation 68. Substituting Equation 68 in Equation 63, the acceleration can be related to the partial derivative of the average distance headway with respect to location, as demonstrated in Equation 69. Finally, the acceleration of the FV can be estimated using the average acceleration rate by introducing the indices of the various vehicles and the perception-reaction time lag (T), as demonstrated in Equation 70. It should be noted that the formulation ensures that the stimulus is offset by a time lag of T seconds, while the sensitivity factor (within braces) is computed for the current conditions.

$$\frac{\partial q}{\partial x} = -\frac{\partial k}{\partial t} = \frac{1}{\overline{h}^2} \cdot \frac{\partial \overline{h}}{\partial t} \quad [3\text{-}67]$$

$$\frac{\partial \overline{h}}{\partial t} = \left\{ \frac{\overline{h}}{\left[\frac{c_2}{\left(u_f - \overline{u}\right)^2} + c_3 \right]} - \overline{u} \right\} \cdot \frac{\partial \overline{h}}{\partial x} \quad [3\text{-}68]$$

$$a = \left\{ \frac{\overline{h}}{\left[\frac{c_2}{\left[u_f - \overline{u}\right)^2} + c_3 \right]^2} \right\} \cdot \frac{\partial \overline{h}}{\partial x} = \left\{ \frac{\overline{h}}{\left[\frac{c_2}{\left[u_f - \overline{u}\right)^2} + c_3 \right]^2} \right\} \cdot \frac{1}{\overline{u}} \frac{\partial \overline{h}}{\partial t} \quad [3\text{-}69]$$

$$a_{n+1}(t) = \left\{ \frac{\widetilde{h}_{n+1}(t)}{u_{n+1}(t)\left[\frac{c_2}{\left[u_f - u_{n+1}(t)\right]^2} + c_3 \right]^2} \right\} \cdot \left[u_n(t-T) - u_{n+1}(t-T) \right] \quad [3\text{-}70]$$

The same derivation can be made for the Greenshields, Greenberg, and Pipes models, as demonstrated in Equations 71, 72, and 73, respectively.

$$a_{n+1}(t) = \left\{ \frac{c_2^2}{\widetilde{h}_{n+1}(t)^3 \cdot u_{n+1}(t)} \right\} \cdot \left[u_n(t-T) - u_{n+1}(t-T) \right] \quad [3\text{-}71]$$

$$a_{n+1}(t) = \left\{ \frac{u_c^2}{\widetilde{h}_{n+1}(t) \cdot u_{n+1}(t)} \right\} \cdot \left[u_n(t-T) - u_{n+1}(t-T) \right] \quad [3\text{-}72]$$

$$a_{n+1}(t) = \left\{ \frac{\widetilde{h}_{n+1}(t)}{c_3^2 . u_{n+1}(t)} \right\} \cdot \left[u_n(t-T) - u_{n+1}(t-T) \right] \quad [3\text{-}73]$$

Figure 3-7 illustrates the variation in the sensitivity factor (shown in braces in Equations 70 through 73) for all four models as a function of the FV speed. A comparison of Figure 3-6 and Figure 3-7 demonstrates that the sensitivity factor in the fluid approach is higher than that in the molecular approach at low speeds. However, as the FV speed approaches the facility free-speed, the sensitivity factors for the Van Aerde and Greenshields models approach zero similar to the molecular approach.

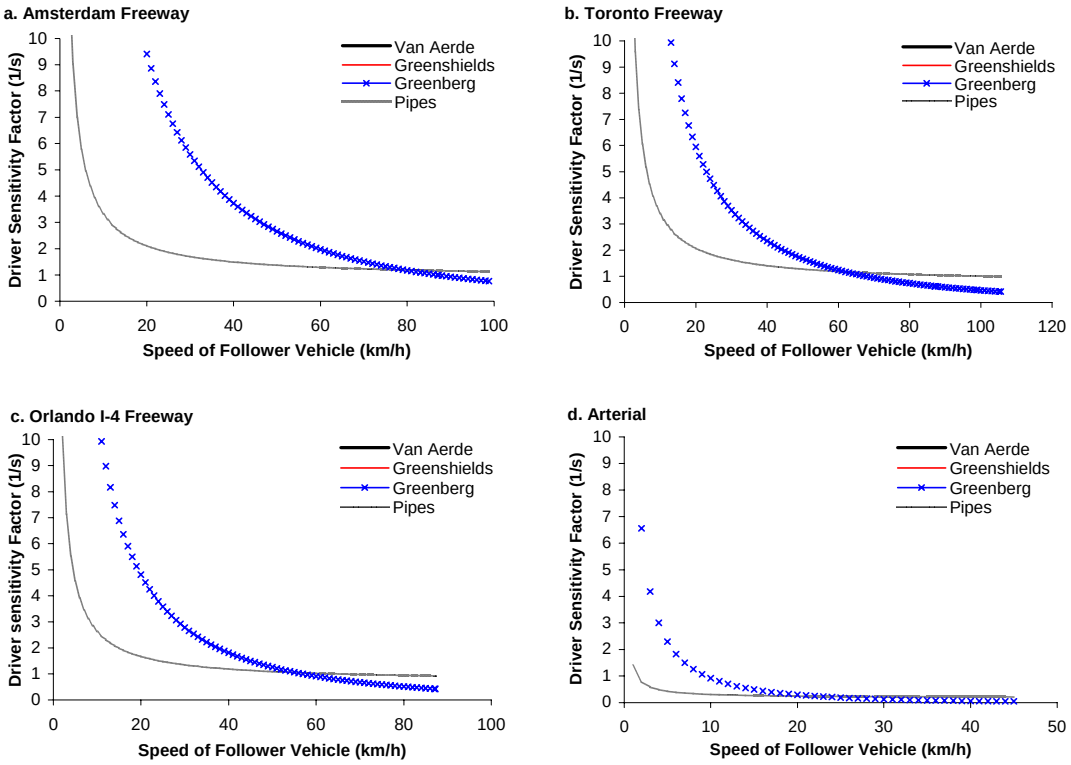

Figure 3-7: Comparison of Driver Sensitivity Factor in Fluid Acceleration Formulation

Comparison of Molecular and Fluid Acceleration Formulation Approaches

Figure 3-8 compares the molecular and fluid formulation acceleration estimates for the Greenshields, Pipes, Greenberg and Van Aerde models, respectively. The figure clearly demonstrates that differences in vehicle accelerations between the molecular and fluid formulations are highest at low FV speeds and smallest at high FV speeds for the four models. To further analyze these findings, Figure 3-9 through Figure 3-12 compare the molecular and fluid formulations for the four models (Van Aerde, Greenshields, Greenberg, and Pipes) using sample freeway facility traffic stream parameters (Amsterdam Ring Road). The figures illustrate the sensitivity of the FV acceleration as a function of the FV speed and the driver stimulus (headway in the case of the speed formulation and speed differential in the case of the acceleration formulation).

The figures clearly illustrate the differences and similarities in the two approaches. In all four models, at lower speeds and lower stimuli, the fluid formulation results in a higher value of acceleration than the molecular formulation. These higher accelerations at lower speeds are caused by differences in the values of the sensitivity factors between the two approaches, as illustrated in Figure 3-6 and Figure 3-7. But at higher speeds, the two approaches have roughly the same profiles. Consistent with the observation made earlier in the molecular approach, the Van Aerde model demonstrates a relatively small variation in FV acceleration at speeds not close to free speed, whereas the Greenshields and

Greenberg models exhibit a high variation with FV speed. In the Pipes molecular formulation, the acceleration of FV remains constant for a particular stimulus irrespective of its speed. This case is because of a constant driver sensitivity factor in the Pipes molecular approach.

Furthermore, it can be observed that as the FV speed approaches the facility free-speed, the Van Aerde and Greenshields models result in very low accelerations/decelerations in comparison to the Greenberg and Pipes models. For example, if an FV traveling at the facility free-speed approaches a stopped vehicle, the Van Aerde and Greenshields models would imply that the FV initially applies mild decelerations that increase as the vehicle speed decreases, whereas the Greenberg and Pipes models imply that the FV applies aggressive decelerations at high speeds. This variance can be explained from Figure 3-6 and Figure 3-7, where the driver sensitivity factor for the Van Aerde and Greenshields models approach zero when the speeds tend to free-speed, whereas those for the Greenberg and Pipes models do not converge to zero. An analysis of field data demonstrates that the Van Aerde and Greenshields model acceleration/deceleration behavior is more realistic and more consistent with typical in-field behavior.

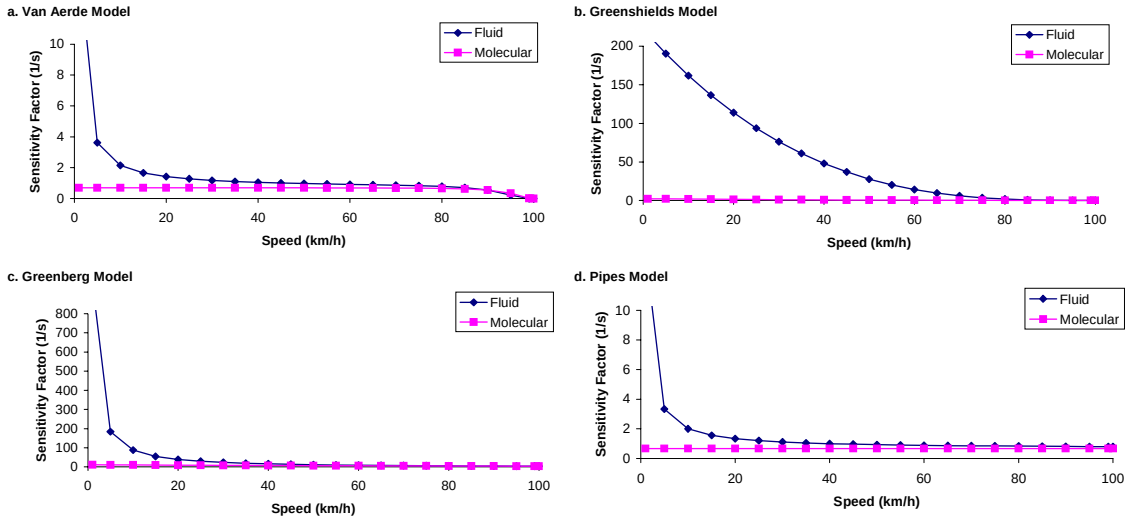

Figure 3-8: Comparison of Molecular and Fluid Formulation Vehicle Driver Sensitivity Factors

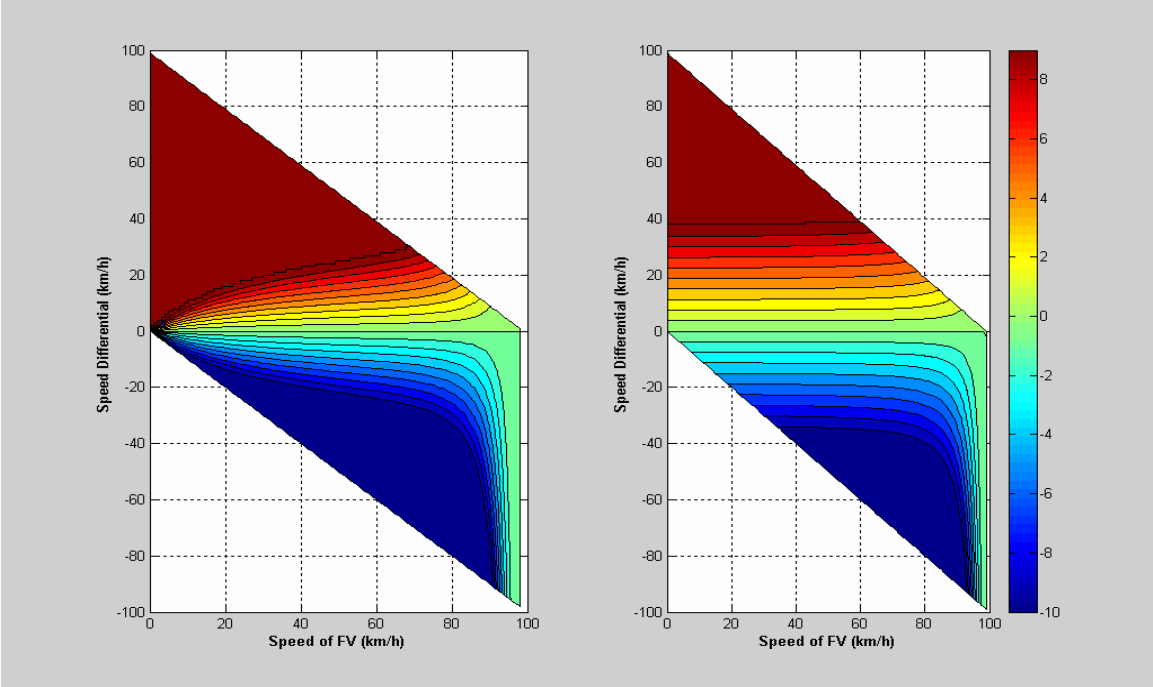

Figure 3-9: Acceleration Variation using Van Aerde Model (a. Fluid Approach; b. Molecular Approach)

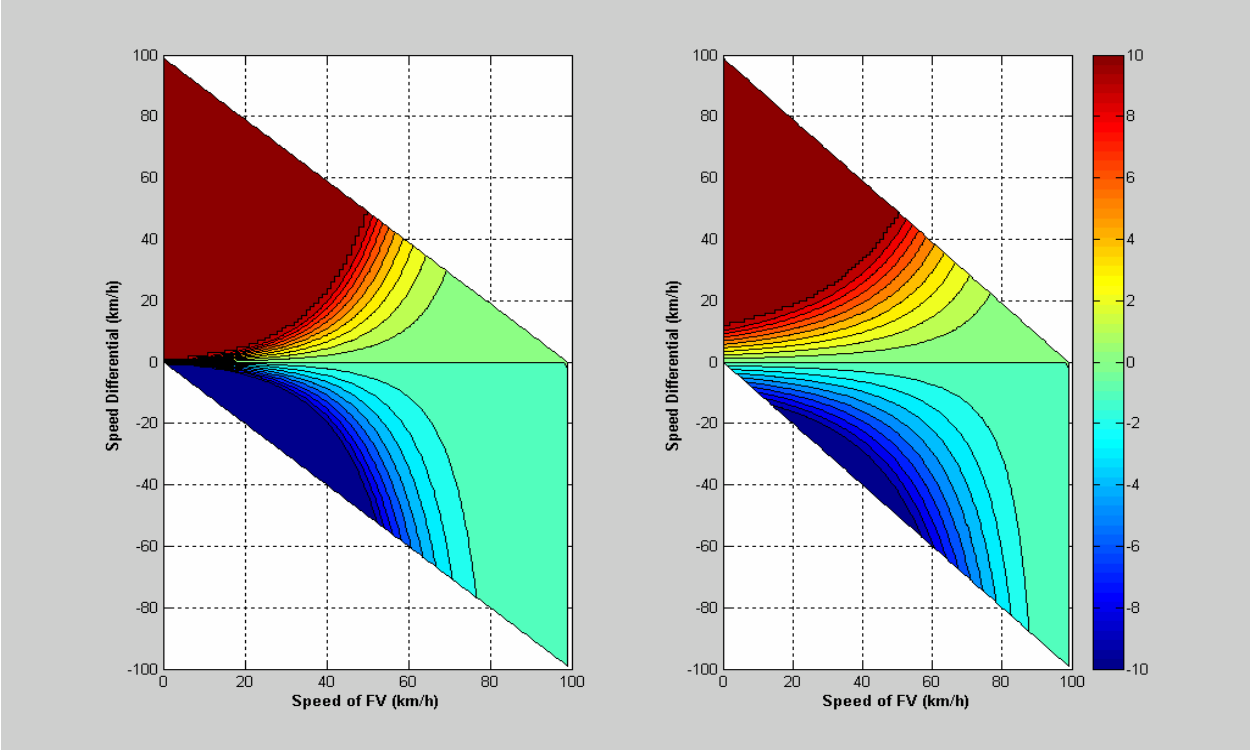

Figure 3-10: Acceleration Variation using Greenshields Model (a. Fluid Approach; b. Molecular Approach)

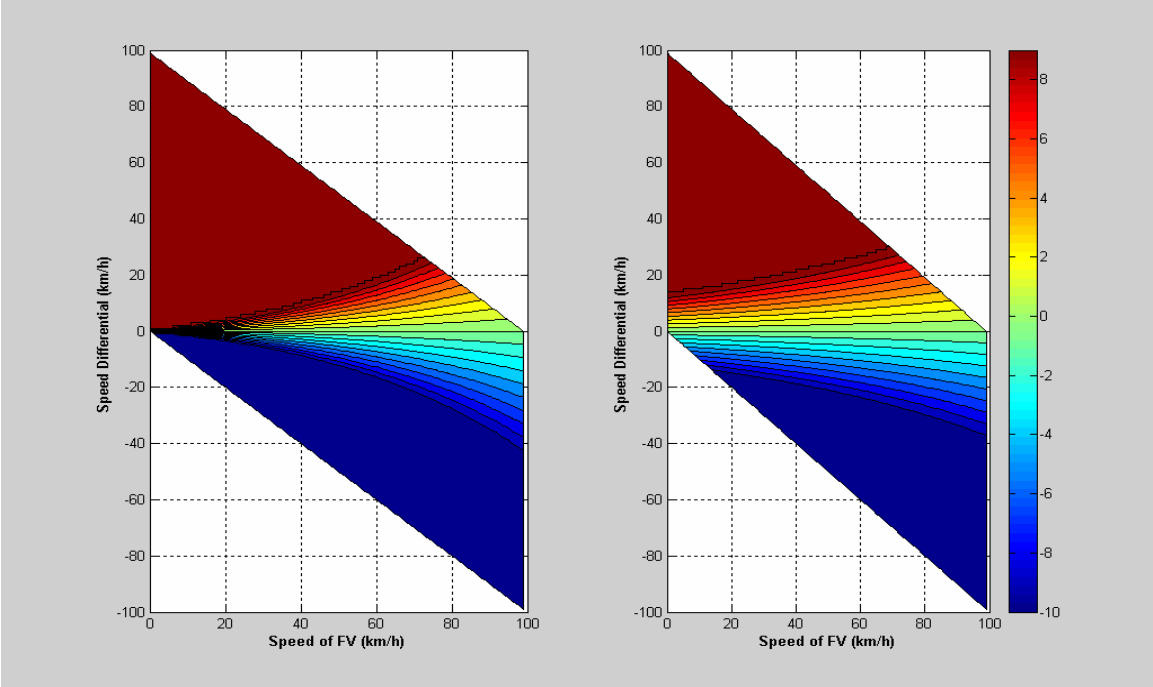

Figure 3-11: Acceleration Variation using Greenberg Model (a. Fluid Approach; b. Molecular Approach)

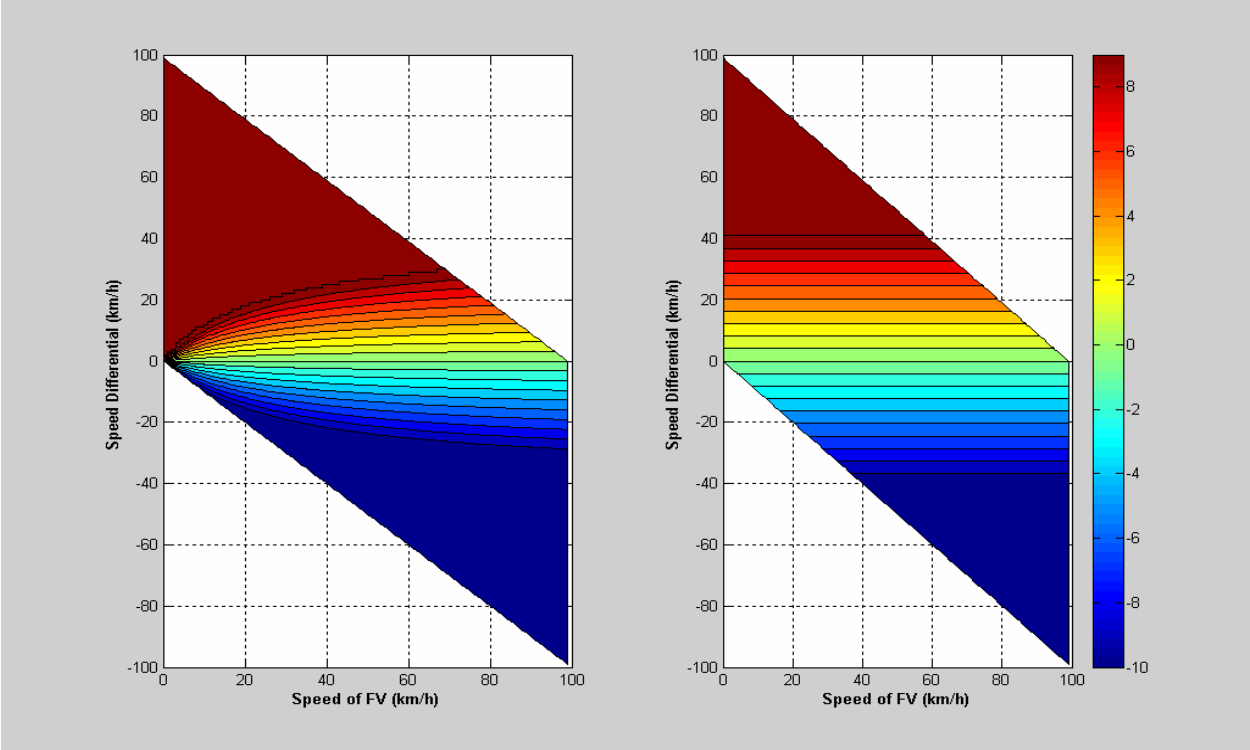

Figure 3-12: Acceleration Variation using Pipes Model (a. Fluid Approach; b. Molecular Approach)

Comment on the different Van Aerde Car-following Formulations

As explained earlier, the functional form of the Van Aerde model combines the Greenshields and the GM-1 model (Pipes car-following model) as demonstrated once again in the following Equation 3-74. So, it is natural that the car-following behavior obtained by the Van Aerde model converges to that of the Greenshields and the Pipes models under certain limiting conditions. It is the aim of this section to identify such limiting conditions under which the Van Aerde model converges to the Greenshields and the Pipes models.

$$\underline{\text{Van Aerde Model:}} \quad \tilde{h}_{n+1}(t-T) = c_1 + \frac{c_2}{u_f - \tilde{u}_{n+1}(t)} + c_3\tilde{u}_{n+1}(t)$$

$$\underline{\text{Greenshields Model:}} \quad \tilde{h}_{n+1}(t-T) = \frac{c_2}{u_f - \tilde{u}_{n+1}(t)} \qquad [3\text{-}74]$$

$$\underline{\text{Pipes Model:}} \quad \tilde{h}_{n+1}(t-T) = c_1 + c_3\tilde{u}_{n+1}(t)$$

As illustrated earlier, the three constants c_1, c_2 and c_3 in the Van Aerde model can be expressed in terms of the four roadway parameters as illustrated in Equation 3-75. These relationships are obtained from the basic equations derived by Van Aerde, 1995 and Van Aerde and Rakha, 1995.

$$c_1 = \frac{u_f}{k_j.u_c^2}.(2u_c - u_f)$$

$$c_2 = \frac{u_f}{k_j.u_c^2}.(u_f - u_c)^2 \qquad [3\text{-}75]$$

$$c_3 = \frac{1}{q_c} - \frac{u_f}{k_j.u_c^2}$$

From the structures of the equations representing the three car-following models, a simple conclusion can be made. The Van Aerde model will converge to the Greenshields model if both c_1 and c_3 are equal to zero; and converge to Pipes model if c_2 is equal to zero. Utilizing the Equation 3-75, the above conclusions can be transformed mathematically to express in terms of the four roadway parameters.

So, the Van Aerde model converges to Greenshields model if:

$$c_1 = c_3 = 0$$

$$\Rightarrow \quad c_1 = 0 \quad \text{and} \quad c_3 = 0$$

$$\Rightarrow \quad \frac{u_f}{k_j.u_c^2}.(2u_c - u_f) = 0 \quad \text{and} \quad \frac{1}{q_c} - \frac{u_f}{k_j.u_c^2} = 0$$

$$\Rightarrow \quad u_f = 2u_c \qquad \text{and} \qquad u_f = \frac{k_j.u_c^2}{q_c} \qquad [3\text{-}76]$$

Further, the Van Aerde model converges to the Pipes model if:

$$c_2 = 0$$

$$\Rightarrow \quad \frac{u_f}{k_j.u_c^2}.(u_f - u_c)^2 = 0$$

$$\Rightarrow \quad u_f = u_c \qquad [3\text{-}77]$$

In summary, the Van Aerde model requires the calibration of four facility-specific parameters (u_f, u_c, q_c and k_j), the Greenshields model requires the calibration of two parameters (u_f & k_j or u_f and q_c) and the Pipes model requires the calibration of three parameters (u_f, k_j and q_c). Further, since all the three car-following formulations are derived from the basic relationships in Equation 3-74, all the three formulations – speed, molecular acceleration and fluid acceleration – for the Van Aerde model converge to the corresponding formulations for the Greenshields and the Pipes models under the above conditions.

3.4 Practical Issues Related to Car-Following Model Implementation

3.4.1 Discrete time step movements of vehicles

The description of car-following models in the literature tends to ignore that simulation software move vehicles at discrete time steps (Δt), which are typically set at a deci-second or a second level of resolution. Furthermore, the movement of the vehicles proceeds from the first down stream vehicle to the farthest upstream vehicle. Consequently, the LV is moved a distance $d_n(t\text{-}T)$ prior to applying the car-following logic, as demonstrated in Equation 78. Specifically, the distance traveled by the LV at instant (t-T) is computed using the speed and acceleration at instant t-T. In order to avoid oscillations in vehicle speed computations, we propose the projection of the FV position based on the estimated distance of travel assuming the vehicle travels at the same speed it traveled in the previous time step, as demonstrated in Equation 79. The predicted headway is then computed as the previous headway plus the difference in distance traveled between the lead and follower vehicles, respectively, as demonstrated in Equations 80 and 81. This procedure has been implemented successfully within the INTEGRATION software (Rakha and Ahn, 2003).

In order to demonstrate the importance of incorporating Equation 37 in the car-following logic, Figure 3-13 illustrates the speed profile of an FV with and without Equation 37. It is evident from the figure that the inclusion of Equation 37 results in a more stable car-following behavior.

$$d_n(t-T) = u_n(t-T)\Delta t + 0.5a_n(t-T)\Delta t^2 \quad [3\text{-}78]$$

$$\tilde{d}_{n+1}(t-T) = u_{n+1}(t-T-\Delta t)\Delta t \quad [3\text{-}79]$$

$$\tilde{h}_{n+1}(t-T) = h_{n+1}(t-T-\Delta t) + d_n(t-T) - d_{n+1}(t-T) \quad [3\text{-}80]$$

$$\tilde{h}_{n+1}(t-T) = h_{n+1}(t-T-\Delta t) + \left[u_n(t-T) - u_{n+1}(t-T-\Delta t)\right]\Delta t + 0.5a_n(t-T)\Delta t^2 \quad [3\text{-}81]$$

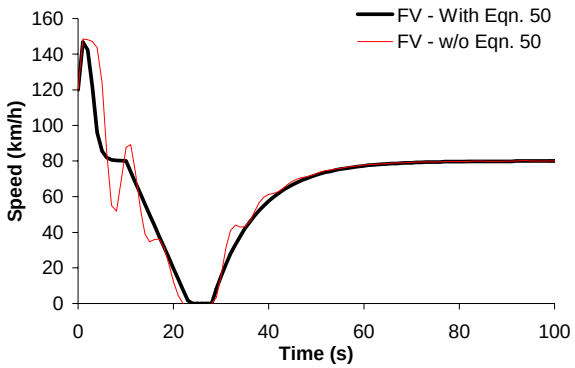

Figure 3-13: Example Illustration of Importance of Vehicle Projections

3.4.2 Acceleration Constraint

A major problem with the state-of-practice car-following models is that the models do not ensure that vehicle accelerations are realistic. Specifically, vehicle accelerations that emerge from car-following models are not constrained by the vehicle dynamics and thus may result in vehicle accelerations that are not feasible. Consequently, car-following behavior is modeled using a system of equations. The first equation characterizes the motion of the FV with respect to the behavior of the LV. The second set of equations constrains the car-following behavior by ensuring that vehicle accelerations are realistic. The third and final set of equations ensures that the traffic stream is asymptotically stable, as will be described in the following section.

In order to ensure feasible accelerations, the use of a variable power vehicle dynamics model that was developed by Rakha and Lucic (2002) is suggested. The model computes the effective tractive force as the minimum of the engine tractive force and the maximum force that can be sustained between the vehicle tires and the roadway pavement, as demonstrated in Equation 82. While this model does not include gear shifting, it does account for the major behavioral characteristics that result from gear shifting, namely, the reductions of power as gearshifts are being engaged. Specifically, the approach uses a simple vehicle dynamics model that captures the more complicated gear shifting behavior while accounting for the buildup of power as a vehicle accelerates from a complete stop.

The model uses a variable power efficiency factor that is dependent on the vehicle speed, as opposed to the constant factor that is currently used in vehicle dynamics models. The factor is a linear relation of vehicle speed with an intercept of $1/u_0$ and a maximum value

of 1.0 at a speed u_0, as demonstrated in Equation 83. The intercept guarantees that the vehicle has enough power to accelerate from a complete stop. The adjustment factor is then multiplied by the vehicle power in computing the tractive force, as demonstrated in Equation 82.

The estimation of the variable power factor "β" requires the calibration of two parameters, namely, the minimum power and the speed at optimum power. This model assumes the minimum power to be a function of the optimum speed, as demonstrated in Equation 83. These parameters were calibrated using four trucks with vehicle rated powers ranging from 260 to 375 kW (350 to 500 hp), each involving 10 weight configurations. The calibration demonstrated that higher weight-to-power ratios required a lower optimum speed and a higher minimum power. The power lower bound addresses this need for a variable parameter while maintaining a single calibration parameter.

Figure 3-14 illustrates the variation in the vehicle power and the resulting vehicle acceleration by incorporating the power adjustment factor presented in Figure 3-15. As illustrated in the figure, the modification reduces the vehicle acceleration levels at the lower speeds while it does not alter the acceleration behavior at higher speeds.

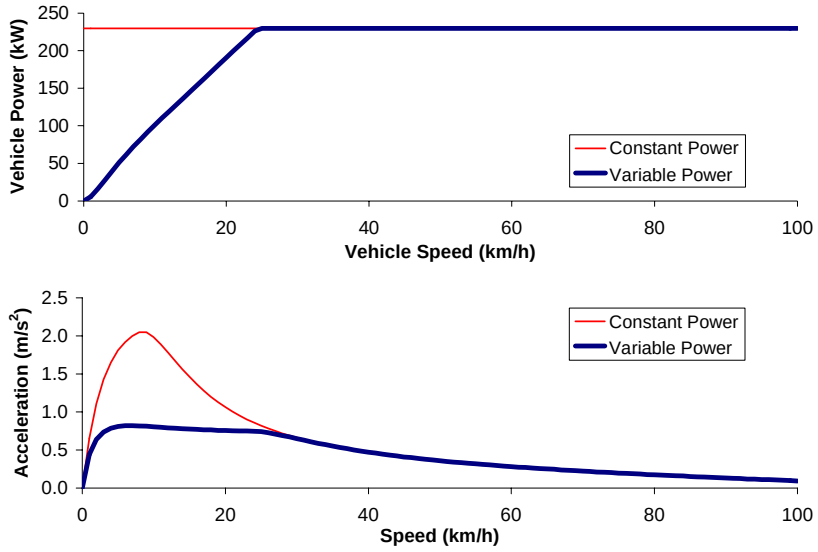

Figure 3-14: Variation in Vehicle Power and Maximum Acceleration as a Function of Vehicle Speed (Rakha and Lucic, 2002)

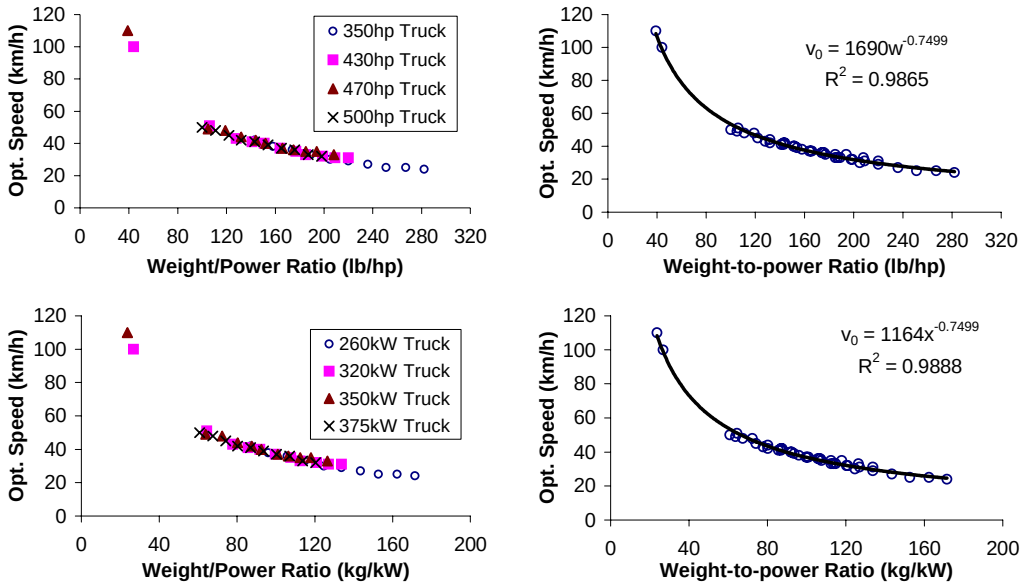

Figure 3-15: Relationship between Vehicle Speed at Optimum Power and Weight-to-Power Ratio (Rakha and Lucic, 2002)

The calibration of the variable power factor involves calibrating the speed at which the vehicle power reaches its maximum (termed the optimum speed). The optimum speed was found to vary as a function of the weight-to-power ratio, as demonstrated in Figure 3-16. The details of how this relationship was derived are not discussed here (Rakha and Lucic, 2002); however, it is sufficient to note at this point that the relationship is a power relationship, as demonstrated by Equation 84. It should be noted that Rakha et al. (2003) demonstrate that the variable power factor should be set to 1.0 for light duty vehicles and trucks (weight-to-power ratio less than 30 kg/kW).

It should be noted that Equation 88 assumes that vehicles accelerate at the maximum rate when they are constrained by their vehicle dynamics. However, Snare and Rakha (2003) have attempted to characterize typical acceleration behavior by incorporating a maximum acceleration factor (γ) in the vehicle dynamics model, as demonstrated in Equation 89. Specifically, Snare and Rakha found that the acceleration factor is, on average, 65 percent and varies between 45 and 85 percent. Specifically, Figure 3-16 illustrates the consistency between the proposed model vehicle speed and acceleration predictions and typical driver behavior collected in the field.

$$F_{n+1}(t) = \min\left[3600 \cdot \eta_d \cdot \beta \cdot \frac{P}{u_{n+1}(t-\Delta t)}, 9.8066 \cdot M_{ta} \cdot \mu \right] \quad [3\text{-}82]$$

$$\beta = \frac{1}{u_0}\left[1 + \min\left(u_{n+1}(t-\Delta t), u_0\right)\left(1 - \frac{1}{u_0}\right)\right] \quad [3\text{-}83]$$

$$u_0 = 1164 w^{-0.75} \quad [3\text{-}84]$$

$$R_{n+1}(t) = c_7 \cdot C_D \cdot C_h \cdot A_f \cdot u_{n+1}^2(t-\Delta t) + 9.8066 \cdot M \cdot C_r \left[c_8 u_{n+1}(t-\Delta t) + c_9\right] + 9.8066 \cdot M \cdot G \quad [3\text{-}85]$$

$$\hat{a}_{n+1}(t) = \frac{F_{n+1}(t) - R_{n+1}(t)}{M} \quad [3\text{-}86]$$

$$\hat{a}_{n+1}(t) = \frac{\hat{u}_{n+1}(t) - u_{n+1}(t-\Delta t)}{\Delta t} = \frac{F_{n+1}(t) - R_{n+1}(t)}{M} \quad [3\text{-}87]$$

$$\hat{u}_{n+1}(t) = u_{n+1}(t-\Delta t) + \left[\frac{F_{n+1}(t) - R_{n+1}(t)}{M}\right]\Delta t \quad [3\text{-}88]$$

$$\hat{u}_{n+1}(t) = u_{n+1}(t-\Delta t) + \gamma\left[\frac{F_{n+1}(t) - R_{n+1}(t)}{M}\right]\Delta t \quad [3\text{-}89]$$

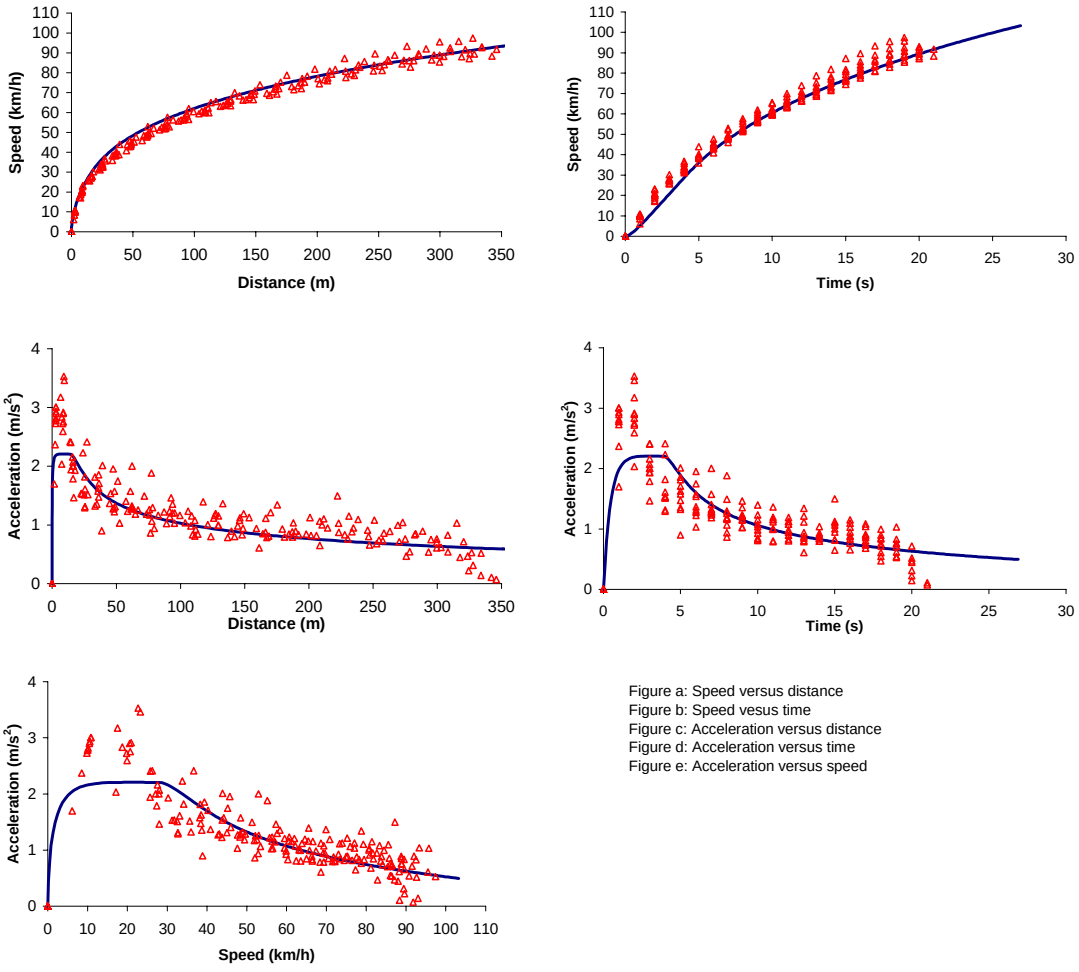

Figure a: Speed versus distance
Figure b: Speed vesus time
Figure c: Acceleration versus distance
Figure d: Acceleration versus time
Figure e: Acceleration versus speed

Figure 3-16: Typical Vehicle Acceleration Levels (Snare and Rakha, 2003)

3.4.3 Collision Avoidance Constraint

The stability of a car-following model is measured as a function of the product of the sensitivity factor (within the braces) and the perception-reaction time (T). Consequently, instability can be introduced into the car-following model by either increasing the driver sensitivity factor or the perception-reaction time (T). Instability can be characterized as being either local or asymptotic. Local stability refers to the stability of two vehicles, while asymptotic stability refers to the stability of a traffic stream of vehicles. When the system is unstable, oscillations in the FV speed are observed. These oscillations may either decrease with time (damped oscillatory) or increase with time (increased oscillatory). Furthermore, the instability of a system may result in vehicles colliding within the traffic stream.

In order to ensure that the traffic stream is stable, a collision avoidance set of equations should be added to the car-following model. Specifically, Equation 90 derives the maximum distance a vehicle can travel to decelerate from its initial speed to the speed of the LV without colliding with the lead vehicle (maintain the minimum jam density headway behind the LV). By solving Equation 90 for the vehicle deceleration rate, Equation 91 can be derived. Finally, Equation 92 computes the maximum speed that the FV can travel at without colliding with the LV. It should be noted that Equation 92 should only be engaged when the lead and follower vehicles approach one another. Specifically, this logic has been implemented successfully within the INTEGRATION microscopic traffic simulation and assignment model when the time headway between the two vehicles is less than 50 seconds. Such a condition ensures that the following vehicle does not respond to a lead vehicle that is too far away to influence the behavior of the following vehicle.

$$\tilde{h}_{n+1}(t) - h_j = \frac{u_n^2(t) - u_{n+1}^2(t-\Delta t)}{2\breve{a}_{n+1}(t)} \quad [3\text{-}90]$$

$$\breve{a}_{n+1}(t) = \frac{\breve{u}_{n+1}(t) - u_{n+1}(t-\Delta t)}{\Delta t} = \frac{u_n^2(t) - u_{n+1}^2(t-\Delta t)}{2\left[\tilde{h}_{n+1}(t) - h_j\right]} \quad [3\text{-}91]$$

$$\breve{u}_{n+1}(t) = u_{n+1}(t-\Delta t) + \frac{u_n^2(t) - u_{n+1}^2(t-\Delta t)}{2\left[\tilde{h}_{n+1}(t) - h_j\right]} \cdot \Delta t \quad [3\text{-}92]$$

3.4.4 Car Following Behavior Formulation

The final car-following model can be viewed as a set of three equations. The first equation characterizes the desired driver behavior as a function of the LV behavior. We have presented a number of state-of-the-art models including the GM, Van Aerde, Greenshields, Greenberg, and Pipes models. In order to ensure that a vehicle converges to its steady-state behavior, the car-following model should be formulated with the speed as the control variable (speed formulation). Such a formulation ensures that vehicles speed up (up to the free-speed) in order to close the gap between the FV and LV.

A second set of equations imposes constraints on the car-following behavior to ensure that the estimated vehicle accelerations are realistic, as illustrated by Equation 93. In this case, the desired speed $\tilde{u}$ of a following vehicle that is accelerating at an instant *t* is constrained by the maximum speed $\hat{u}$ allowed by vehicle dynamics at instant *t*. This equation alone clearly points to the importance of modeling vehicle dynamics within car-following behavior.

$$u_{n+1}(t) = \begin{cases} \hat{u}_{n+1}(t) & \text{if } (\tilde{u}_{n+1}(t) > \hat{u}_{n+1}(t)) \\ \tilde{u}_{n+1}(t) & \text{if } (\tilde{u}_{n+1}(t) \le \hat{u}_{n+1}(t)) \end{cases} \quad [3\text{-}93]$$

A third, and final set of equations further ensures that the traffic stream is asymptotically stable by enforcing collision-avoidance rules when the lead vehicle is traveling at a lower speed than the following vehicle ($u_n(t) < u_{n+1}(t)$), as demonstrated in Equation 94. Specifically, this set of constraints ensures that the following vehicle is able to decelerate to a complete stop without colliding with the lead vehicle. Again, Equation 94 is invoked when the time headway between the two vehicles is less than 50 seconds.

$$u_{n+1}(t) = \begin{cases} \breve{u}_{n+1}(t) & \text{if } (\tilde{u}_{n+1}(t) > \breve{u}_{n+1}(t)) \\ \tilde{u}_{n+1}(t) & \text{if } (\tilde{u}_{n+1}(t) \le \breve{u}_{n+1}(t)) \end{cases} \quad [3\text{-}94]$$

In summary, the provision of the acceleration and collision avoidance constraints within the car-following framework ensures that vehicle accelerations are realistic and that the traffic stream is asymptotically stable.

3.5 Conclusions

This chapter presented the different formulations of car-following behavior for four selected models – Pipes, Greenshields, Greenberg and Van Aerde. Specifically, speed and acceleration forms are described and detailed and a new acceleration formulation which considers the fluid nature of traffic is proposed. A comparison of the existing and the proposed approaches for acceleration formulation is also presented. Further, the valid range for Van Aerde speed formulation is analyzed. Then a comprehensive car-following behavior encompassing the steady state conditions and the two constraints – acceleration and collision avoidance – is presented. Specifically, the variable power vehicle dynamics model proposed by Rakha and Lucic (2002) is utilized for the acceleration constraint.

The next step after deriving the different formulations is to analyze them under different traffic scenarios. Specifically, it should be analyzed which car-following formulation produces realistic representation in the different conditions. The next chapter is devoted for this purpose. It identifies the scenarios that are best for the comparison purpose. Further, the question of capacity drop is also addressed by using the car-following formulations derived in this chapter.

CHAPTER FOUR:

COMPARISON OF CAR-FOLLOWING MODELS

4.1 Introduction

The previous chapter presented three different possible formulations for car-following behavior – Speed formulation, molecular acceleration formulation and fluid acceleration formulation. And these formulations were presented for four state-of-the art car-following models – Pipes, Greenshields, Greenberg and Van Aerde models. The next question will be to study how these formulations compare with each other under different scenarios and analyze the differences and/or similarities. The selection of scenarios for the purpose of comparison is very critical since it gives a chance to analyze a wide range of possible traffic flow scenarios. Vehicle flow on transportation facilities may generally be classified into two types, as illustrated by examples in Table 4-1:

- Uninterrupted flow
- Interrupted flow

Uninterrupted flow occurs on facilities on which there are no external factors causing periodic interruptions to the traffic stream. Such flows exist primarily on freeway and other limited-access facilities, where there are no traffic signals, stop or yield signs, or at-grade intersections to interrupt the continuous movement of vehicles. Such flows can also occur on long sections of surface highways between signalized intersections where the geometric and driving characteristics approach those usually found on a limited-access facility. On uninterrupted flow facilities, traffic flow conditions are thus primarily the result of the interactions among the vehicles within the stream and the interactions between the vehicles and the geometric characteristics of the roadway. If congestion occurs, the breakdown of traffic flow then is strictly the results of frictions internal to the traffic stream and not the result of external causes.

Uninterrupted Flow	Freeways
	Multi-lane Highways
	Two-lane Highways
Interrupted Flow	Signalized Streets
	Un-signalized Streets with Stop Signs
	Arterials
	Transits
	Pedestrian Walkways
	Bicycle Paths

Table 4-1: Types of Transportation Facilities

Interrupted flow occurs on transportation facilities that have fixed elements causing periodic interruptions to the traffic stream irrespective of existing traffic conditions. These flows occur on facilities on which traffic signals, stop signs, yield signs, and other types of control devices force motorists to interrupt their progression at specific locations. On these facilities, traffic flow characteristics thus not only depend on the interactions between the vehicles within the stream and with the roadway geometry, but also on the external factors causing the interruptions.

This chapter first presents an overview of the formulations presented in the previous chapter and then goes on to describe the various scenarios selected for comparing them. The next two sections describe the results and analyses of the three car-following formulations for the selected scenarios. Finally, the issue of capacity drop after queue formation is also addressed by studying the flow processes downstream of two shockwaves – backward moving and stationary.

4.2 Overview

4.2.1 Car-following Models

In the previous chapter, three possible formulations were presented and illustrated for four state of the art car-following models. The mathematical relationships for all these formulations and models are presented here in a tabular form for the purpose of summarization and as a quick reference. Table 4-2 shows the summary of formulae.

In this chapter, for the purpose of comparison during the analysis of a platoon of vehicles, a fifth model is selected. This model currently implemented in TRANSIMS is known as Cellular Automata (CA). In the next few lines, the logic behind this model is summarized. CA considers the roadway to be divided into cells of length 7.5 m. So, the vehicles in this model are moved forward also in cells. So, at any given time, a vehicle can be either in a cell or not; and partial presence of a vehicle in 2 cells is considered impossible. The car-following logic for this model can be summarized in the following three steps:

- Find the headway (number of empty cells ahead) of the vehicle at time t.
- If u (speed of vehicle expressed in cells/sec) > headway, then decrease the speed to u-1 cells/sec.
- If u < headway, then increase the speed to the minimum of u + 1 and free-speed.

Further, in TRANSIMS this logic is applied every second. So, for the purpose of calculations in this research work, the vehicles are moved every sec based on the logic described above.

Formulations / Models	**Speed** $\tilde{u}_{n+1}(t) =$	**Molecular Acceleration** $a_{n+1}(t) =$	**Fluid Acceleration** $a_{n+1}(t) =$
Pipes	$\min\left\{\frac{1}{c_3}\cdot\left[\tilde{h}_{n+1}(t-T)-h_j\right], u_f\right\}$	$\left\{\frac{1}{c_3}\right\}\cdot\left[u_n(t-T)-u_{n+1}(t-T)\right]$	$\left\{\frac{\tilde{h}_{n+1}(t)}{c_3^2.u_{n+1}(t)}\right\}\cdot\left[u_n(t-T)-u_{n+1}(t-T)\right]$
Greenshields	$u_f-\frac{c_2}{\tilde{h}_{n+1}(t-T)}$	$\left\{\frac{c_2}{\tilde{h}_{n+1}(t-T)^2}\right\}\cdot\left[u_n(t-T)-u_{n+1}(t-T)\right]$	$\left\{\frac{c_2^2}{\tilde{h}_{n+1}(t)^3\cdot u_{n+1}(t)}\right\}\cdot\left[u_n(t-T)-u_{n+1}(t-T)\right]$
Greenberg	$u_c\ln\left(k_j\cdot\tilde{h}_{n+1}(t-T)\right)$	$\left\{\frac{u_c}{\tilde{h}_{n+1}(t-T)}\right\}\cdot\left[u_n(t-T)-u_{n+1}(t-T)\right]$	$\left\{\frac{u_c^2}{\tilde{h}_{n+1}(t)\cdot u_{n+1}(t)}\right\}\cdot\left[u_n(t-T)-u_{n+1}(t-T)\right]$
Van Aerde	$\frac{-c_1+c_3u_f+\tilde{h}_{n+1}(t-T)}{2c_3}$ $-\frac{\sqrt{\left[c_1-c_3u_f-\tilde{h}_{n+1}(t-T)\right]^2-4c_3\left[\tilde{h}_{n+1}(t-T)u_f-c_1u_f-c_2\right]}}{2c_3}$	$\left\{\frac{u_f-u_{n+1}(t)}{c_3(u_f-2u_{n+1}(t))-c_1+\tilde{h}_{n+1}(t-T)}\right\}$ $\times\left[u_n(t-T)-u_{n+1}(t-T)\right]$	$\left\{\frac{\tilde{h}_{n+1}(t)}{u_{n+1}(t)\left[\frac{c_2}{\left[u_f-u_{n+1}(t)\right]^2}+c_3\right]^2}\right\}$ $\times\left[u_n(t-T)-u_{n+1}(t-T)\right]$

Table 4-2: Summary of Car-Following Formulations for Pipes, Greenshields, Greenberg and Van Aerde Models

4.2.2 Scenarios Considered

As explained previously, there exist in general two traffic flow conditions in practice – uninterrupted and interrupted flow conditions. So, it is best to compare the three car-following formulations under these two conditions. First, the comparison is done using the car-following behavior for a pair of vehicles – under both uninterrupted and interrupted conditions. Then, in order to compare the discharge headways of vehicles departing a signalized intersection and to address the issue of capacity drop, the comparison is also performed for a platoon of vehicles (uninterrupted condition). Thus on the whole, four scenarios are selected for the comparison purposes. This section describes in detail all the scenarios considered for analyses.

Scenario I: Uninterrupted Flow Condition – Two Vehicles:

As explained earlier, uninterrupted flow occurs on facilities like freeways on which there are no external factors causing periodic interruptions to the traffic stream. This scenario tries to compare the behavior of a follower vehicle obtained from the three formulations under such uninterrupted conditions on freeways. Then under such conditions, three distinct cases can be analyzed. They are:

- Follower vehicle (FV) following a Lead vehicle (LV) traveling at the same speed on a roadway.
- FV approaching a slow moving LV after exiting from a freeway facility.
- FV approaching a fast moving LV after entering a freeway facility.

In case 1, both the FV and LV are assumed to be traveling at a speed of 80 km/h initially with an initial headway of 75 m on a freeway. In case 2, the initial speed of FV is taken to be 70 km/h, whereas that of LV is taken to be 40 km/h. The initial headway between the vehicles was considered to be 100 m. In case 3, the initial speed of FV is taken to be 50 km/h, whereas that of LV is taken to be 80 km/h. Similarly, initial headway is considered to be 100m.

Scenario II: Interrupted Flow Condition – Two Vehicles:

Interrupted flow occurs on transportation facilities that have fixed elements like traffic signals, causing periodic interruptions to the traffic stream irrespective of existing traffic conditions. This scenario attempts to compare the behavior of FV obtained from the three formulations under such interrupted conditions.

Specifically, a profile of LV as it travels on a roadway with a stop sign is selected and the behavior of FV following this LV is analyzed. For the purpose of calculations, the initial speed of FV is assumed to be 65 km/h and the initial headway is taken as 75 meters. In order to study the effect of initial headway on the car-following behavior, the headway is increased to 150 meters and the simulation results are analyzed. The selected profile of the LV as it travels on the roadway with a traffic signal is taken as shown in Figure 4-1:

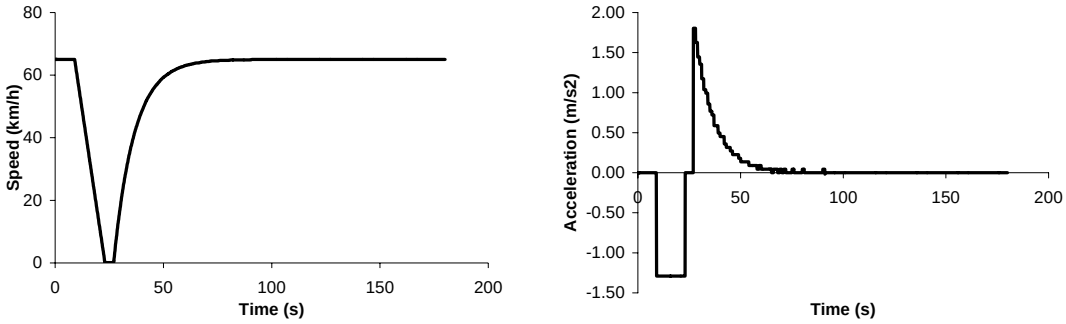

Figure 4-1: Example Lead Vehicle Speed and Acceleration Profile

Scenario III: Interrupted Flow Condition – Study of Discharge Headways:

As stated in the thesis objectives section of the introduction chapter, one of the objectives of this research work is to study the discharge headways of a platoon of vehicles leaving an intersection. This scenario tries to achieve this goal. For this purpose, a platoon of 20 vehicles leaving an intersection after the traffic signal turns green is considered. The discharge headways for those vehicles are analyzed using five models – four models mentioned in previous chapter and another model called cellular automata implemented in TRANSIMS. The analysis is conducted under four scenarios to reflect the effect of various parameters on discharge headways. The following Table 4-3 describes the different cases considered for this scenario.

Case No.	Free Flow Speed (km/h)	Position of	
		Truck	Turning Vehicle
1	80	-	-
2	100	-	-
3	80	1	-
4	80	-	4

Table 4-3: Description of Different Cases in Scenario III

Scenario IV: Interrupted Flow Condition – Study of Capacity Drop:

Careful study of the literature revealed that there is a large debate on whether the capacity of freeway drops after the formation of a queue. Several studies have been conducted and theories proposed for and against the concept of a capacity drop, but none of them were found to be convincing by the researchers. In this scenario, this issue is addressed using the state-of-art car-following models under two situations – at a backward moving shockwave and at a stationary shockwave. Further the differences and/or similarities observed in the flow rates of traffic stream for both the speed and acceleration formulations are also analyzed. Understanding the significance of the maximum

acceleration factor proposed by Rakha and Snare (2003), its effect on the roadway capacity is also studied.

A backward moving shockwave is obtained at a signalized intersection when the signal turns green and a stationary shockwave on the sections of a roadway with lane drops. For the purposes of analyses, the backward moving shockwave is simulated by considering a platoon of 20 stopped vehicles at a signalized intersection. To replicate a stationary shockwave, a section of the freeway with a single lane drop is considered. Further, to understand the effect of the level of congestion on the flow processes, the initial speed of vehicles in the region of lane drop is varied.

4.2.3 General Assumptions

In order to solve the car-following behavior for various scenarios numerically, certain assumptions have to taken and values for certain parameters including vehicles and roadway have to be fixed. This section describes such assumptions made.

- All the cars are assumed to have the same characteristics i.e., same power, mass, acceleration behavior, etc. Further, all the vehicles including cars and trucks are assumed to be using radial tires – which affect the rolling resistance coefficients. The characteristics of cars and trucks used in this research work are tabulated below:

	Car	**Truck**	
Power	98	336	KW
Mass	1497	44806	Kg
% Mass on Tractive Axle	0.65	0.37	
Frontal Area	1.9	9.0	m^2

- Unless otherwise stated, the roadway parameters are fixed as follows:

	Arterial	**Freeway**	
$\mathbf{u_f}$ =	80	110	km/h
$\mathbf{u_c}$ =	45	85	km/h
$\mathbf{q_c}$ =	1600	2300	veh/h/lane
$\mathbf{k_j}$ =	125	125	veh/km/lane

- Further, the roadway is considered to be made up of asphalt in good condition. In addition, the grade of the roadway is considered to be zero with a coefficient of friction of 0.6.

4.3 Car-Following Behavior Comparison

As explained and illustrated in the previous chapter, the process of car-following is modeled as an equation of motion under steady-state conditions plus a number of constraints that govern the behavior of vehicles while moving from one steady state to another (decelerating and accelerating). The steady-state car-following formulations for the four state-of-the art models are summarized in Table 4-2 above. The first constraint governs the vehicle acceleration behavior, which is typically a function of the vehicle dynamics. The second and final constraint ensures that vehicles maintain a safe position relative to the lead vehicle in order to ensure asymptotic stability within the traffic stream.

This section compares the behavior of FV obtained from the three car-following formulations for the four models. For this purpose, the steady-state formulations summarized in Table 4-2 along with the acceleration and collision avoidance constraints are used together to generate the car-following behavior. Further, the comparison is performed for a pair of lead and follower vehicles under two distinct scenarios – uninterrupted and interrupted traffic flow conditions.

4.3.1 SCENARIO I: Uninterrupted Flow Conditions

As explained in section 1.2.2, three distinct cases to illustrate the similarities and/or differences between the three formulations are considered in this scenario. The car-following behavior of the FV as it follows a LV is obtained by using spreadsheet simulation in EXCEL. The results of these cases are described below and analyzed in detail:

FV traveling at the same speed as LV with an initial headway of 75 m

In this case, both the lead and follower vehicles are assumed to be traveling at the same speed of 80 km/h with a headway of 75 meters initially (at time, $t = 0$). Stable distance headway (SDH) of the FV (i.e. the headway between a pair of vehicles at a stable speed of FV) for a speed of 80 km/h can be obtained from the four car-following models by calculating the distance headway, h at a speed of 80 km/h. This value for the four models is as follows:

$$\underline{\textit{Van Aerde}} - \; h_{n+1}(@u_{n+1} = 80) = c_1 + c_3.80 + \frac{c_2}{u_f - 80} = 42 \text{ meters}$$

$$\underline{\textit{Greenshields}} - \; h_{n+1}(@u_{n+1} = 80) = \frac{c_2}{u_f - 80} = 40 \text{ meters}$$

$$\underline{\textit{Greenberg}} - \; h_{n+1}(@u_{n+1} = 80) = \frac{1}{k_j} e^{80/u_c} = 43 \text{ meters}$$

$$\underline{\textit{Pipes}} - \; h_{n+1}(@u_{n+1} = 80) = c_1 + c_3.80 = 45 \text{ meters}$$

Now, since the initial headway is considered to be 75 meters, it is to be expected that all the four models result in FV being accelerated as the SDH for a speed of 80 km/h is less than 75 meters. The behavior of the FV from the four models and for the three formulations is obtained from spreadsheet simulation and the results are given below.

It can be noted from Figure 4-2 that the speed formulation of the four car-following models results in the FV being accelerated initially. As a result, the FV speeds up for some time initially and later on converges to the speed of the LV. This can be explained on the basis that, initially at $t = 0$ the headway of the FV is less than the SDH prescribed for the FV at its speed of 80 km/h. Consequently, the speed formulation results in the FV being accelerated and this helps the FV to close up the gap between it and the LV. Finally, as the distance headway reduces, the FV decelerates and finally converges to the speed of LV.

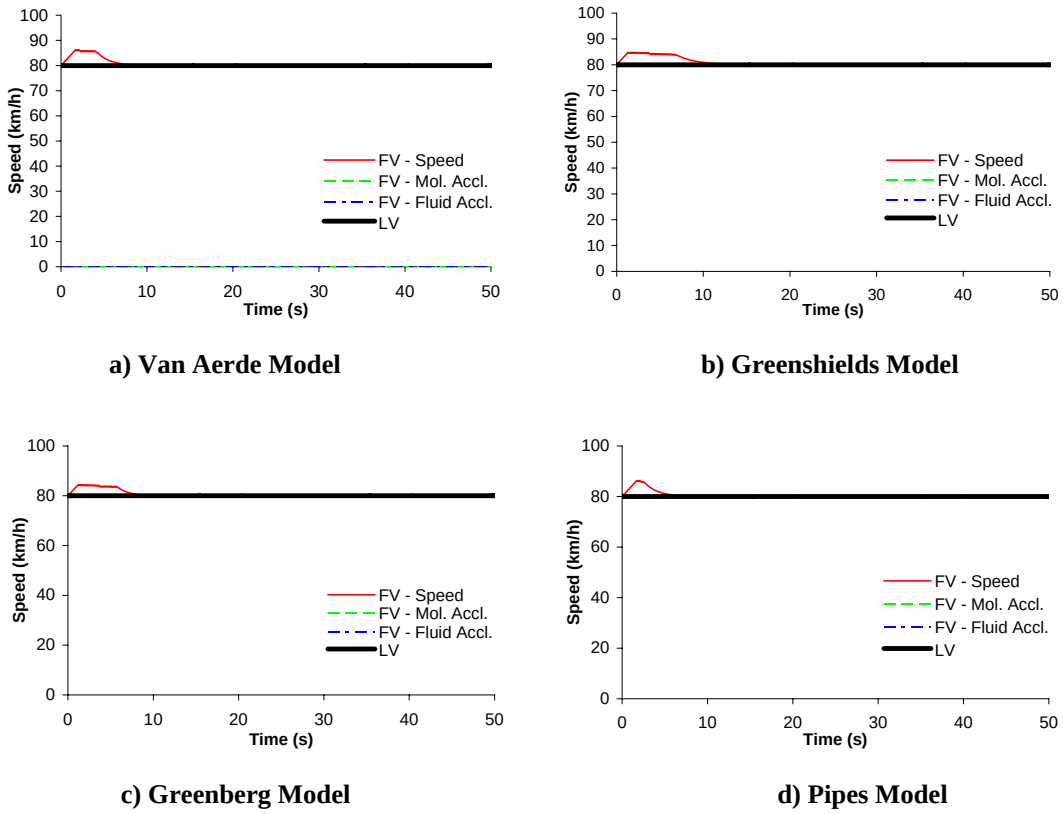

a) Van Aerde Model **b) Greenshields Model**

c) Greenberg Model **d) Pipes Model**

Figure 4-2: Speed Profiles of FV under Uninterrupted Flow Conditions – Case 1

On the other hand, both acceleration formulations – molecular and fluid – result in a different behavior for the FV. From the figures, it can be observed that the profile of FV for the acceleration formulations is identical to that of LV. That is, the acceleration formulations result in the FV traveling at the same speed as the LV for the entire duration without any acceleration or deceleration. This can be explained by analyzing the

mathematical equations for both acceleration formulations. As explained in the previous chapter, the acceleration formulations of car-following models express the acceleration of the FV as a function of the stimulus and sensitivity. The stimulus term is expressed by the speed difference between the LV and FV and the sensitivity is a function of headway and/or speed of FV. Since the speed difference between the LV and FV at $t = 0$ is zero, the formulations result in zero acceleration for the FV. And as the LV travels at the same speed of 80 km/h for the entire trip, the stimulus term remains zero and as a result the vehicle does not accelerate. It can further be observed that this behavior is expected irrespective of the distance headway between the LV and FV, as long as the speed difference remains zero. So, as long as the LV and FV travel at the same speed, the FV does not try to close the gap between it and LV and travels at the same speed.

FV approaching a slow moving LV with an initial headway of 100 m

This case replicates a vehicle exiting from a freeway and approaching a vehicle which is traveling at a lower speed. Specifically, the FV is assumed to be traveling at 70 km/h; LV at a speed of 40 km/h; at an initial distance headway of 100 meters. In this case, it can be expected that the deceleration constraint plays a role in the initial stages as the FV approaches the LV. After the FV converges to the speed of LV, it should maintain a distance headway equal to that of SDH prescribed at 40 km/h (the final speed of FV). As illustrated in the previous case, this SDH can be computed for the four models as follows:

$$\underline{\textit{Van Aerde}} - \; h_{n+1}(@u_{n+1} = 40) = c_1 + c_3.40 + \frac{c_2}{u_f - 40} = 26 \text{ meters}$$

$$\underline{\textit{Greenshields}} - \; h_{n+1}(@u_{n+1} = 40) = \frac{c_2}{u_f - 40} = 25 \text{ meters}$$

$$\underline{\textit{Greenberg}} - \; h_{n+1}(@u_{n+1} = 40) = \frac{1}{k_j} e^{40/u_c} = 31 \text{ meters}$$

$$\underline{\textit{Pipes}} - \; h_{n+1}(@u_{n+1} = 40) = c_1 + c_3.40 = 27 \text{ meters}$$

The results for this scenario are displayed in Figure 4-3. By observing the speed profiles of the FV for all the four models, it can be concluded that the speed of FV in the case of the speed formulation is maintained for a larger value and a larger time than that of both the acceleration formulations. In the case of both the acceleration formulations, the speed of the FV decreases rapidly to the speed of the LV. This can be explained on the basis of the presence of the stimulus term in the acceleration formulations. Because of this term, as the speed of the FV approaches that of LV, the acceleration value remains negative and approaches zero and hence the speed rapidly approaches that of LV. Further, from Figures 3-6 and 3-7, it can be seen that the value of driver sensitivity factor for the molecular acceleration formulation is less than that of the fluid acceleration formulation for most of the speed range of the FV. As a result, it should be expected that the speed of

FV based on the molecular approach converges slower to that of LV than that from the fluid formulation.

Another significant observation can be made by observing the distance and time headway profiles for the four models and the three formulations. The speed formulation results in the FV converging to a distance and time headway equal to the SDH for 40 km/h. Whereas the acceleration formulations do not ensure this behavior and the final headway between lead and follower vehicles is larger than the SDH. This can be explained on the basis that the speed of FV is maintained for a longer time in the speed formulation than that in the acceleration formulations. This results in a reduction of distance and time headway in the case of speed formulation.

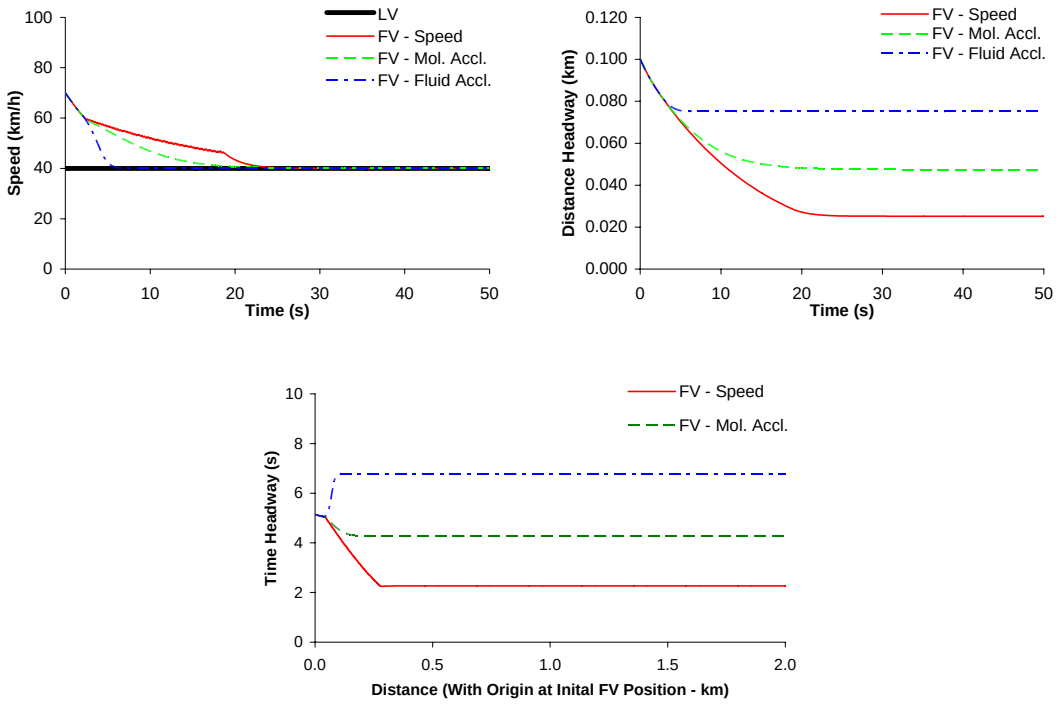

a) Van Aerde Model

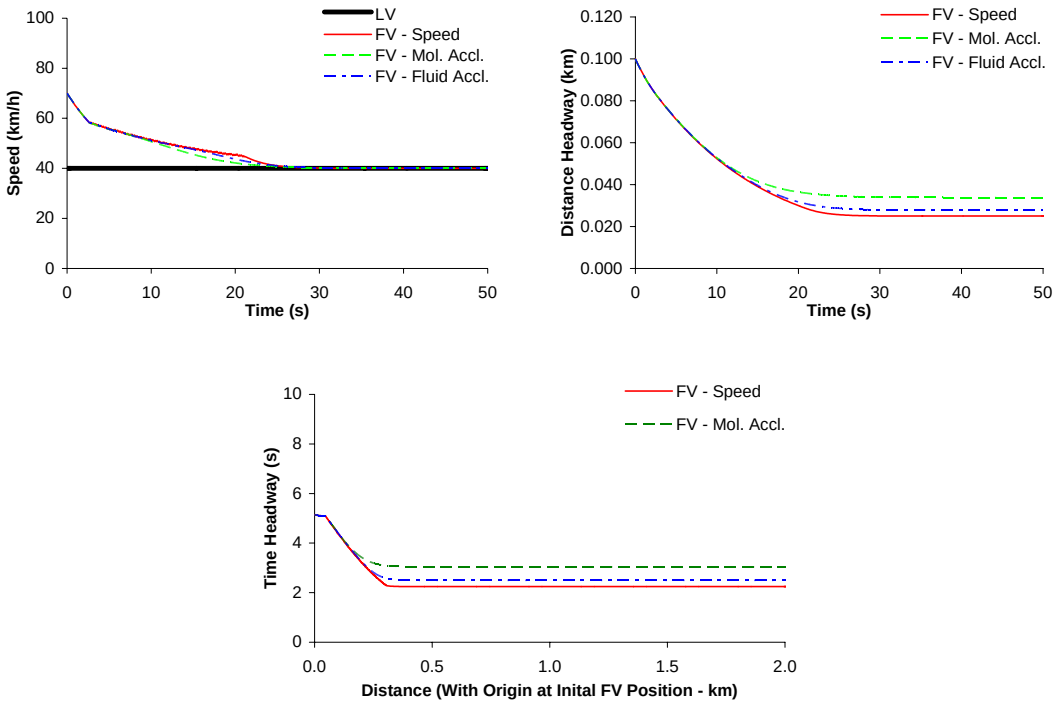

b) Greenshields Model

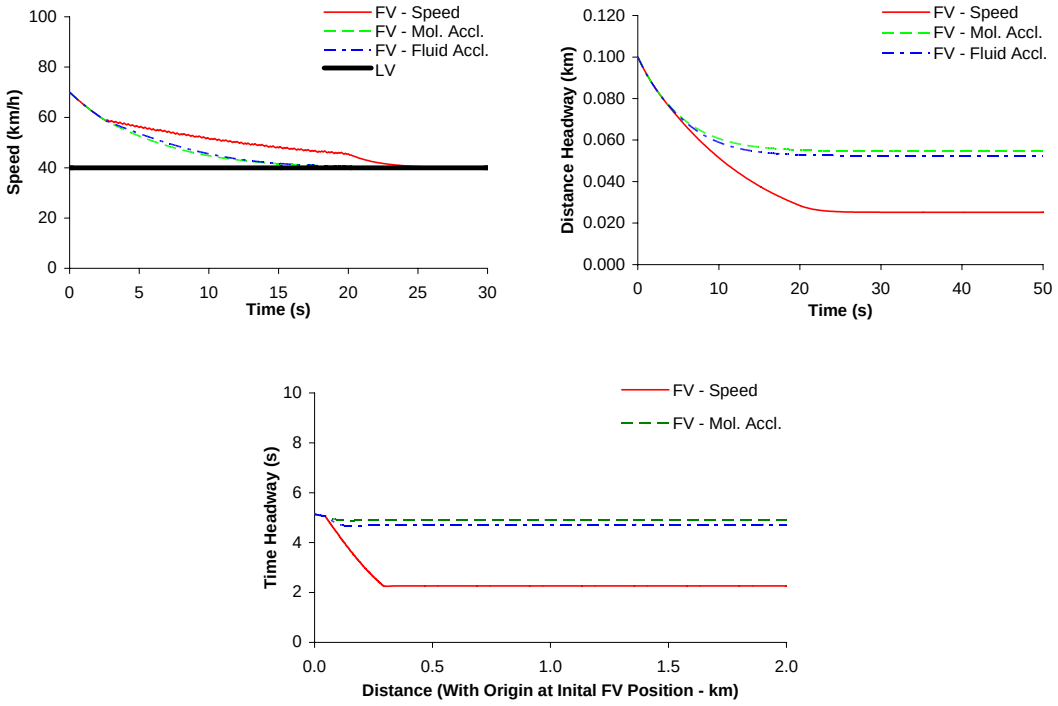

c) Greenberg Model

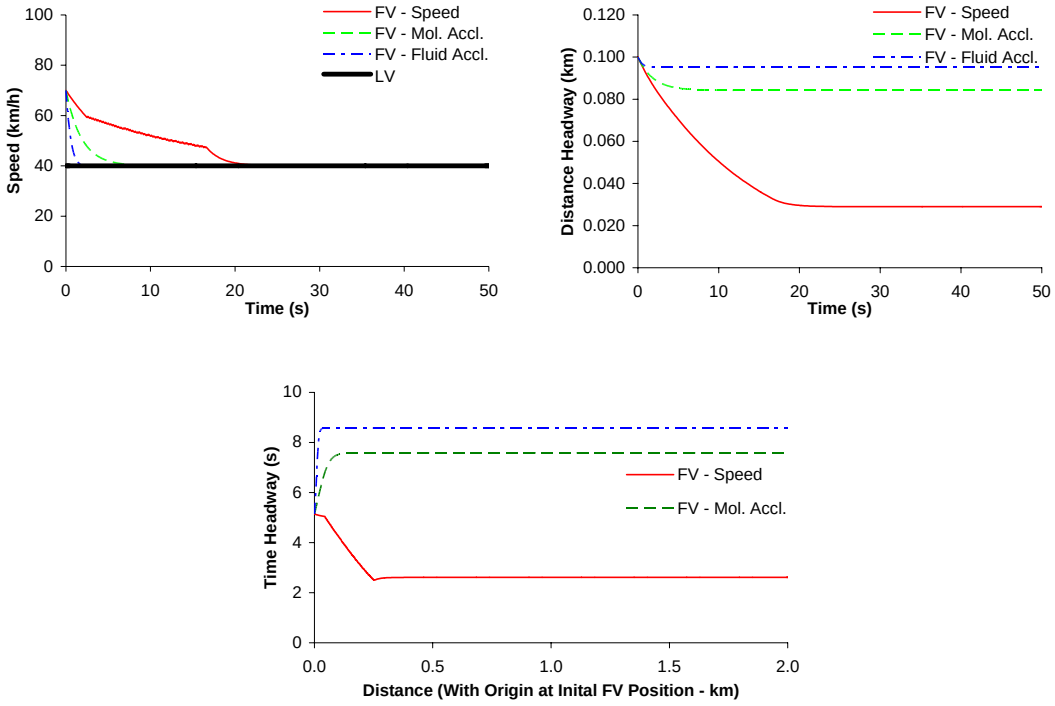

d) Pipes Model

Figure 4-3: Speed and Headway Profiles of FV under Uninterrupted Flow Conditions – Case 2

FV approaching a fast moving LV with an initial headway of 100 m

This case replicates a vehicle entering a freeway and approaching a vehicle which is traveling at a faster speed. Specifically, the FV is assumed to be traveling at 50 km/h; LV at a speed of 80 km/h; and the distance headway is 100 meters initially. In this case, it can be expected that the acceleration constraint plays a role in the initial stages as the FV approaches the LV; because the distance headway is greater than the SDH for a speed of 40 km/h. And after the FV converges to the speed of LV, it should maintain a distance headway equal to that of SDH prescribed at 80 km/h (the final speed of FV).

The results for this case are illustrated in Figure 4-4. From the figures it can be clearly seen that a behavior as that observed in the previous cases is also seen here but is more profound. The speed profiles show a clear difference between the three formulations. In all the three formulations, the FV accelerates initially because the headway is greater than the SDH for 50 km/h. In this region, the acceleration constraint plays a role and hence a linear speed profile is observed. It should be noted that the linear relationship of speed is obtained here just because of the chosen values of parameters like speed and headway. For other values of speed and headway, a non-linear relationship might be obtained. But the difference in the three formulations can be observed at such a time when the speed of the FV exceeds that of the LV as produced by the speed formulation; whereas this situation is not observed in acceleration formulations.

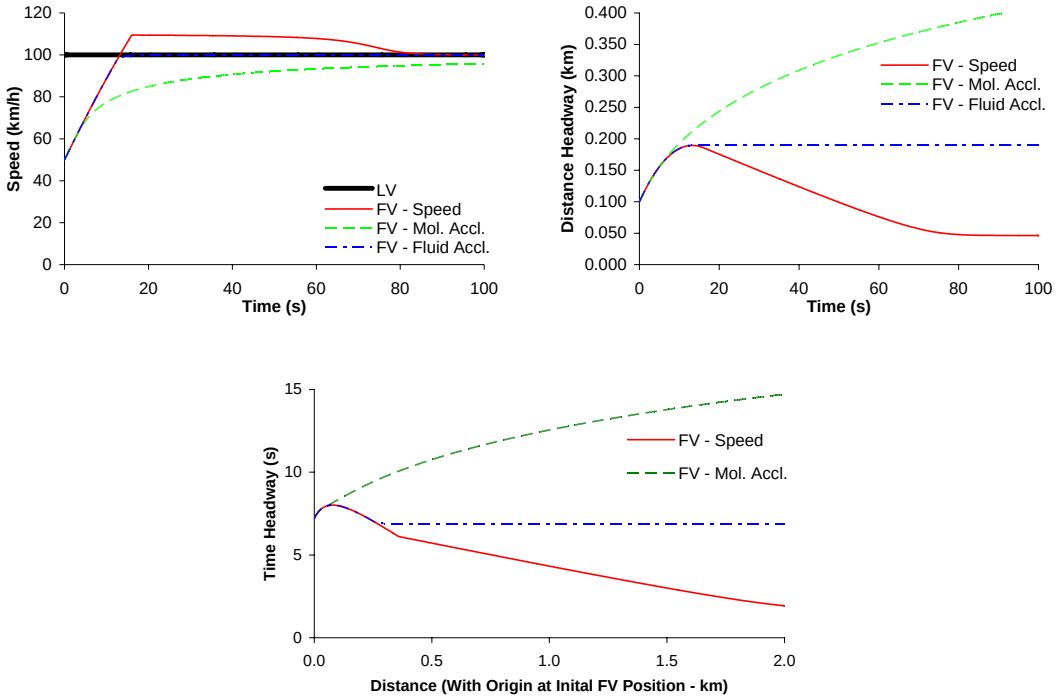

a) Van Aerde Model

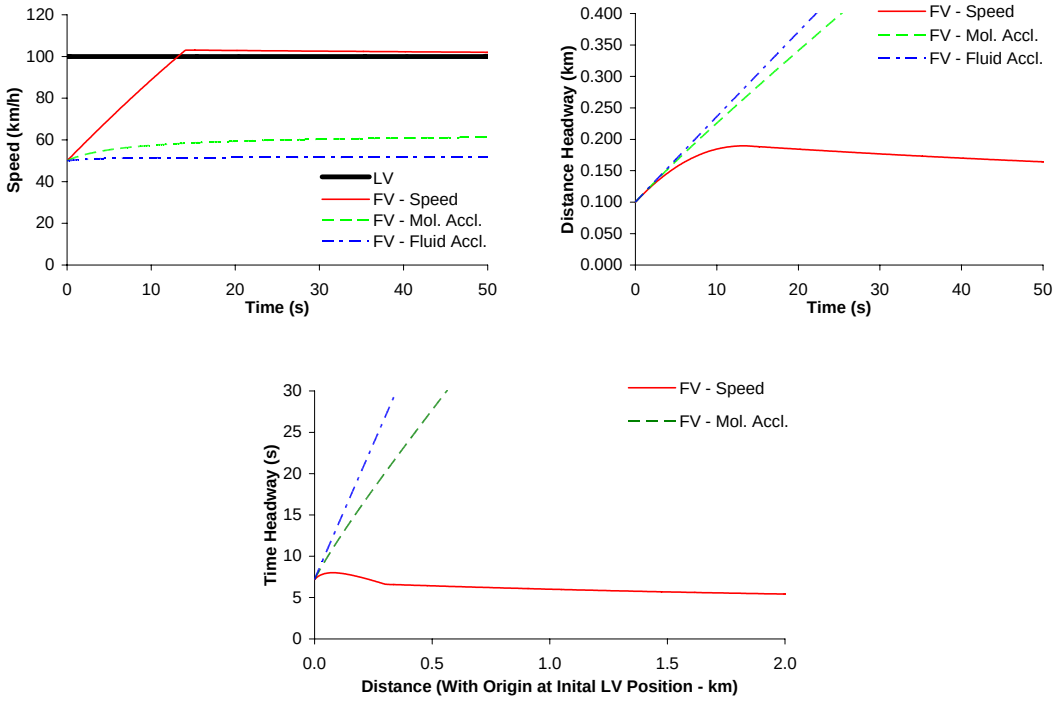

b) Greenshields Model

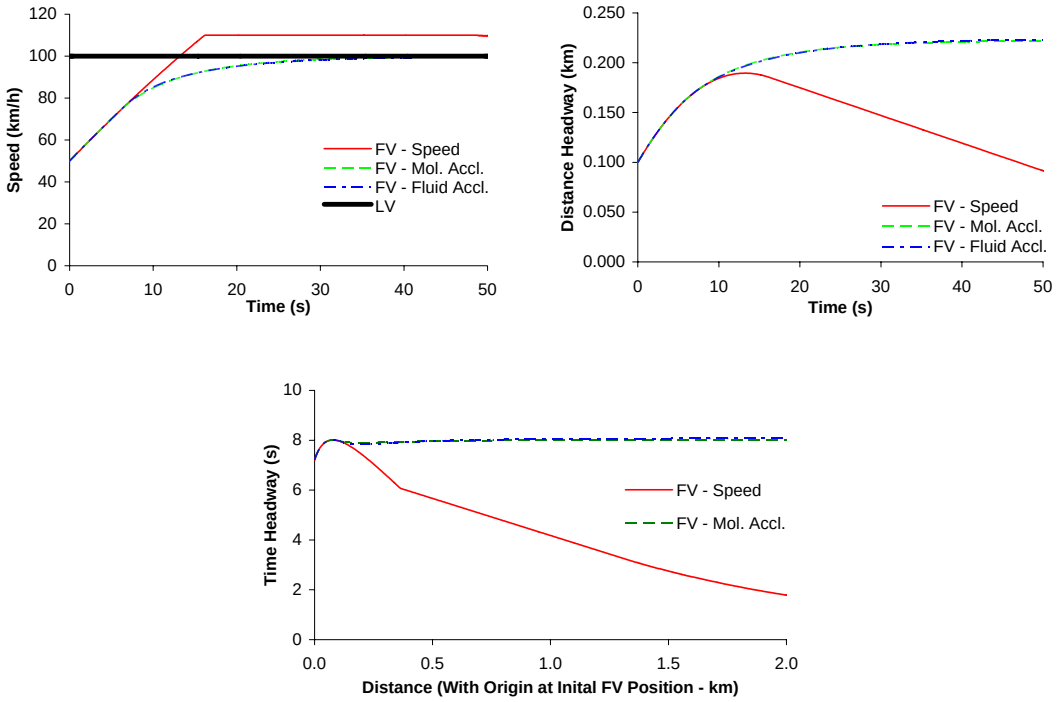

c) Greenberg Model

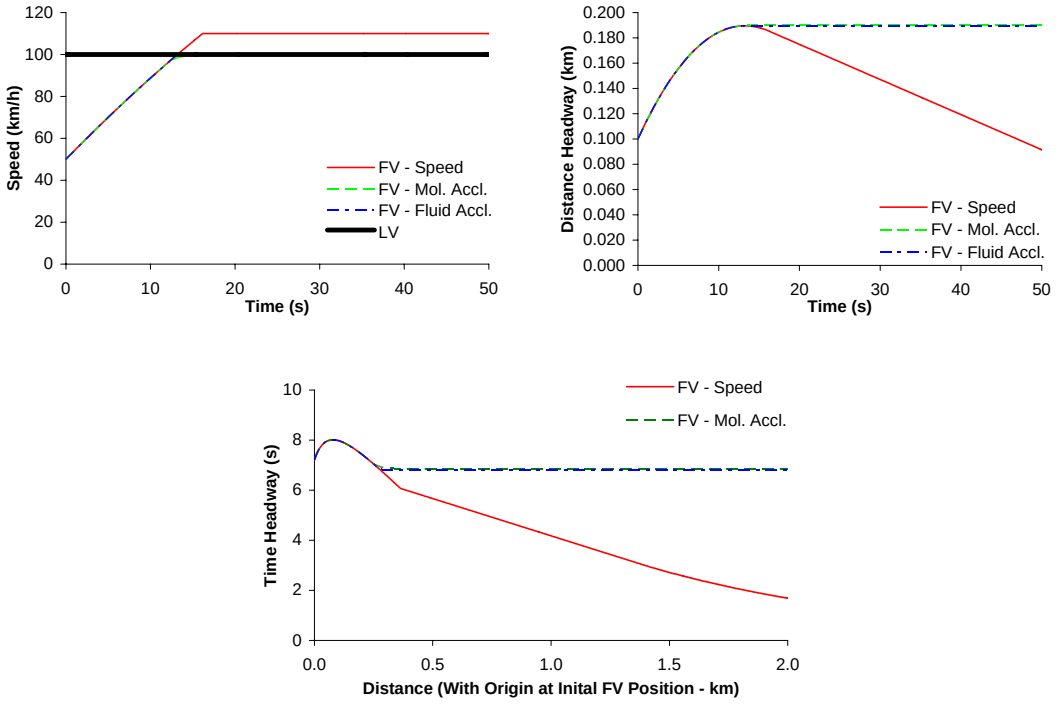

d) Pipes Model

Figure 4-4: Speed and Headway Profiles of FV under Uninterrupted Flow Conditions – Case 3

As a result of the observed speed profile of the FV, the effects are also visible in the headway plots. In the speed formulation, because the FV accelerates to a speed that is greater than the speed of the LV, the gap between it and LV is reduced. This ensures that the FV converges to a SDH for a speed of 80 km/h (final speed of FV) for all the four models. However, in the case of acceleration formulations, the FV does not exceed the speed of the LV and hence the gap between them is not reduced. As a result, the acceleration formulations do not ensure that the FV converges to the SDH. The analysis demonstrates that the speed formulation always converges to steady-state conditions. On the other hand, the acceleration formulations are unable to converge to steady-state conditions when the system experiences an unstable condition.

4.3.2 SCENARIO II: Interrupted Flow Conditions

In this scenario, the car-following formulations are compared for interrupted traffic flow conditions. Such an analysis helps one to compare the car-following behavior that can be observed on typical arterials and local streets. As explained previously, a profile of LV as it travels on a roadway with a traffic signal is selected as shown in Figure 4-1. The FV is assumed to be traveling at a speed of 65 km/h and a headway of 75 meters. The car-following behavior of FV as it follows this LV is obtained for the three formulations. The effect of initial headway on the car-following behavior is also studied by considering two separate cases in which the only parameter that is varied is the distance headway. The results of the analysis are described in detail below.

This analysis further combines the three cases that were presented earlier in scenario I. Because of the profile of the LV and initial conditions of FV, the acceleration constraint plays a critical role initially for a brief period of time and during the acceleration from a stop, while the deceleration takes over in the intermediate period. The results of this analysis are presented in Figure 4-5.

From the speed profile of FV for all four models, the difference between the three formulations can be observed. In the initial region, only the speed formulation results in the FV accelerating. The acceleration formulations do not result in a similar behaviour of FV because the stimulus term is zero. This behaviour is consistent with what was presented in case 1 of scenario I. After this initial period, the LV decelerates to a complete stop (either because of a stop sign or traffic signal) and then starts to accelerate again to its original speed. The behaviour of FV obtained from the three formulations is similar in this region because of the influence of acceleration and collision avoidance constraints. The clear difference in the various formulations demonstrates that the speed formulation ensures that the system converges to steady-state conditions even when the system experiences perturbations from steady-state conditions.

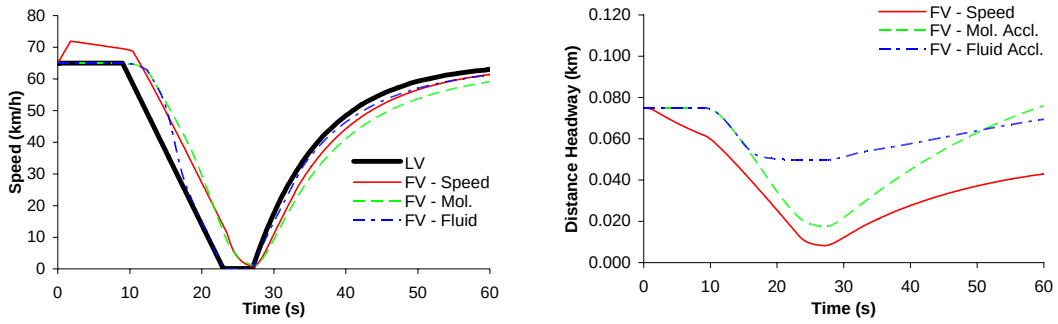

a) Van Aerde Model

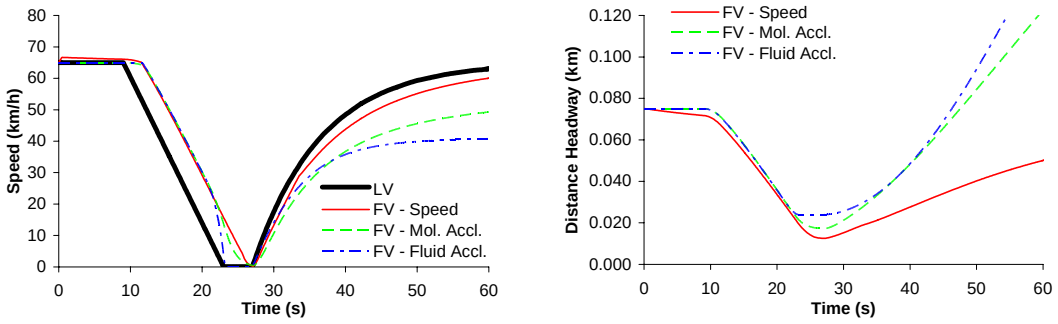

b) Greenshields Model

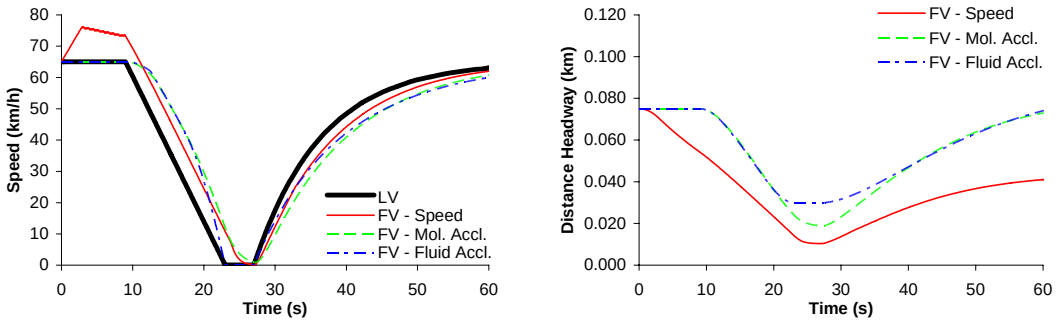

c) Greenberg Model

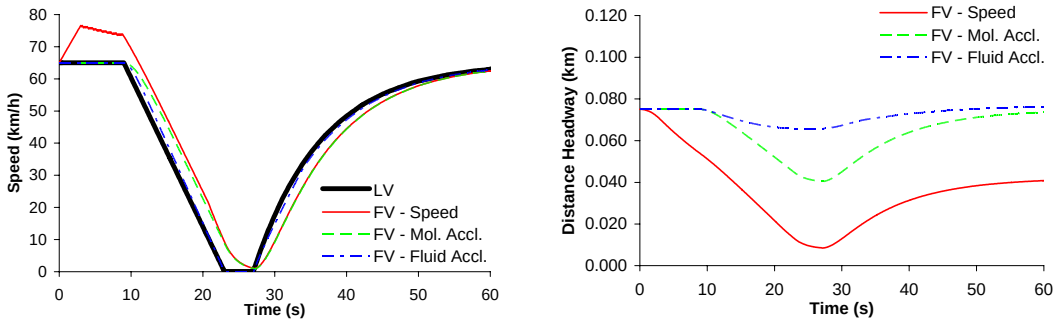

d) Pipes Model

Figure 4-5: Speed and Headway Profiles of FV under Interrupted Flow Conditions

The effect of the above described speed profiles is clearly visible in the headway plots for the four models. The speed formulation results in the FV converging to a SDH for a speed of 80 km/h whereas the acceleration formulations do not ensure this. This observation is similar to the one made in cases 2 and 3 of scenario I. Specifically, if we match the speed and headway profiles, it can be seen that in the speed formulation, the time when the FV's speed is higher than the LV's corresponds to the time when the headway decreases. This allows the FV to maintain a SDH at the end of the maneuver.

In order to study the effect of initial headway on the car-following behavior, the initial headway is increased to 150 meters and the profile of FV is simulated. Figure 4-6 shows the comparison of headway profiles for the three formulations corresponding to the Van Aerde model. Similar results are obtained for the other three models.

From a study of the Figure 4-6, it can be observed that in the speed formulation the FV converges to the SDH (corresponding to a speed of 65 km/h in this case) irrespective of the initial headway. Alternatively, the acceleration formulation converges to different states (speed and headway) depending on the initial state.

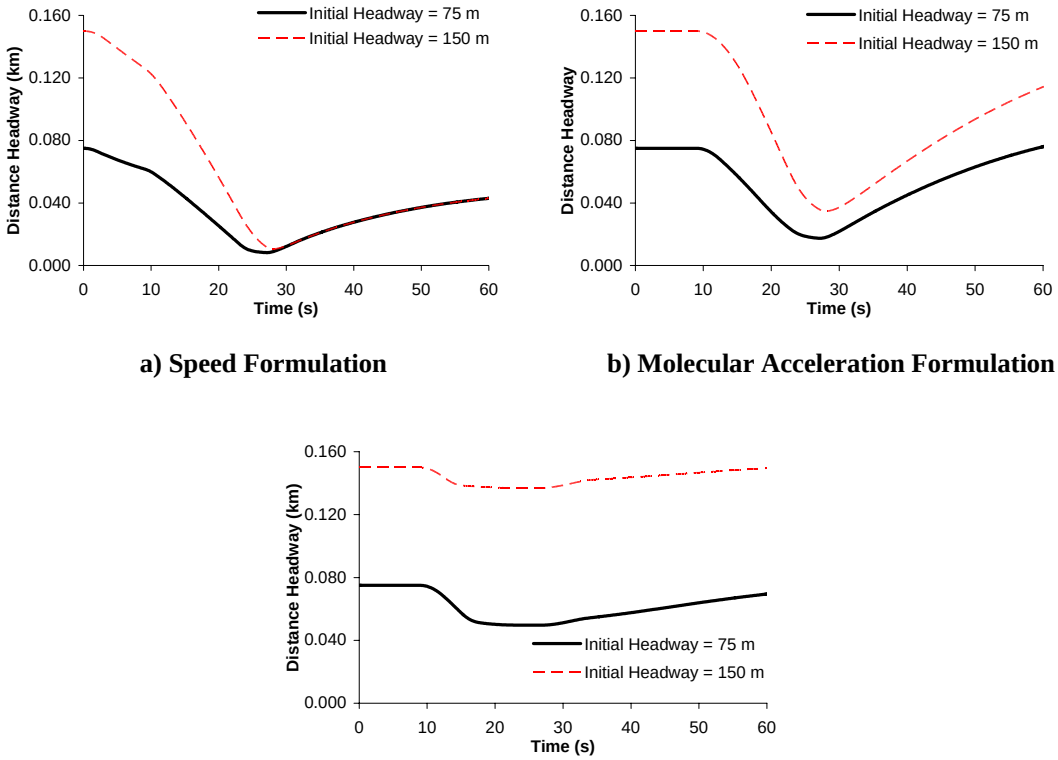

a) Speed Formulation

b) Molecular Acceleration Formulation

c) Fluid Acceleration Formulation

Figure 4-6: Insensitivity of Speed Formulation to Initial Distance Headway – Van Aerde Model

4.4 Discharge Headways

After having analyzed the car-following behavior of a pair of vehicles for a variety of scenarios, this section describes the comparison of the formulations for a platoon of vehicles entering a signalized intersection. This comparison is performed by studying the discharge headways of 20 identical vehicles entering an intersection. As mentioned in section 1.2.2, four distinct cases are considered here in order to study the effect of various parameters on discharge headways and car-following behavior.

The car-following formulations are applied to queue discharge problem as follows:

- The first vehicle starts moving after a lost time of 3 s has expired. The movement is assumed to be governed by the Van Aerde model together with the two constraints.
- The second vehicle in the queue responds to the motion of the leader through the car-following system with no additional lost time added.
- Each subsequent vehicle in the queue then responds to the motion of its leader in the same way.

The following pages describe in detail the results for the four cases.

Case 1 – Base Case:

From a study of the plots of discharge headways for the three car-following formulations as displayed in the Figure 4-7, a number of observations can be made. In all the formulations and all models (except the cellular automata model), the discharge headway converges rapidly to a constant value. But the difference occurs in how rapidly the headways drop and the final value in each of the three formulations.

In the speed formulation, the discharge headways fall rapidly for the first 6 vehicles in queue before converging to a steady-state discharge headway. Specifically the headway of the first vehicle is 4.72 s in the case of the Van Aerde model, 5.48 s in the Greenshields model, 6.13 s in the Greenberg and 4.8 s in the Pipes model. Alternatively, the 20^{th} vehicle has a headway of 1.93 s in the case of the Van Aerde model, 1.81 s in the Greenshields model, 1.9 s in the Greenberg model, 2.02 s in the Pipes model and 2 s in the Cellular Automata model.

Similarly, in the case of the molecular acceleration formulation, the vehicle headways decrease within the queue. The values of the discharge headways of the first and 20^{th} vehicle in queue are roughly the same as the speed formulation. This observation can be explained on the basis that as long as the FV maintains a SDH prescribed for its speed, the molecular acceleration formulation results in the same behaviour of FV as that of the speed formulation. This is due to the mathematical derivation of the molecular formulation. But if the headway of the FV is different from the SDH for its speed, the speed and acceleration formulations result in different behaviours as illustrated in the previous two scenarios.

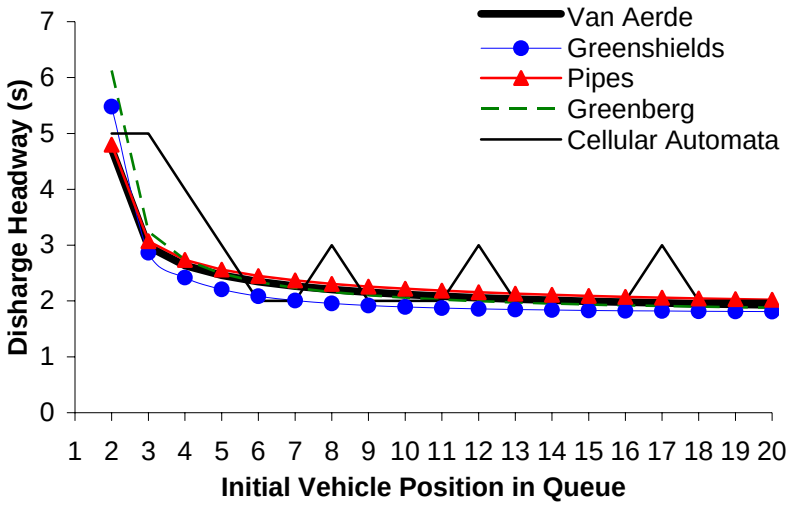

a) Speed Formulation

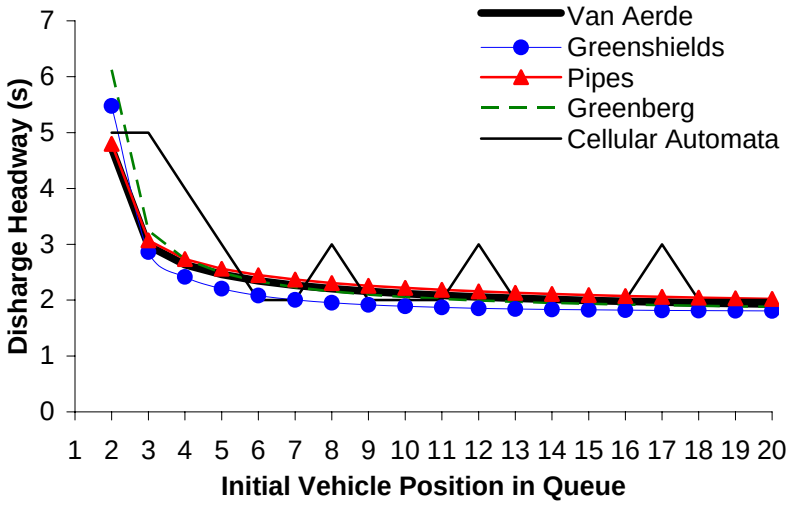

b) Molecular Acceleration Formulation

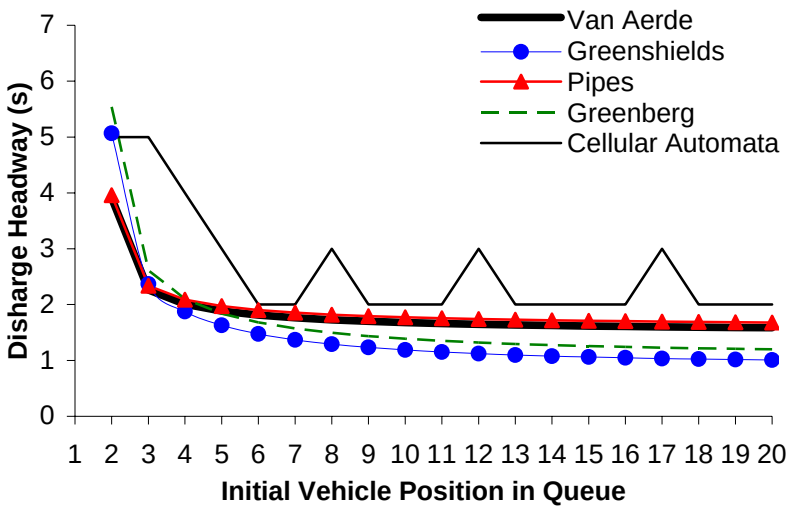

c) Fluid Acceleration Formulation

Figure 4-7: Discharge Headways for Case 1

In the fluid acceleration formulation, though a fall in the discharge headways is observed for vehicles within the queue, a significant difference can be observed. Specifically, the discharge headways for the vehicles are comparatively less in the fluid formulation than in the other two formulations. For example, the discharge headway of the first vehicle was observed to be 3.91 s in the Van Aerde model, 5.07 s in the Greenshields model, 5.54 s in the Greenberg and 3.96 s in the Pipes model. Whereas the discharge headway for the 20^{th} vehicle was observed to be 1.59 s in the Van Aerde model, 1 s in the Greenshields model, 1.2 s in the Greenberg and 1.67 s in the Pipes model. This decrease in the headways can be explained by observing closely the driver sensitivity term in the fluid acceleration formulation. This sensitivity factor includes the speed of the FV in the denominator and hence at very low speeds, the acceleration obtained from the fluid formulation tends to be very high. So, at very low speeds the acceleration constraint takes over and this results in a higher acceleration rate for the FV than in the speed and molecular acceleration formulations (where the acceleration is determined by the model and not by the acceleration constraint). Because of this high acceleration rate of vehicles compared to the other formulations, the discharge headways are also shorter.

Finally, the profile of discharge headways obtained from the cellular automata display a peculiar behaviour. This can be explained by the fact that in this model, the vehicles are moved in steps of cells of size 7.5 meters every second. So, at any given time a vehicle can either be in a cell or not and hence the issue of a vehicle being partially in one cell is not considered. Because of this granularity effect of vehicle movement, the discharge headways do not fall off smoothly as observed in other four models. Though the discharge headway of 20^{th} vehicle is 2 s, it does not guarantee that the vehicle behind it have the same 2 s headway.

Case 2 – Base Case w/ Free flow speed increased by 20 km/h

In this case, the effect of free-flow speed on discharge headways is analyzed. For this purpose, the free-flow speed in increased to 100 km/h from its earlier value of 80 km/h with the rest of the parameters being the same. Though the profiles of the headways as illustrated in Figure 4-8 look similar to the ones obtained in the previous case, significant conclusions can be drawn by observing the values of the headways.

In the speed formulation, the discharge headway of the first vehicle was 4.7 s, 6.3 s, 6.1 s and 4.8 s for the Van Aerde, Greenshields, Greenberg and Pipes models respectively. Alternatively for the 20th vehicle, the time headways are observed to be 1.9 s in the Van Aerde model, 1.84 s in the Greenshields model, 1.9 s in the Greenberg model and 2.08 s in the Pipes model. By comparing these values with those in the speed formulation of case 1, it can be observed that the discharge headways decreased in the Van Aerde and the Greenshields models increased in the Pipes model and remained unchanged in the Greenberg model. This can be explained by looking at the mathematical expressions for the speed of FV in Table 4-2. For Van Aerde and Greenshields models, the speed of FV increases with increase in free-flow speed. Whereas in the Pipes model, the increase of free-flow speed causes the parameter c_3 to increase and as a result the speed of the FV decreases. The Greenberg model is not affected by the free-flow speed as is clearly visible from the equation.

In the molecular acceleration approach, the discharge headway of the first vehicle was observed to be 4.68 s in the Van Aerde model, 6.3 s in the Greenshields model, 6.1 s in the Greenberg model and 4.84 s in the Pipes model. Alternatively for the 20th vehicle, the time headways are 1.9 s, 1.84 s, 1.9 s and 2.08 s for the Van Aerde, Greenshields, Greenberg and Pipes models respectively. This shows that the headways increased in the case of Greenshields and Pipes models; decreased in the case of Van Aerde model and remain unchanged in Greenberg model. The reasoning for this behaviour is the same as that explained earlier.

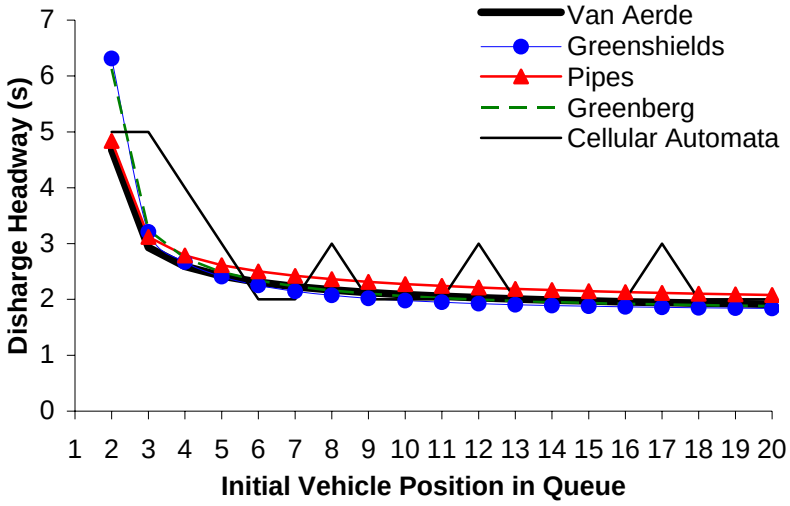

a) Speed Formulation

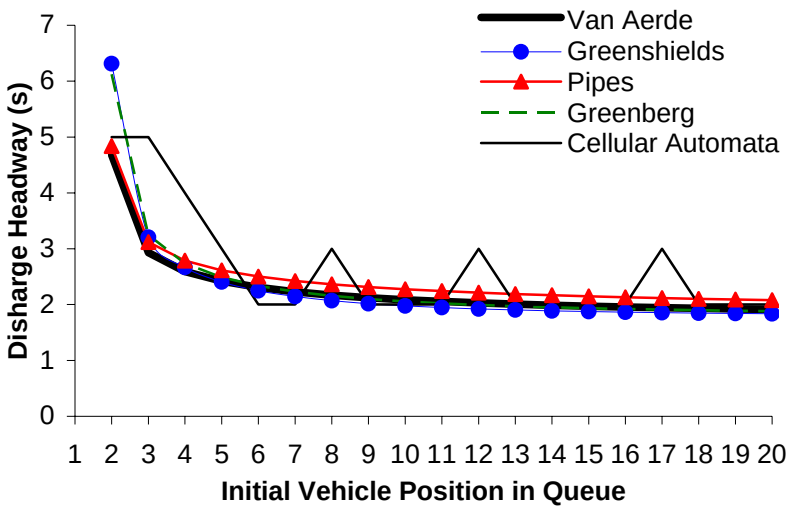

b) Molecular Acceleration Formulation

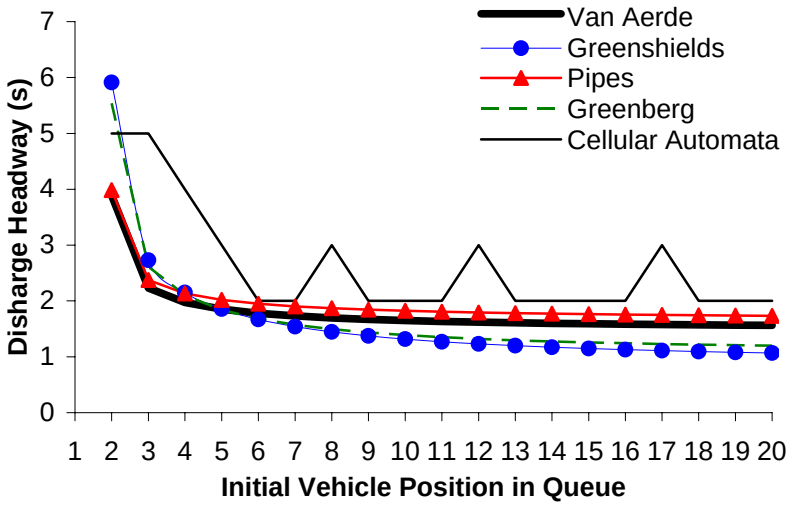

c) Fluid Acceleration Formulation

Figure 4-8: Discharge Headways for Case 2

The fluid acceleration formulation displays a similar behaviour as in the previous case by generating low discharge headways compared to the speed and molecular acceleration formulations. Further, the discharge headway of the first vehicle was observed to be 3.9 s in Van Aerde model, 5.9 s in Greenshields model, 5.5 s in Greenberg model and 4.0 s in Pipes model. And that for the 20th vehicle is observed as 1.6 s in Van Aerde model, 1.1 s in Greenshields model, 1.2 s in Greenberg model and 1.7 s in Pipes model. This shows that the headways increased in the case of Greenshields and Pipes models; decreased in the case of Van Aerde model and remain unchanged in Greenberg model. The reasoning for this behaviour is the same as that explained earlier.

Case 3 – Base Case w/ the first vehicle as a truck

This case describes the effects of a tractor-trailer truck on the discharge headways of the following vehicles. Vehicle 1 is assumed to be a truck and its speed profile is obtained by using its corresponding vehicle dynamics parameters given in the assumptions section earlier. The results of this case are presented in Figure 4-9. There is a similarity and difference between the results of this case and the previous two cases. The similarity is that all three formulations show a similar profile of headways for vehicles in queue. The difference is the value of the discharge headways in the case of the first vehicle since it is a truck.

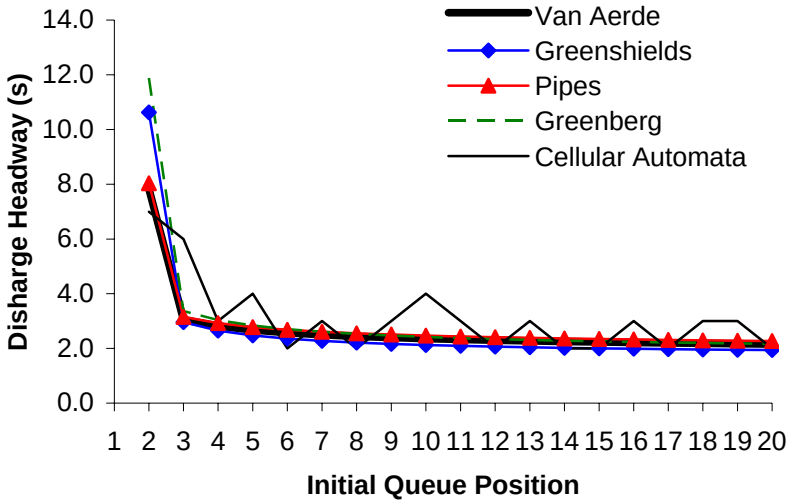

a) Speed Formulation

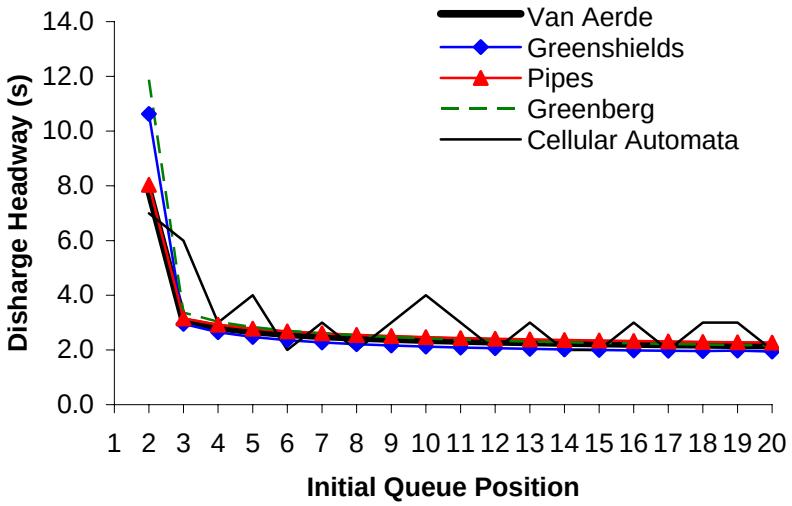

b) Molecular Acceleration Formulation

Figure 4-9: Discharge Headways for Case 3

Further, the values of the discharge headways obtained from the speed and molecular acceleration formulations are identical because the vehicle starts from steady-state conditions. However, in the fluid formulation, the headways are lower when compared to the other formulations.

Another major point of observation is the effect the truck has on the values of discharge headways. The discharge headway of the first vehicle was observed to be 7.8 s in Van Aerde model, 10.6 s in Greenshields model, 11.9 s in Greenberg, 8 s in Pipes model and 7 s in cellular automata model. Whereas the discharge headway for the 20^{th} vehicle was observed to be 2.2 s in Van Aerde model, 1.9 s in Greenshields model, 2.2 s in Greenberg, 2.3 s in Pipes model and 2 s in cellular automata model. This increased headway is the result of the slow acceleration characteristics of the truck which causes an increased discharged headway for the entire platoon of vehicles.

Case 4 – Vehicle 4 turns left

This case describes the effects of a left-turning bay on the discharge headways of the following vehicles. Vehicle 4 is assumed to turn left into the turn bay after its rear bumper has moved forward enough to allow the lane change. This section describes the results of the turning bay analysis in further detail.

From the graphs of both the formulations illustrated in Figure 4-10, it can be seen that the 5^{th} vehicle has a longer headway in comparison to the base case scenario. This is because, the acceleration constraint played a role and prevented vehicle 5 from closing up the gap between it and vehicle 3. However, vehicle 5 was able to speed up faster than in case 1 because of the longer headway. Also, all the vehicles after vehicle 5 were also able to speed up, and hence they have a lesser discharge headway compared to case 1.

Another point of observation is the difference observed in the discharge headways of vehicles 5 and afterwards for the speed and molecular acceleration formulations. This difference can be attributed to the fact that after vehicle 4 turns left, the headway available for vehicle 5 is not the SDH for its speed and hence as explained previously, the profile of this vehicle differs between the speed and acceleration formulations.

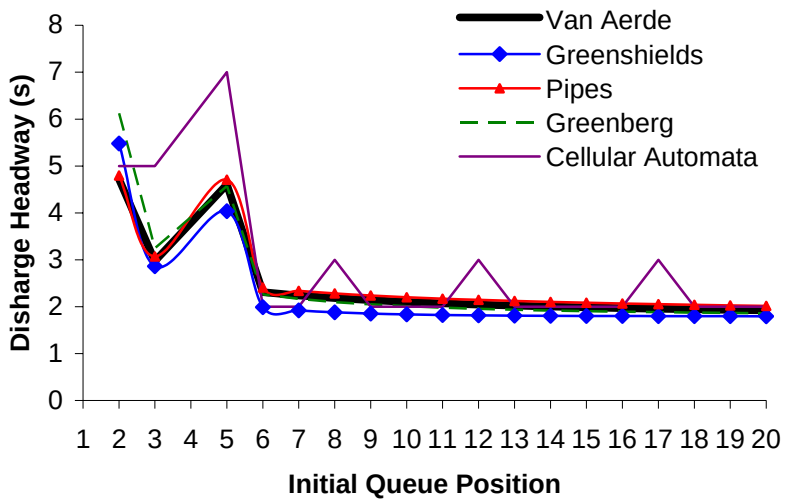

a) Speed Formulation

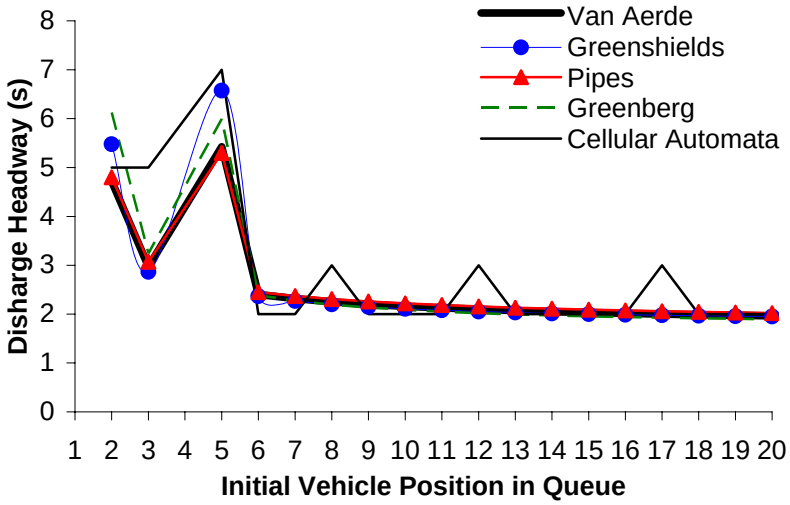

b) Molecular Acceleration Formulation

Figure 4-10: Discharge Headways for Case 4

4.5 Capacity Drop Issue

As stated in the literature review, there is a large debate among the researchers on the issue of capacity drop i.e. whether a drop in capacity of the roadway occurs after the formation of a queue. Many studies have been conducted by researchers to understand the effect of bottlenecks on freeway capacity using field data. While some studies reported that the freeway capacity diminishes by an average of 5 – 10% following the formation of an upstream queue, other studies found no such reductions. Further, some researchers (Cassidy, et al) claimed that the findings from most of the studies were inconclusive. This

was attributed to the methods used in processing the measured data which altered important traffic features. In order to overcome these drawbacks in coming to any conclusions by analyzing the field data, this research effort attempts to address the capacity-drop issue using car-following models. This is achieved by simulating different real-world scenarios using the four state-of-the-art car-following models and was described earlier.

The phenomenon of backups and queuing on a highway occur due to the changes in flow-speed-density states over space and time. These changes of state could be attributed to accidents, reduction of the number of lanes, restricted bridge sizes, work zones, a signal turning red and so forth creating a situation where the capacity on the highway drops to a lower value with a corresponding change in speed and density. When these changes of state (bottlenecks) occur, a boundary is established that demarks the time-space domain of one flow state from another. This boundary is referred to as a shock wave. The aim of this section is to understand the flow processes further downstream of these bottlenecks where their effect is no longer felt.

Depending on the direction of movement of the wave and the change in the area of congestion, shock waves are classified into different categories – forward and backward forming, stationary and recovery shockwaves. Each of these conditions affects the flow processes in a different way. In this research effort, the effect on freeway capacity is studied under two scenarios – at backward recovery shockwave and at stationary shockwave. The former is observed at a traffic signal when the light turns to green; while the latter is observed at a lane drop section. The following pages are devoted to show and explain the results observed for these scenarios and to hypothesize the reasons for such observations.

4.5.1 Signalized Intersection

The speed and acceleration formulations of the Van Aerde car-following model result in the flow rate of the traffic stream to vary as illustrated in Figures 4-11 and 4-12. As the vehicles travel downstream of the intersection, they speed up and try to attain the free-speed. Correspondingly, the flow rate of the traffic stream increases initially to the capacity of the roadway and drops off later on. In the speed formulation, the flow rate of the vehicles reaches the capacity (1600 vph) when they are traveling at speed-at-capacity (45 km/h). The distance required by the vehicles to reach 45 km/h increases with the increase in the initial vehicle position in queue because of the lower speed of the vehicle ahead of it. As the speed of the vehicles increases, the dispersion of traffic stream is observed and as a result the flow rates diminish.

A similar behavior in the flow rate is observed for the acceleration formulation. But the difference here is that the flow rate attained by the vehicles when they reach the speed-at-capacity. When the vehicles attain a speed of 45 km/h, the flow rate from the first two vehicles was observed to be 1591 whereas that from 15^{th} and 16^{th} vehicles was observed to be 1599. So, the vehicles do not actually reach the capacity of roadway but only tend to. As the vehicles travel downstream of the intersection, they are no longer in the steady

state conditions and in such situations the acceleration formulation does not result the follower vehicles to close up the gap in front of it as observed in previous sections. As a result of this, the vehicles travel far more widely than in the speed formulation and hence the flow rates do not reach the roadway capacity.

Further, the flow rate of traffic stream is analyzed at specific locations downstream of the intersection in both the congested and uncongested regimes. The speed and acceleration formulations result in similar profiles but with small differences in values. At a distance of 50 m downstream, all the vehicles are traveling roughly at speed-at-capacity in both formulations and hence the flow rates are close to capacity. At 500 m downstream of the intersection, the vehicles experience no effect of the upstream bottleneck conditions. The flow rate of the traffic stream observed in speed formulation is slightly higher than that in acceleration formulation because of reason explained above. However, the flow rate in both the formulations approaches to capacity when an infinite number of vehicles are considered. The lower flow rate that is observed downstream at the 50 m location is a result of traffic dispersion. Specifically, the first vehicle in queue experiences an infinite headway and thus accelerates to the free-speed. The next vehicle observes a shorter headway and thus accelerates to a lower speed. This domino effect continues until vehicles travel at the speed-at-capacity. It should be noted that the analysis conducted here ignored the random differences in driver behavior.

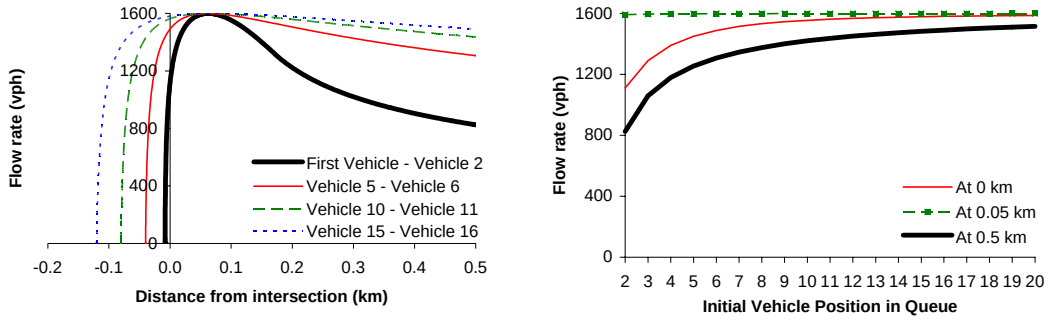

Figure 4-11: Flow Rate of Traffic Stream for Van Aerde Speed Formulation

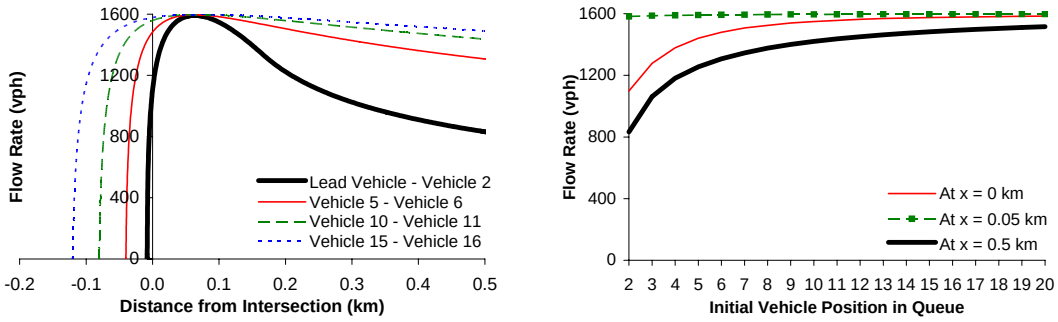

Figure 4-12: Flow Rate of Traffic Stream for Van Aerde Acceleration Formulation

4.5.2 Lane Drop

The speed formulation of the Van Aerde car-following model results in the flow rate of the traffic stream to vary as shown in the Figure 4-13. As the vehicles travel downstream of the intersection, they speed up and try to attain the free-speed. But as observed from the figures, the profile of the flow rates is not the same as that for backward recovery shockwave. As the vehicles start entering the region of lane drop, the speed of vehicles is governed by the acceleration constraint than that obtained from the model. As the vehicles travel further downstream, the speed is no longer governed by the acceleration constraint and hence the change in the profile of the flow rate. As a result of this influence of vehicle dynamics in the initial period, the flow rate of traffic stream does not reach the roadway capacity when the vehicles' speed reaches speed-at-capacity. But as the initial speed of vehicles is increased, the effect of vehicle dynamics is felt for a lesser time period and hence, the flow rate approaches the capacity when the vehicle is at speed-at-capacity. Another way of interpreting this result is that as the level of congestion in the bottleneck increases, the distance required for the traffic stream to reach the roadway capacity also increases.

When the flow rates are analyzed in congested regime (for e.g. 50 m downstream of intersection), a roughly constant flow rate is observed irrespective of the initial speed of the vehicles. This is because; in this region all the vehicles are traveling at the same speed as a result of the influence of vehicle dynamics. In the uncongested regime, 500 m downstream of the intersection, the effect of initial speed on the flow rates can be observed. As the initial speed of vehicles increases, the flow rate of the traffic stream approaches rapidly to the roadway capacity. This is because of the lesser influence of vehicle dynamics as the initial vehicle speed increases. But if a sufficiently large number of vehicles are considered in the analysis, the flow rate will be observed to approach the roadway capacity which indicates that there is no drop in capacity before and after the bottleneck.

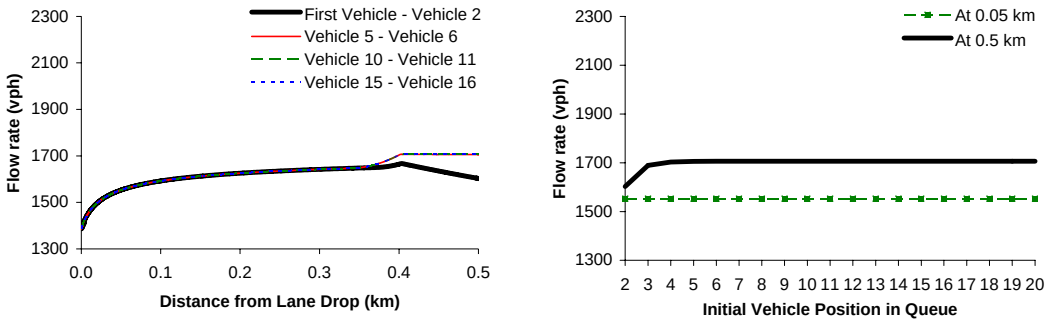

(a)

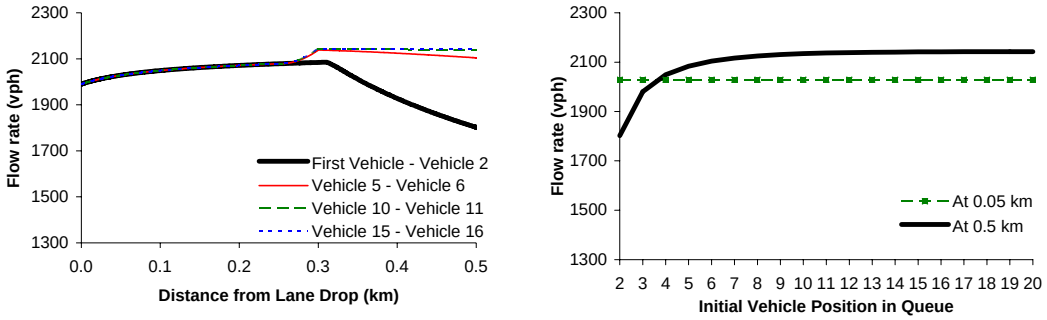

(b)

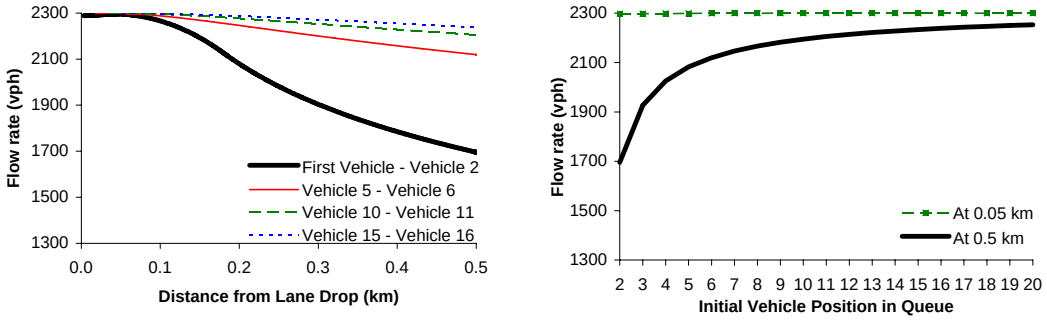

(c)

Figure 4-13: Flow Rate of Traffic Stream for Van Aerde Speed Formulation

a) Initial Speed – 20 km/h; b) Initial Speed – 45 km/h; c) Initial Speed – 80 km/h

The acceleration formulation of the Van Aerde car-following model results in the flow rate of the traffic stream to vary as shown in the following Figure 4-14. It can be observed from these figures that there is a very close resemblance between the profiles for speed and acceleration formulations for distances close to the lane drop. This is because in these regions the vehicle dynamics will control the movement of vehicles in both the car-following formulations. But once the vehicles depart from the steady state conditions, the molecular acceleration formulation results in a lesser acceleration than the speed formulation and hence the flow rate never reaches the value attained in the speed formulation. As a result, the acceleration formulation does not result in the traffic stream reaching the roadway capacity.

When the flow rates in congested regions downstream of the bottleneck are analyzed, a similarity can be observed in the results for speed and acceleration formulations. This is because, in this region the vehicle dynamics controls the movement of vehicles and not the car-following formulation. But the exact relationship depends on the location of analysis downstream of the bottleneck. In the uncongested regions also, like 500 m downstream of bottleneck, the flow rate profile is similar to that in speed formulation. But the values of flow rates attained in acceleration formulation are lower than that in speed formulation because of the reason explained above.

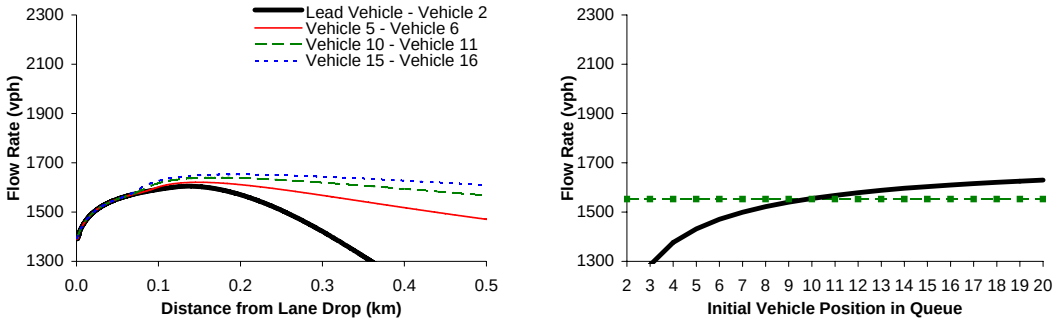

(a)

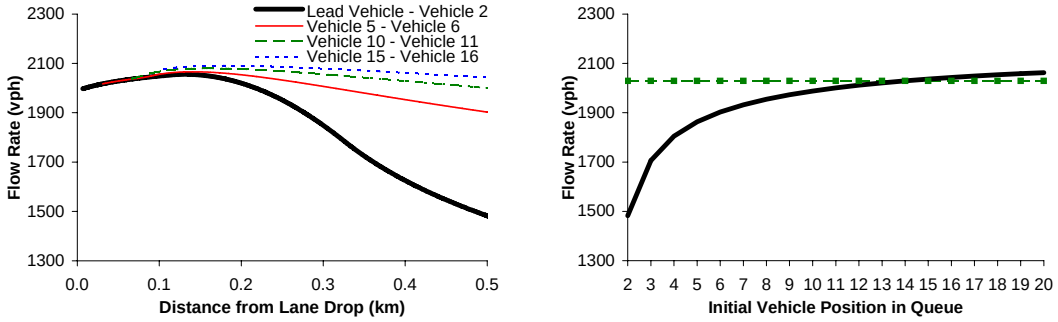

(b)

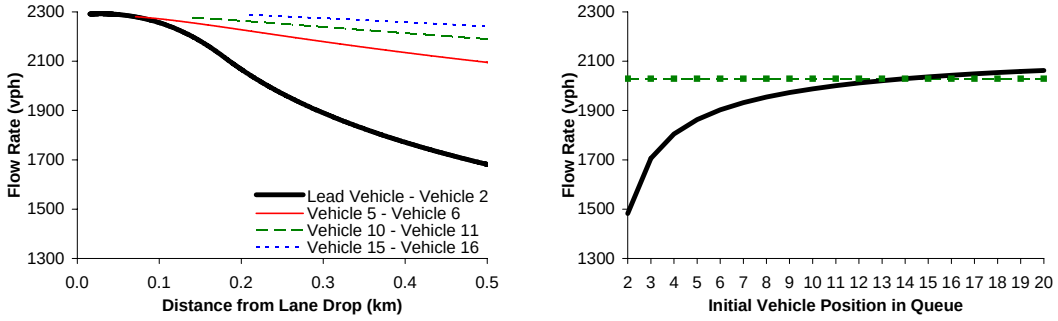

(c)

Figure 4-14: Flow Rate of Traffic Stream for Van Aerde Molecular Acceleration Formulation

a) Initial Speed – 20 km/h; b) Initial Speed – 45 km/h; c) Initial Speed – 80 km/h

4.5.3 Effect of Typical Acceleration Factor

As seen in the previous few paragraphs, the acceleration constraint plays a significant role in understanding the flow processes on a roadway after the formation of a bottleneck. It should be noted in the above analyses; it has been assumed that vehicles accelerate at the maximum rate when they are constrained by their vehicle dynamics. However, Snare

and Rakha (2003) have attempted to characterize typical acceleration behavior by incorporating a maximum acceleration factor (γ) in the vehicle dynamics model, as explained in the previous chapter. Specifically, Snare and Rakha found that the acceleration factor is, on average, 65 percent and varies between 45 and 85 percent. In order to study the effect of maximum acceleration factor on the flow processes and also to simulate a real-world situation, this factor is accounted into the above analyses and the results are explained.

First, the effect of maximum acceleration factor on the flow rate of traffic stream is analyzed for the backward moving shockwave at the signalized intersection previously considered. The figure 4-15 compares the flow rate for speed and acceleration formulations as vehicles depart from a signalized intersection with three different acceleration factors. As it can be observed from the figure, the acceleration factor does not affect the car-following behavior in both the speed and acceleration formulations. This is because as observed in the earlier section, the vehicle dynamics does not play a part in the car-following behavior as vehicles depart from the intersection. This is because as vehicles start from complete stop, the desirable speed obtained from the model is less than that dictated by vehicle dynamics. As a result, the profiles of flow rate for both the car-following formulations are similar.

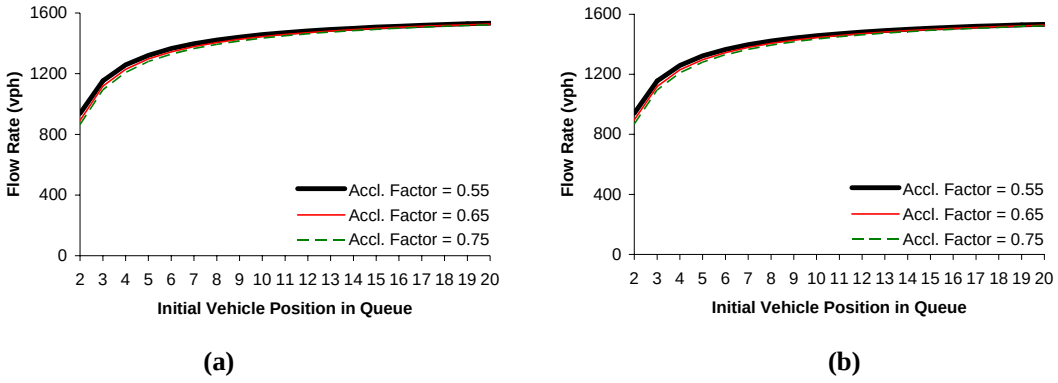

Figure 4-15: Flow Rate of Traffic Stream at a Backward Moving Shockwave

a) Van Aerde Speed Formulation; b) Van Aerde Molecular Acceleration Formulation

Next, the effect of the acceleration factor on flow rate is studied in uncongested and congested regions downstream of a stationary shockwave. The results are displayed in Figure 4-16. From the figures, it can be seen that as the acceleration factor increases the flow rate of the traffic stream also increases. In the congested region (for e.g. 50 m) downstream of the stationary shockwave, the flow rate remains constant for all the vehicles in both the formulations. This is because in this region all the vehicles are being affected by the vehicle dynamics only. Further with the increase in acceleration factor, the speed of the vehicles increases and hence the flow rate. Further, 500m downstream of the shockwave, a similar result is observed. In the speed formulation, the vehicles queued

up far behind are affected by the vehicle dynamics, whereas in the acceleration formulation, the vehicles' motion is not affected by the vehicle dynamics. As explained earlier, the acceleration formulation does not result in the vehicle to close up a large headway once the steady state conditions are disrupted. As a result, the acceleration formulation results in a lower flow rate compared to the speed formulation for all the values of acceleration factors.

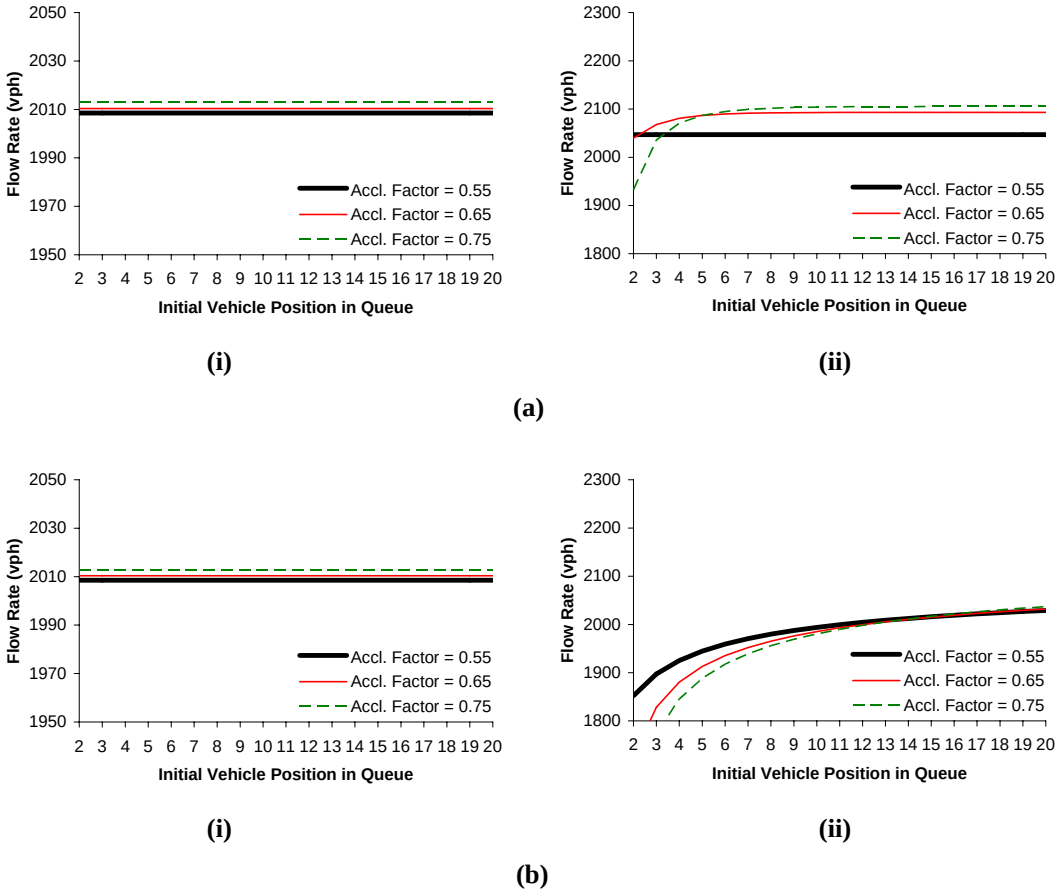

Figure 4-16: Flow Rate of Traffic Stream at a Stationary Shockwave

a) Van Aerde Speed Formulation; b) Van Aerde Molecular Acceleration Formulation

i) 50 m Downstream; ii) 500 m Downstream

4.6 Conclusions

This chapter described in detail the issues faced in comparing the car-following formulations derived in the previous chapter. Realising that many different traffic flow conditions exist in reality, three distinct scenarios are selected in this chapter for the purpose of comparing the models. The first scenario compared the formulations in uninterrupted traffic flow conditions found on freeways. Next, the comparison was performed on a roadway facility with a stop sign reflecting an interrupted flow condition.

Further, the behaviour of a platoon of 20 vehicles queued up at an intersection is analyzed to compare the discharge headways. Finally, the issue of capacity drop is addressed through considering two specific cases – stationary and backward moving shockwaves.

During the course of this chapter, many important results were obtained and the reasoning was explained appropriately. In conclusion, it would be best to summarize the main findings of this chapter below:

- If both LV and FV are travelling at the same speed, then both the acceleration formulations do not result in an acceleration of the FV whatever the headway is. But speed formulation results in FV being accelerated or decelerated depending on the headway.
- Speed formulation ensures that the FV converges to a SDH for its speed irrespective of the initial headway; whereas, both the acceleration formulations do not ensure this behaviour.
- If a vehicle travels such that it maintains a SDH prescribed for its speed, then the speed and molecular acceleration formulations result in a same behaviour for that vehicle. However, this is not the case with the fluid acceleration approach.
- Discharge headways obtained from any of the four models – Van Aerde, Greenshields, Greenberg or Pipes – converge to a constant value after a long time. However, this is not the case with Cellular Automata model.
- Free-flow speed has a different effect on the discharge headways of vehicles departing from an intersection for each of the four car-following models and three formulations.
- The influence of trucks and turning vehicles is profound on discharge headways and should be accounted for.
- In the case of backward moving shockwave, both the speed and acceleration formulations result in no loss of roadway capacity as long as a very large number of vehicles are considered in the analysis.
- In the case of a stationary bottleneck, acceleration factor plays a major role in defining the flow processes after the shockwave. If the level of congestion in the stationary bottleneck is high, the capacity of the traffic stream drops off because of vehicle dynamics. But at low congestion, this is not the case and the speed formulation does not result in a loss of capacity. However, the acceleration formulation results in a capacity drop irrespective of the level of congestion in the bottleneck.
- The maximum acceleration factor has no effect on the roadway capacity and flow processes before and after the formation of a queue at a backward moving shockwave.
- The acceleration factor affects the roadway capacity to a great extent in the case of a stationary bottleneck. The higher the acceleration factor, the higher the flow rate of vehicles on the vehicles once the steady-state conditions are attained.
- So, in conclusion it can be stated that the capacity loss which has been observed in the filed studies may either be due to the effect of acceleration factor or due to collection of data before the steady-state conditions are again attained or because of the high level of congestions.

CHAPTER FIVE:

SUMMARY, CONCLUSIONS AND RECOMMENDATIONS

5.1 Summary

This thesis first presented the different formulations of car-following behavior for four selected models – Pipes, Greenshields, Greenberg and Van Aerde. Specifically, speed and acceleration forms are described and detailed and a new acceleration formulation which considers the fluid nature of traffic is proposed. A comparison of the existing and the proposed approaches for acceleration formulation is also presented. Further, the valid range for Van Aerde speed formulation is analyzed. Then a comprehensive car-following behavior encompassing the steady state conditions and the two constraints – acceleration and collision avoidance – is presented. Specifically, the variable power vehicle dynamics model proposed by Rakha and Lucic (2002) is utilized for the acceleration constraint.

Next, the thesis focused on describing in detail the issues faced in comparing the car-following formulations derived earlier. Realising that many different traffic flow conditions exist in reality, three distinct scenarios were selected for the purpose of comparing the models. The first scenario compared the formulations in uninterrupted traffic flow conditions found on freeways. Next, the comparison was performed on a roadway facility with a stop sign reflecting an interrupted flow condition. Further, the behaviour of a platoon of 20 vehicles queued up at an intersection is analyzed to compare the discharge headways. Finally, the issue of capacity drop is addressed through considering two specific cases – stationary and backward moving shockwaves.

5.2 Conclusions

An analysis of the sensitivity factor derived in molecular and fluid acceleration approaches revealed a number of interesting results. At lower speeds and lower stimuli, the fluid formulation results in a higher value of acceleration than the molecular formulation. These higher accelerations at lower speeds are caused by differences in the values of the sensitivity factors between the two approaches. But at higher speeds, the two approaches have roughly the same profiles. Furthermore, the Van Aerde and Greenshields model acceleration/deceleration behavior is found to be more realistic and more consistent with typical in-field behavior than the Greenberg and Pipes models.

Following a comparative analysis of the different formulations for the four selected car-following models, following conclusions can be made. It has been observed that the speed formulation always allows the vehicles to converge to steady-state conditions. On the other hand, both the acceleration formulations are unable to converge to steady-state conditions when the system experiences an unstable condition. Further, if both the LV and FV are travelling at the same speed, then both the acceleration formulations do not result in an acceleration of the FV whatever the headway is. But speed formulation

results in the FV being accelerated or decelerated depending on the headway. This is attributed to the '*response*' term in the acceleration formulations which goes to zero if the speed differential is zero.

A study of the discharge headways of vehicles departing from a signalized intersection revealed that the four state-of-art car-following models result in a constant headway after steady-state conditions are arrived. However, this is not the case with the Cellular Automata model. This has been attributed to the fact that in this model, vehicles are moved in steps of cells of size 7.5 meters every second. Because of this kind of vehicle movement, the discharge headways do not fall off smoothly as observed in other four models. Further, it has been observed that the free-flow speed has a different effect on the discharge headways of vehicles departing from an intersection for each of the four car-following models and three formulations. The influence of trucks and turning vehicles is profound on discharge headways and should be accounted for.

The other topic addressed here is the question of capacity drop. In the case of backward moving shockwave, both the speed and acceleration formulations result in no loss of roadway capacity as long as a very large number of vehicles are considered in the analysis. However, in the case of a stationary bottleneck, acceleration factor plays a major role in defining the flow processes after the shockwave. If the level of congestion in the stationary bottleneck is high, the capacity of the traffic stream drops off because of vehicle dynamics. But at low congestion, this is not the case and the speed formulation does not result in a loss of capacity. However, the acceleration formulation results in a capacity drop irrespective of the level of congestion in the bottleneck. The maximum acceleration factor has no effect on the roadway capacity and flow processes before and after the formation of a queue at a backward moving shockwave. However, it affects the roadway capacity to a great extent in the case of a stationary bottleneck. The higher the acceleration factor, the higher the flow rate of vehicles on the vehicles once the steady-state conditions are attained. So, in conclusion it can be stated that the capacity loss which has been observed in the filed studies may either be due to the effect of acceleration factor or due to collection of data before the steady-state conditions are again attained.

5.3 Recommendations for Further Research

Based on the research that was presented in this thesis further research is required in a number of areas:

a. Microscopic field data of vehicle departures from stationary and backward recovery shockwaves is critical in validating the findings of this research effort.
b. Further research is required to investigate the effect of heavy-duty vehicles on capacity drops downstream of bottlenecks.
c. Attempt to incorporate acceleration constraints with the solution of macroscopic traffic stream differential equations.

REFERENCES

1. Agyemang-Duah, K. and Hall, F. L. (1991). *Some Issues Regarding the Numerical Value of Capacity*. Proceedings of the International Symposium of Highway Capacity. A.A. Balkema Press, Germany, pp. 1-15.

2. Aycin, M. F. and Benekohal, R. F. (1998). *Linear Acceleration Car-Following Model Development and Validation*. Transportation Research Record 1644, TRB, National Research Council, Washington, D.C., pp. 10-19.

3. Banks, J. H. (1990). *Flow Processes at a Freeway Bottleneck*. Transportation Research Record 1287, TRB, National Research Council, Washington, D.C., pp. 20-28.

4. Banks, J. H. (1991). *Two-Capacity Phenomenon at Freeway Bottlenecks: A Basis for Ramp Metering?* Transportation Research Record 1320, TRB, National Research Council, Washington, D.C., pp. 83-90.

5. Bekey, G. A., G. O. Burnham and J. Seo. (1977). *Control Theoretical Models of Human Drivers in Car Following*. Human Factors, Vol. 19, No. 4, pp. 399-413.

6. Bonneson, J. A. (1992). *Modeling Queued Driver Behavior at Signalized Junctions*. Transportation Research Record 1365, TRB, National Research Council, Washington, D.C., pp. 99-107.

7. Carstens, R. L. (1971). *Some Traffic Parameters at Signalized Intersections*. Traffic Engineering, Vol. 41, No. 11, pp. 33-36.

8. Cassidy, M. J. and Bertini, R. L. (1999). *Some Traffic Features at Freeway Bottlenecks*. Transportation Research, Part B, Vol. 33, pp. 25-42.

9. Ceder, A. (1976). *A Deterministic Traffic Flow Model for the Two Regime Approach*. Transportation Research Record 567, TRB, National Research Council, Washington, D.C., pp. 16-30.

10. Ceder, A. (1978). *The accuracy of Traffic Flow Models: A Review and Preliminary Investigation*. Traffic Engineering and Control, December, pp. 541-544.

11. Ceder, A. and A. D. May, Jr. (1976). *Further evaluation of single and two regime traffic flow models*. Transportation Research Record 567, TRB, National Research Council, Washington, D.C., pp. 1-30.

12. Chandler, F. E., R. Herman and E. W. Montroll (1958). *Traffic Dynamics: Studies in Car Following. Operations Research*, Vol. 6, pp. 165-184.

13. Cohen, S. L. (2002). *Application of Car-Following Systems in Microscopic Time-Scan Simulation Models*. Transportation Research Record 1802, TRB, National Research Council, Washington, D.C., pp. 239-247.

14. Cohen, S. L. (2002). *Application of Car-Following Systems to Queue Discharge Problem at Signalized Intersections*. Transportation Research Record 1802, TRB, National Research Council, Washington, D.C., pp. 205-213.

15. Drake, J., Scofer, J. and May, A. D., Jr. (1965). *A Statistical Analysis of speed-density hypotheses*. Proceedings of Third International Symposium on Theory of Traffic Flow, New York, June 1965. Published as Vehicular Traffic Science, American Elsevier, New York (1967), pp. 112-117.

16. Drew, D. R. (1968). *Traffic Flow Theory and Control*. New York: McGraw-Hill.

17. Edie, L. C. (1961). *Car-following and Steady State Theory for Noncongested Traffic*. Operations Research, Vol. 7, pp. 66-76.

18. Gazis, D. C., R. Herman and R. B. Potts (1959). *Car Following Theory of Steady State Traffic Flow*. Operations Research, Vol. 7, No. 4, pp. 499-505.

19. Gazis, D. C., R. Herman and R. W. Rothery (1961). *Non-Linear Follow the Leader Models of Traffic Flow*. Operations Research, Vol. 9, pp. 545-567.

20. Gerlough, D. L. and Wanger, F A. (1967). *Improved Criteria for Traffic Signals at Individual Intersections*. NCHRP Report 32, HRB, National Research Council, Washington, D. C., p. 34.

21. Gipps, P. G. (1981). *A Behavioral Car Following Model for Computer Simulation*. Transportation Research, Part B, Vol. 15, pp. 105-111.

22. Greenberg, H. (1959). *An Analysis of Traffic Flow*. Operations Research, Vol. 7, pp. 79-85.

23. Greenshields, B. D. (1935). *A study in Highway Capacity*. Highway Research Board, Proceedings, Vol. 14, p. 458.

24. Greenshields, B. D., D. Schapiro and E. L. Ericksen. (1947). *Traffic Performance at Urban Street Intersections*. Eno Foundation for Highway Traffic Control.

25. Hall, F. L. and Hall, L. M. (1990). *Capacity and Speed-Flow Analysis of the Queen Elizabeth Way in Ontario*. Transportation Research Record 1287, TRB, National Research Council, Washington, D.C., pp. 108-118.

26. Helly, W. (1959). *Simulation of Bottlenecks in Single Lane Traffic Flow*. Proceedings of the Symposium on Theory of Traffic Flow, Research Laboratories, General Motors, New York: Elsevier, pp. 207-238.

27. Heyes, M. P. and Ashworth, R. (1972). *Further Research on Car Following Models*. Transportation Research, Vol. 6, pp. 287-291.

28. Highway Capacity Manual. (1950). U.S.Government Printing Office, Washington, D.C.

29. Khan, S., Maini, P. and Thanasupsin, K. (2000). *Car-Following and Collision Constraint Models for Uninterrupted Traffic*. Transportation Research Record 1710, TRB, National Research Council, Washington, D.C., pp. 37-46.

30. Kikuchi, C. and Chakroborty, P. (1992). *Car Following Model Based on a Fuzzy Inference System*. Transportation Research Record 1365, TRB, National Research Council, Washington, D.C., pp. 82-91.

31. Kometani, E. and T. Sasaki. (1959). *Dynamic Behavior of Traffic with a Non-linear Spacing-Speed Relationship*. Proceedings of the Symposium on Theory of Traffic Flow, Research Laboratories, General Motors, New York: Elsevier, pp. 105-119.

32. Lee, G. (1966). *A Generalization of Linear Car-Following Theory*. Operations Research, Vol. 14, No.4, Jul. – Aug., pp. 595-606.

33. Lee, J. and Chen, R. L. *Entering Headway at Signalized Intersections in a Small Metropolitan Area*. Transportation Research Record 1091, TRB, National Research Council, Washington, D.C., pp. 117-126.

34. Lighthill, M. J. and G. B. Whitham, (1955). *On Kinematic Waves: II. A Theory of Traffic Flow on Long Crowded Roads*. Proceedings of the Royal Society: A 229, pp. 317-347, London.

35. May, A. D. (1990). *Traffic Flow Fundamentals*. Englewood Cliffs, NJ: Prentice-Hall.

36. May, A. D., Jr. and H. E. M. Keller (1967). *Non-Integer Car Following Models*. Highway Research Record 199, pp. 19-32.

37. Michalopoulos, P. G., Lyrintzis, A. S. and Liu, G. (1994). *Development and Comparative Evaluation of High-Order Traffic Flow Models*. Transportation Research Record 1457, TRB, National Research Council, Washington, D.C., pp. 174-183.

38. Nelson, P. (1995). *On Deterministic Developments of Traffic Stream Models*. Transportation Research, Vol. 29 B, No. 4, pp. 297-302.

39. Newell, G. F. (1961). *Non-Linear Effects in the Dynamics of Car Following*. Operations Research, Vol. 9, No. 2, pp. 209-229.

40. Papageorgiou, M., J. M. Blosseville and H. Hadj-Salem. (1989). *Macroscopic Modeling of Traffic Flow on the Boulevard Peripherique in Paris*. Transportation Research, Vol. 23 B, No. 1, 1989, pp. 29-47.

41. Payne, H. J. (1971). *Models of Freeway Traffic and Control*. Proc., Simulation Council, Mathematical Models of Public Systems, Vol. 1, No. 1, pp. 51-61.

42. Payne, H. (1984). *Discontinuity in Equilibrium Traffic Flow*. Transportation Research Record 971, TRB, National Research Council, Washington, D.C., pp. 140-146.

43. Pipes, L. A. (1953). An Operational Analysis of Traffic Dynamics. Journal of Applied Physics, Vol. 24, pp. 271-281.

44. Pipes, L. A. (1967). *Car Following Models and the Fundamental Diagram of Road Traffic*. Transportation Research, Vol. 1, No. 1, pp. 21-29.

45. Prigogine, I. and R. Herman, (1971). *Kinematic Theory of Vehicular Traffic*. American Elsevier Publications, New York.

46. Ross, P. (1988). *Traffic Dynamics*. Transportation Research, Vol. 22 B, No. 4, pp. 421-435.

47. Tolle, J. E. (1974). *Composite Car Following Models*. Transportation Research, Vol. 8, pp. 91-96.

48. Special Report 209: *Highway Capacity Manual*. TRB, National Research Council, Washington, D. C., 1985.

49. Underwood, R.T. (1961). *Speed, Volume and Density Relationships, Quality and Theory of Traffic Flow*. Yale Bureau of Highway Traffic, New Haven, Conn., pp. 141-188.

50. Van Aerde, M. (1995). *Single Regime Speed-Flow-Density Relationship for Congested and Uncongested Highways*. Presented at the 74th TRB Annual Conference (Paper No. 95080), Washington, D. C.

51. Van Aerde, M and Rakha, H. (1995). *Multivariate Calibration of Single Regime Speed-Flow-Density Relationships*. Proceedings of the Vehicle Navigation and Information Systems (VNIS) Conference, Seattle, WA.

52. Wattleworth, J. A. (1963). *Some Aspects of Macroscopic Freeway Traffic Flow Theory*. Traffic Engineering, Vol. 34, No. 2, pp. 15-20.

VITA

Venkata Siva Praveen Pasumarthy was born in Machilipatnam, India to Lakshmi and Murthy Pasumarthy. He later moved to Hyderabad, India where he finished his high school education. Praveen attended Indian Institute of Technology, Madras after high school and he received a Bachelor of Technology degree in Civil Engineering in May 2002. He elected to pursue a higher degree in Civil Engineering and attended Virginia Tech for his Masters degree. Praveen will be relocating to Richmond, Virginia after his graduation where he accepted a temporary employment with Wilbur Smith Associates.